

COMPARING DIGESTIBILITY OF A- AND B- TYPE CRYSTALS AND PROVIDING  
INSIGHT ON DIGESTIBILITY OF STARCHES

by

LIMING CAI

B.E., Wuhan Polytechnic University, China, 2004  
M.E., South China University of Technology, 2007

AN ABSTRACT OF A DISSERTATION

submitted in partial fulfillment of the requirements for the degree

DOCTOR OF PHILOSOPHY

Department of Grain Science and Industry  
College of Agriculture

KANSAS STATE UNIVERSITY  
Manhattan, Kansas

2011

## Abstract

Starch is the most important source of food energy. However, the information about the metabolic quality of starchy foods is scarce. It is well known that native starches with a B-type X-ray diffraction pattern are more resistant to  $\alpha$ -amylase digestion than those starches with an A-type X-ray pattern, but the underlying mechanism is not well understood. It is not clear whether the enzyme resistance of B-type starch is due to its B-type crystalline structure or the other structural features in starch granules. The objective of this study was to compare the structure and enzyme digestibility of highly pure A- and B-type starch crystals, and understand the roles of crystalline types in starch digestibility. Highly pure A- and B-type starch crystals were prepared from short linear  $\alpha$ -glucans (short-chain amylose) generated from completely debranched waxy starches by manipulating the processing conditions such as starch solids concentration, crystallization temperature and chain length. High concentration, high temperature and short chain length favored the formation of the A-type structure, whereas reverse conditions resulted in the B-type polymorph. Digestion results using a mixture of  $\alpha$ -amylase and glucoamylase showed that A-type crystals were more resistant to enzyme digestion than B-type crystals. The A-type crystalline product obtained upon debranching 25% waxy maize starch at 50°C for 24 h gave 16.6% digestion after 3 h, whereas B-type crystals produced by debranching 5% waxy maize starch at 50°C for 24 h followed by holding at 25°C for another 24 h had 38.9% digested after 3 h. The A-type crystals had a higher melting temperature than the B-type crystals as determined by differential scanning calorimetry. Annealing increased the peak melting temperature of the B-type crystals, making it similar to that of the A-type crystals, but did not improve the enzyme resistance. The possible reason for these results was due to more condensed packing pattern of double helices in A-type crystallites. It seems that the crystalline types are not the key factor that controls the digestibility of native starch granules. The resistance of native starches with B-type X-ray diffraction pattern is probably attributed to the other structural features in starch granules.

COMPARING DIGESTIBILITY OF A- AND B- TYPE CRYSTALS AND PROVIDING  
INSIGHT ON DIGESTIBILITY OF STARCHES

by

LIMING CAI

B.E., Wuhan Polytechnic University, China, 2004  
M.E., South China University of Technology, 2007

A DISSERTATION

submitted in partial fulfillment of the requirements for the degree

DOCTOR OF PHILOSOPHY

Department of Grain Science and Industry  
College of Agriculture

KANSAS STATE UNIVERSITY  
Manhattan, Kansas

2011

Approved by:

Major Professor  
Dr. Yong-Cheng Shi

# **Copyright**

LIMING CAI

2011

## Abstract

Starch is the most important source of food energy. However, the information about the metabolic quality of starchy foods is scarce. It is well known that native starches with a B-type X-ray diffraction pattern are more resistant to  $\alpha$ -amylase digestion than those starches with an A-type X-ray pattern, but the underlying mechanism is not well understood. It is not clear whether the enzyme resistance of B-type starch is due to its B-type crystalline structure or the other structural features in starch granules. The objective of this study was to compare the structure and enzyme digestibility of highly pure A- and B-type starch crystals, and understand the roles of crystalline types in starch digestibility. Highly pure A- and B-type starch crystals were prepared from short linear  $\alpha$ -glucans (short-chain amylose) generated from completely debranched waxy starches by manipulating the processing conditions such as starch solids concentration, crystallization temperature and chain length. High concentration, high temperature and short chain length favored the formation of the A-type structure, whereas reverse conditions resulted in the B-type polymorph. Digestion results using a mixture of  $\alpha$ -amylase and glucoamylase showed that A-type crystals were more resistant to enzyme digestion than B-type crystals. The A-type crystalline product obtained upon debranching 25% waxy maize starch at 50°C for 24 h gave 16.6% digestion after 3 h, whereas B-type crystals produced by debranching 5% waxy maize starch at 50°C for 24 h followed by holding at 25°C for another 24 h had 38.9% digested after 3 h. The A-type crystals had a higher melting temperature than the B-type crystals as determined by differential scanning calorimetry. Annealing increased the peak melting temperature of the B-type crystals, making it similar to that of the A-type crystals, but did not improve the enzyme resistance. The possible reason for these results was due to more condensed packing pattern of double helices in A-type crystallites. It seems that the crystalline types are not the key factor that controls the digestibility of native starch granules. The resistance of native starches with B-type X-ray diffraction pattern is probably attributed to the other structural features in starch granules.

## Table of Contents

List of Figures .....	xi
List of Tables .....	xv
Acknowledgements.....	xvii
Dedication .....	xviii
Chapter 1 - Introduction.....	1
Structure levels related to enzymatic hydrolysis .....	2
Granular structure .....	2
Supramolecular structure .....	3
Molecular structure .....	4
A- and B-type starch crystals.....	5
Preparation and crystallization of SCA.....	5
Characterization and digestibility of A- and B-type crystals.....	7
Objectives .....	7
References.....	9
Chapter 2 - Debranching and crystallization of waxy maize starch in relation to enzyme digestibility * .....	13
Abstract.....	13
Introduction.....	13
Materials and methods .....	14
Materials .....	14
Debranching of starch .....	14
Gel permeation chromatography (GPC) .....	15
Scanning electron microscopy .....	15
Transmission Electron Microscopy (TEM) .....	15
Differential scanning calorimetry (DSC).....	15
Synchrotron X-ray scattering and diffraction measurements .....	16
In vitro digestion method .....	16
Isolation of resistant starch .....	17
Results.....	17

Degree of debranching and Molecular weight distribution .....	17
Crystallization and precipitation .....	17
Morphology.....	18
Thermal properties .....	18
Synchrotron SAXS results .....	19
Synchrotron WAXD results .....	20
In vitro digestion profile .....	21
Molecular origin of RS .....	22
Discussion .....	22
Conclusions.....	24
References.....	25
Chapter 3 - Structure and digestibility of crystalline short-chain amylose from debranched waxy wheat, waxy maize and waxy potato starches* .....	38
Abstract.....	38
Introduction.....	38
Materials and methods .....	39
Materials .....	39
Debranching of starch and preparation of CSCA .....	40
Gel permeation chromatography (GPC) .....	40
High-performance anion-exchange chromatograph (HPAEC).....	40
Average CL determination.....	41
Wide-angle X-ray diffraction.....	41
Differential scanning calorimetry (DSC).....	41
In vitro digestion method .....	41
Statistical analysis .....	41
Results and discussion .....	42
Molecular weight distribution by GPC .....	42
CL distribution .....	42
Yield and average CL .....	43
Crystalline structure .....	43
Thermal properties .....	44

In vitro digestion .....	44
Conclusions.....	46
References.....	47
Chapter 4 - Study on melting and crystallization of short-chain amylose by <i>in situ</i> synchrotron wide-angle X-ray diffraction .....	58
Abstract.....	58
Introduction.....	58
Materials and methods .....	59
Materials .....	59
Starch debranching and preparation of SCA.....	59
Preparation of amorphous SCA .....	59
Synchrotron WAXD .....	60
Differential scanning calorimetry (DSC).....	60
Results.....	61
Synchrotron WAXD of powder and hydrated SCA .....	61
Melting and crystallization of SCA from waxy starches .....	61
Thermal properties of SCA from waxy starches.....	63
Discussion.....	64
Conclusions.....	66
References.....	67
Chapter 5 - Manipulation of A- and B-type crystals from short-chain amylose in relation to their digestibility .....	79
Abstract.....	79
Introduction.....	80
Materials and methods .....	80
Manipulation of A- and B- type crystals from short-chain amylose (SCA) .....	81
Annealing of starch crystals.....	81
Gel permeation chromatography (GPC) .....	82
Scanning electron microscopy (SEM) .....	82
Particle size distribution.....	82
Wide-angle X-ray diffraction.....	82



In vitro digestion method .....	82
Results and Discussion .....	82
Formation of A- and B- starch crystals.....	82
Molecular weight distribution of A- and B- starch crystals.....	83
Morphology and particle size distribution of A- and B- starch crystals .....	84
Thermal properties of A- and B- starch crystals .....	84
In vitro digestibility of A- and B- starch crystals .....	85
Conclusions.....	87
References.....	89
Chapter 6 - Formation of spherulites from short-chain amylose in relation to their digestibility	
.....	107
Abstract.....	107
Introduction.....	107
Materials and methods .....	109
Materials .....	109
Starch debranching and spherulites formation.....	109
Light microscopy .....	109
Gel permeation chromatography (GPC) .....	110
Scanning electron microscopy (SEM) .....	110
Wide-angle X-ray diffraction.....	110
DSC.....	110
Synchrotron small-angle X-ray scattering .....	110
In vitro digestion method .....	110
Results.....	111
Molecular weight (MW) distribution and yield .....	111
Morphology.....	111
Characterization of crystalline structure .....	112
In vitro digestion profile .....	113
Discussion.....	115
Conclusions.....	116
References.....	117

Chapter 7 - Conclusions and Perspectives ..... 132

## List of Figures

- Figure 2.1 Molecular weight distribution of (A) waxy maize starch (25% solids) debranched and crystallized at 50°C at different times, and (B) waxy maize starch debranched and crystallized at 50°C for 24 h and its corresponding isolated resistant starch..... 32
- Figure 2.2 (A) Yield of starch precipitate based on the weight of waxy maize starch at different debranching times; —◆— crystallization at 50°C; —■— crystallization at 25°C after the debranched starch was crystallized at 50°C for 24 h; (B) Starch polymer solution at the beginning of debranching and cloudy slurry after 24 h of crystallization at 50°C; and (C) SEM images of waxy maize starch debranched and crystallized at 50°C for 24 h recovered by filtration and drying in an oven at 40°C..... 33
- Figure 2.3 Transmission electron microscopic images of waxy maize starch (25% solids) debranched at different times at 50°C: (A) 1 h, (B) 2 h, (C) 4 h, (D) 8 h, (E) 16 h, and (F) 24 h..... 34
- Figure 2.4 Thermal properties of native waxy maize starch and waxy maize starch debranched at different times as determined by differential scanning calorimetry ..... 35
- Figure 2.5 Small-angle X-ray scattering of native waxy maize starch and freeze-dried digests of waxy maize starch debranched and crystallized at 50°C at different times with (A) 4% moisture (except that native starch was 11% moisture), (B) 45% moisture; (C) log-log plots, 4% moisture (except that native starch was 11% moisture) and (D) log-log plots, 45% moisture..... 36
- Figure 2.6 Wide-angle X-ray diffraction of native waxy maize starch and freeze-dried digests of waxy maize starch debranched and crystallized at 50°C at different times with (A) 4% moisture (except that native starch was 11% moisture) and (B) 45% moisture ..... 37
- Figure 3.1 Molecular weight distributions of (A) debranched waxy wheat, waxy maize, and waxy potato starches; (B) crystalline short-chain amylose (CSCA) products from debranched waxy wheat, waxy maize and waxy potato starches ..... 54
- Figure 3.2 Chain length distributions of (A) debranched waxy wheat starch and its CSCA product; (B) debranched waxy maize starch and its CSCA product; (C) debranched waxy potato starch and its CSCA product..... 55

Figure 3.3 X-ray diffraction patterns of waxy wheat, waxy maize, waxy potato starches and debranched crystalline short-chain amylose (CSCA) products .....	56
Figure 3.4 Differential scanning calorimetry thermograms of waxy wheat, waxy maize, waxy potato starches and debranched crystalline short-chain amylose (CSCA) products.....	57
Figure 4.1 Synchrotron wide-angle X-ray diffraction of short-chain amylose (as is and hydrated) from (A) waxy wheat starch; (B) waxy maize starch; and (C) waxy potato starch.....	73
Figure 4.2 Dynamic synchrotron wide-angle X-ray diffraction results of short-chain amylose from debranched waxy wheat starch during (A) heating and (B) cooling.....	74
Figure 4.3 Dynamic synchrotron wide-angle X-ray diffraction results of short-chain amylose from waxy maize starch during (A) heating and (B) cooling .....	75
Figure 4.4 Dynamic synchrotron wide-angle X-ray diffraction results of short-chain amylose from waxy potato starch during (A) heating and (B) cooling.....	76
Figure 4.5 Thermal properties of short-chain amylose from (A) debranched waxy wheat starch, (B) debranched waxy maize starch and (C) debranched waxy potato starch as determined by differential scanning calorimetry: (a) Samples (50% moisture) were heated from 10 to 160°C at 10°C/min; (b) Samples (75% moisture) were heated from 10 to 160°C at 10°C/min; (c) Samples (50% moisture) were heated from 10 to 100°C at 10°C/min; and (d) Samples (50% moisture) were heated from 10 to 160°C at 10°C/min, after heating from 10 to 100°C at 10°C/min, holding at 100°C for 5min, and cooling from 100°C to 10°C at 10°C/min ....	77
Figure 4.6 The diagram of melting and crystallization of short-chain amylose studied by using synchrotron wide-angle X-ray diffraction.....	78
Figure 5.1 Production of A- and B-type crystals from short-chain amylose by changing (A) starch solids; (B) crystallization temperature; and (C) chain length.....	95
Figure 5.2 Wide-angle X-ray diffraction of short-chain amylose prepared from debranched waxy maize starch with different (A) solids concentration, (B) crystallization temperatures, and (C) debranched waxy potato starch before and after annealing .....	96
Figure 5.3 Molecular weight distribution of short-chain amylose prepared from debranched waxy maize starch with different (A) solids concentration, and (B) crystallization temperatures, and (C) debranched waxy potato starch before and after annealing .....	97

Figure 5.4 Scanning electron microscopic images of short-chain amylose prepared from debranched waxy maize starch with different starch solids concentration: A and B, 5% solids; C and D, 15% solids; E and F, 25% solids .....	98
Figure 5.5 Scanning electron microscopic images of short-chain amylose prepared from debranched waxy maize starch with different crystallization temperature: A and B, 4°C; C and D, 25°C; E and F, 50°C .....	99
Figure 5.6 Scanning electron microscopic images of short-chain amylose prepared from debranched waxy potato starch: A and B, before annealing; C and D, after annealing .....	100
Figure 5.7 Particle size distributions of short-chain amylose prepared from debranched waxy maize starch at different starch solids concentration: A, 5% solids; B, 15% solids; C, 25% solids .....	101
Figure 5.8 Particle size distributions of short-chain amylose prepared from debranched waxy maize starch with different crystallization temperature: A, 4°C; B, 25°C; C, 50°C .....	102
Figure 5.9 Particle size distributions of short-chain amylose prepared from debranched waxy potato starch: A, before annealing; B, after annealing.....	103
Figure 5.10 Thermal properties of short-chain amylose prepared from debranched waxy maize starch with different (A) solids concentration, and (B) crystallization temperatures, and (C) debranched waxy potato starch before and after annealing .....	104
Figure 5.11 <i>In vitro</i> digestion profile of short-chain amylose prepared from debranched waxy maize starch with different (A) solids concentration, and (B) crystallization temperatures, (C) debranched waxy potato starch before and after annealing, and (D) the method by Planchot et al (1997) .....	105
Figure 5.12 Arrangement of double helices in A- and B-type short-chain amylose (Dot represents double helix) .....	106
Figure 6.1 Molecular weight distribution of short-chain amylose spherulites produced by heating debranched waxy maize starch (25% w/w) to 180°C and crystallized at different temperatures .....	121
Figure 6.2 Microscopic images of short-chain amylose spherulites produced by heating debranched waxy maize starch (25% w/w) to 180°C and crystallized at different temperatures: A and B, 4°C; C and D, 25°C; E and F, 50°C. All scale bars represent 10 μm .....	122

Figure 6.3 Microscopic images of short-chain amylose produced by cooling debranched waxy maize starch (25% w/w) from A and B, 170°C; C and D, 190°C, and crystallized at 4°C. All scale bars represent 10 μm .....	123
Figure 6.4 Scanning electron microscopic images of short-chain amylose spherulites produced by heating debranched waxy maize starch (25% w/w) to 180°C and crystallized at different temperatures: A and B, 4°C; C and D, 25°C; E and F, 50°C.....	124
Figure 6.5 Wide-angle X-ray diffraction of short-chain amylose spherulites produced by heating debranched waxy maize starch (25% w/w) to 180°C and crystallized at different temperatures .....	125
Figure 6.6 Thermal properties of short-chain amylose spherulites produced by heating debranched waxy maize starch (25% w/w) to 180°C and crystallized at different temperatures as determined by differential scanning calorimetry .....	126
Figure 6.7 Synchrotron small-angle X-ray scattering of short-chain amylose spherulites produced by heating debranched waxy maize starch (25% w/w) to 180 °C and crystallized at different temperatures: (A) 4 °C, as it; (B) 4 °C, hydrated; (C) 25 °C, as it; (D) 25 °C, hydrated; (E) 50 °C, as it; and (F) 50 °C, hydrated.....	127
Figure 6.8 <i>In vitro</i> digestion profile of (A) short-chain amylose spherulites produced by heating debranched waxy maize starch (25% w/w) to 180 °C and crystallized at different temperatures; and (B) their digestive residues.....	128
Figure 6.9 Microscopic images of digestive residues from short-chain amylose spherulites produced by heating debranched waxy maize starch (25% w/w) to 180 °C and crystallized at different temperatures: A and B, 4 °C; C and D, 25 °C; E and F, 50 °C. All scale bars represent 10 μm.....	129
Figure 6.10 Scanning electron microscopic images of digestive residues from short-chain amylose spherulites produced by heating debranched waxy maize starch (25% w/w) to 180 °C and crystallized at different temperatures: A and B, 4 °C; C and D, 25 °C; E and F, 50 °C. ....	130
Figure 6.11 Schematic drawing of transition from starch granule to short-chain amylose spherulites. ....	131

## List of Tables

Table 2.1 Percentage of debranched starch at different debranching times <sup>A</sup> .....	28
Table 2.2 Thermal properties of native waxy maize starch and waxy maize starch debranched at different times as determined by differential scanning calorimetry <sup>A</sup> .....	29
Table 2.3 Average size of polymorph crystallites of native waxy maize starch and waxy maize starch debranched at different times as determined by wide-angle X-ray diffraction.....	30
Table 2.4 Levels of rapidly digestible starch (RDS), slowly digestible starch (SDS), and resistant starch (RS) content in native waxy maize starch, debranched waxy maize starch produced at different times at 50°C and isolated crystalline materials <sup>A</sup> .....	31
Table 3.1 Molecular weight distributions of debranched waxy wheat, waxy maize, waxy potato starches and their crystalline short-chain amylose (CSCA) products.....	50
Table 3.2 Yields and average chain lengths (CL) of debranched waxy wheat, waxy maize, waxy potato starches and their corresponding crystalline short-chain amylose (CSCA) products <sup>A, B</sup> .....	51
Table 3.3 Thermal properties of waxy wheat, waxy maize, waxy potato starches and debranched crystalline short-chain amylose (CSCA) products as determined by differential scanning calorimetry <sup>A, B</sup> .....	52
Table 3.4 Levels of rapidly digestible starch (RDS), slowly digestible starch (SDS), and resistant starch (RS) in waxy wheat, waxy maize, waxy potato starches and debranched crystalline short-chain amylose (CSCA) products <sup>A, B</sup> .....	53
Table 4.1 Relative crystallinity and approximate average size of polymorph crystallites of short-chain amylose from debranched waxy wheat starch, debranched waxy maize starch and debranched waxy potato starch as determined by synchrotron wide-angle X-ray diffraction <sup>A, B</sup> .....	70
Table 4.2 Melting and crystallization of short-chain amylose from debranched waxy wheat starch, debranched waxy maize starch and debranched waxy potato starch as determined by differential scanning calorimetry <sup>A, B</sup> .....	71

Table 4.3 Thermal properties of short-chain amylose from debranched waxy wheat starch, debranched waxy maize starch and debranched waxy potato starch as determined by differential scanning calorimetry <sup>A, B</sup> .....	72
Table 5.1 Yields and average particle size of crystalline short-chain amylose products prepared by different approaches .....	91
Table 5.2 Thermal properties of short-chain amylose prepared at different solids concentration of debranched waxy maize starch as determined by differential scanning calorimetry <sup>A</sup> .....	92
Table 5.3 Thermal properties of short-chain amylose prepared at different crystallization temperature of debranched waxy maize starch as determined by differential scanning calorimetry <sup>A</sup> .....	93
Table 5.4 Thermal properties of short-chain amylose prepared from debranched waxy potato starch before and after annealing <sup>A</sup> .....	94
Table 6.1 Yield of short-chain amylose spherulites produced by heating debranched waxy maize starch (25% w/w) to 180°C and crystallized at different temperatures <sup>A</sup> .....	119
Table 6.2 Thermal properties of short-chain amylose spherulites produced by heating debranched waxy maize starch (25% w/w) to 180°C and crystallized at different temperatures as determined by differential scanning calorimetry <sup>A</sup> .....	120



## **Acknowledgements**

First of all, I would like to express my appreciations to my major advisor Dr. Yong-Cheng Shi for his guide and supports for the past four years. His broad knowledge, kind encouragement, and endless patience help me grow a lot, not only in my academic career but also in my personal life. Anytime I have questions, his door is open and he is there to assist me. I am grateful to Dr. Paul Seib for his useful suggestions on my manuscripts and dissertation, Dr. Jeff Wilson and Dr. Christopher Sorensen for their valuable advices and kind technical supports on my project and Dr. Christopher Culbertson for his time and serving as my committee chair.

I would like to thank my labmates Dr. Yijun Sang, Dr. Lijia Zhu, Yanjie Bai, Rhett Kaufman, Lauren Brewer, Navneet Grewal, Radhiah Shukri, Shiva Garimella, Xinyi E, Anikka Ahmed, Emin Akarcay, Meng Xu, Dr. Zhigang Luo, Dr. Yan Hong, Dr. Dan Qiu, Dr. Xiangli Kong, Lan Guan, and Xiaoli Xu for their help and cheerful working attitudes that make it a pleasure for me to work in the lab.

I would like to extend my further thanks to the people in the Department of Grain Science and Industry. I have had a great experience by studying here. Special thanks go to Dr. Susan Sun and Dr. Sajid Alavi for allowing me to use the DSC instruments in their labs.

Last but not least, I would like to thank my parents, my brother Liguang Cai, and my friends Yonghui Li, Zhaofeng Li, Dr. Zhigang Xiao, Feng Xu, Dr. Xiaoming Pan, for their sharing of life experiences and kind supports.

## **Dedication**

This dissertation is dedicated to my parents.

## Chapter 1 - Introduction

Starch is one of the most abundant polymers in nature and consists of two types of  $\alpha$ -D-glucose polymers: amylose and amylopectin. Amylose is a mixture of lightly branched and linear molecules with a molecular weight of approximately  $1 \times 10^5$ - $1 \times 10^6$  g/mol, whereas amylopectin is a much larger molecule with a molecular weight of  $1 \times 10^7$ - $1 \times 10^9$  g/mol and a highly branched structure consisting of about 95%  $\alpha$ -1, 4- and 5%  $\alpha$ -1, 6- linkages (Hizukuri et al, 2006; Tester, et al, 2004a). The ratio of amylose to amylopectin in starch varies depending on botanical sources. Normal starches consist of 20-30% amylose and 70%-80% amylopectin. Waxy starch is comprised of essentially 100% amylopectin.

Native starches are biosynthesized as granules in higher plants. When the starch granules are viewed under polarized light, a characteristic Maltese cross with clear birefringence is observed (Buleon et al, 1998). Based on the X-ray diffraction patterns, native starch granules have been reported in A-, B-, C- and V-type forms (Zobel, 1988). A-type crystalline structure occurs in cereal starches, while B-type structure is found in tuber, root and amylose-rich starches. C-type polymorph is basically a mixture of A- and B- type polymorphs and occurs in some tuber and legume starches (Bogracheva et al., 1998). The V-type diffraction pattern could be observed from amylose-lipids or iodine, alcohols complexes (Biliaderis and Galloway, 1989).

Starch is the most important source of food energy and there is growing interest in understanding the relationships between digestion of starch and its impacts on human health (Lehmann and Robin, 2007; Zhang and Hamaker, 2009). The fundamental knowledge with respect to the relationship of starch structure and digestion is of particular interest to the food industry and has been reviewed in the literature (Tester et al, 2004b, 2006). It is known that native starches with an A-type X-ray pattern, such as corn starch, waxy corn starch, wheat starch or rice starch, are less resistant to alpha-amylase digestion than those starches with a B-type X-ray pattern such as high-amylose cereal starch or potato starch (Dreher et al 1984; Gallant et al, 1972; Gallant et al 1997; Jane et al, 1997; McCleary and Monaghan 2002; Planchot et al, 1995; Srichuwong et al, 2005a, b). However, the underlying reasons of different enzyme susceptibilities of starch polymorphs are not clearly understood and remained to be investigated.

## **Structure levels related to enzymatic hydrolysis**

The susceptibility of starch granules to enzymes and extent of enzymatic hydrolysis are controlled by many factors such as starch botanical origins, enzyme sources, enzyme and substrate concentration, hydrolysis temperature and time as well as the presence of other components (Tester et al, 2004b). Within starch granules, there are different structural levels (granular structure, supramolecular structure and molecular structure) that could impact on the rate and extent of enzyme digestion (Buleon et al, 1998).

### ***Granular structure***

Features of granular morphology such as shape, size and surface of starch granules could affect diffusion of enzyme molecules, adsorption of enzymes onto the solid substrates, and hydrolysis of substrates (Colonna et al, 1992). According to Fannone et al (1992), pores along with grooves were observed on the surfaces of many cereal starch granules. The pores may be the site of initial enzyme attack and allow the enzymes to penetrate into the granule interior. The surface area of starch granule is another critical factor in hydrolysis (Colonna et al, 1992). Large granules (i.e. potato starch) showed a small surface area to volume ratio, thus limiting access of enzymes and the hydrolysis of the granules (Tester et al, 2006). Noda et al (2005) studied the effects of granule size on the physicochemical properties and amylopectin structures of potato starches, and found that the hydrolysis rate of starch by glucoamylase increased as granule size decreased.

For different granular structure, enzymes may have different hydrolysis patterns (Bird et al, 2009; Evans and Thompson, 2004; Helbert et al, 1996; Planchot et al, 1995; Sarikaya et al, 2000; Zhang and Hamaker, 2009). The erosion profile of starch granules was normally obtained by analyzing the internal granule structure after digestion using scanning electron microscopy or transmission electron microscopy. Evans and Thompson (2004) observed that partially digested high-amylose maize starch showed a radial digestion pattern in the interior and an enzyme-resistant layer near the surface. Helbert et al (1996) studied the diffusion of *Bacillus licheniformis*  $\alpha$ -amylase into corn starch granules by analyzing the internal degradation of starch with a concomitant visualization of enzymes at the site of hydrolysis. They found that  $\alpha$ -amylase molecules first proceed from the surface of granules toward the center (centripetal hydrolysis) and act by progressing along the polysaccharide chains, then the core was completely degraded

by even erosion of its periphery (centrifugal hydrolysis) with a more diffusive motion of the enzymes. According to Planchot et al (1995), normal and waxy maize starch showed highly eroded layered structure after digestion by alpha-amylase, while potato and high-amylose maize starches produced much less endo-eroded granules with pronounced superficial porosity. Sarikaya et al (2000) examined the degradation abilities of  $\alpha$ -amylases on raw granules and observed that  $\alpha$ -amylases showed both centrifugal and centripetal hydrolysis on corn, rice and wheat starch granules, but only centrifugal hydrolysis on potato starch granules.

The interaction of starch molecules with the minor components attached in granules should be considered as well. In the case of cereal starch with high amylose content (i.e high-amylose maize starch), the presence of lipid and lipid-amylose complex could provide some resistance to enzyme hydrolysis (Tester et al, 2006). Lauro et al (2000) also reported that lipid-complexed amylose appeared to be more resistant to the  $\alpha$ -amylolysis than free amylose and amylopectin.

### *Supramolecular structure*

Native starch internal granules have been proposed to contain three different types of regions: amorphous growth rings, amorphous and crystalline lamella in a repeating stack (Donald et al, 2001a, b). The crystalline lamellae represent the side chain clusters of amylopectin whereas the amorphous lamellae contain branching regions of amylopectin and amylose (Donald et al, 2001a, b; Gallant et al, 1997). The supramolecular structure, such as arrangement of crystalline and amorphous regions in the granule, size of blocket that containing both amorphous and crystalline lamellae, could have impacts on the extent and rate of hydrolysis of starch granules.

Generally, a slow rate of hydrolysis or even some resistance to the enzymes is observed in the crystalline region. This is due to the double helices being present in crystalline area that could inhibit the access of enzyme to starch molecules (Jiang and Liu, 2002; Planchot et al., 1995; Tester et al, 2006). However, in the absence of amorphous lamellae structure, the extent of hydrolysis of lintnerized starch (acid resistant residues) increased. It is suggested the removal of the amorphous lamellae by acid could increase the accessibility of enzyme to the substrate (Srichuwong et al, 2005a). When heated in an aqueous environment, starch undergoes a process known as “gelatinization,” which is manifested by irreversible changes in properties such as

granular swelling, crystallite melting, loss of birefringence. The gelatinized starch is then totally amorphous and becomes digestible by enzymes (Colonna et al, 1992; Tester et al, 2006).

Spherical blocklets organized from amylopectin lamella have effects in the hydrolysis of starch granules as well (Gallant et al, 1997). The enzyme resistance of potato and high amylose starch may be linked to their large blocklet size. Those starch granules appear to have a thick peripheral layer of large stacked blocklets comprising of the crystalline and amorphous lamellae of the amylopectin that are organized into larger, more or less spherical structures (Gallant et al, 1997). However, as pointed out by Gallant et al (1997), wrinkled pea starch has a smaller blocklet size than smooth pea but is more resistant to enzyme digestion (Gallant et al 1992), indicating that other factors besides blocklet size determine resistance to  $\alpha$ -amylase.

### ***Molecular structure***

On the molecular level, the fine structure of amylose and amylopectin, crystal perfection and interrelations as well as crystalline types also play an important role in the hydrolysis of native starch granules.

Starches with B-type crystallinity are more resistant to enzyme hydrolysis than starches with A-type crystallinity (Dreher et al 1984; Gallant et al, 1972; Gallant et al 1997; Jane et al, 1997; McCleary and Monaghan 2002; Planchot et al, 1995; Srichuwong et al, 2005a, b) and are believed to be related to the fine structure of amylopectin and amylose (Jane et al, 1997; Jiang and Liu, 2004; Srichuwong et al, 2005b; Zhang and Oates, 1999). According to Jane et al (1997), A-type starch had more short A-chains (Degree of polymerization, DP 6-12) than B-type starch. The short double helices derived from those chains, and the branch linkages present in the crystalline region were more susceptible to enzymatic hydrolysis and resulted in pinholes and pits to the A-type starches. Jiang and Liu (2004) characterized the residues from partially hydrolyzed potato and high amylose corn starches by pancreatic  $\alpha$ -amylase and found that the relative portion of short chains (DP <16) in the residues decreased for both starches. It was suggested that the short chains in native starches were more susceptible to enzyme hydrolysis and preferred to be digested first. According to Srichuwong et al (2005b), digestion of starch granules was positively and negatively correlated with the proportions of amylopectin unit-chains with DP 8-12 and DP 16-26. Crystalline regions packed by high proportion of longer chains were more stable and more resistant to enzymatic hydrolysis than that of shorter chains.

## **A- and B-type starch crystals**

Native starch granules contain A- type, B-type or mixed (C-type) crystallites (Zobel, 1988). The main differences between these crystallites are the packing way of double helices and the amount of water molecules in the crystal unit cell (Imberty et al, 1988; Imberty and Perez, 1988; Popov et al, 2009; Takahashi et al, 2004). A-type structure is more dense and characterized as a monoclinic unit cell ( $a=2.12$  nm,  $b=1.17$  nm,  $c=1.07$  nm and  $\gamma=123.5^\circ$ ) with 8 water molecules per unit cell. B-type polymorph displays a more open hexagonal unit cell ( $a=b=1.85$  nm,  $c=1.04$  m and  $\gamma=120.0^\circ$ ) with 36 water molecules per unit cell.

The crystallinity of native starches is approximately 15 to 40% as measured by wide-angle X-ray diffraction (Gidley and Bociek, 1985; Zobel 1988). In order to prepare starch crystals with high crystallinity, short linear chains (or short chain amylose, SCA) were first prepared, followed by recrystallization of those chains into highly crystalline materials. (Buleon et al, 2007; Cai et al, 2010; Cai and Shi, 2010; Gidley and Bulpin, 1987; Helbert, 1993; Lebail et al, 1993; Pfannemuller, 1987; Planchot et al, 1997; Ring et al, 1987; Whittam et al, 1990; Williamson et al, 1992).

### ***Preparation and crystallization of SCA***

SCA is a short linear segment of  $\alpha$ -1, 4-glucan and can be prepared by mild acid hydrolysis, *in vitro* synthesis, and by enzyme debranching. Mild acid hydrolysis, called “lintnerization”, removes the amorphous region and isolates the crystalline fraction of native starch granules. For example, extensive hydrolysis of native potato starch in 2.2N HCl at 35°C extracts amylose chains of average DP equal to 15 (Robin et al, 1974). The  $\alpha$ -glucan chains can also be synthesized *in vitro* by phosphorylase (Gidley and Bulpin, 1989; Pfannemuller, 1987) or amylosucrase (Potocki-Veronese et al, 2005).

Enzyme debranching of glycogen, maltodextrin and starch is another way to release SCA (Cai et al, 2010; Cai and Shi, 2010; Gidley and Bulpin, 1987; Pohn et al, 2004). According to Gidley and Bulpin (1987), enzymatically debranched glycogen produced linear chains with average DP=11. Pohn et al (2004) reported that split crystallization of A- and B-type starch crystals occurred during debranching of high concentrations of maltodextrins by isoamylase. Recently, the structure and digestibility of crystalline SCA from debranched waxy wheat, waxy maize, and waxy potato starches were investigated and compared (Cai and Shi, 2010).

The branching points in starch, or  $\alpha$ -1, 6-linkages, can be cleaved by debranching enzymes such as isoamylase and pullulanase (Hizukuri et al, 2006; Manners, 1989). For an amylose-containing starch, debranching enzymes cleave the branch points in both amylose and amylopectin and produce a mixture of long and short linear  $\alpha$ -1, 4-glucan chains; for a waxy starch, debranching releases short linear side chains from amylopectin (Shi et al, 1998). The type of enzyme used in the debranching process has a different reaction pattern. Isoamylase and pullulanase, the two commonly used debranching enzymes, do not act the same on starch (Hizukuri et al, 2006; Manners and Matheson, 1981; Yokobaya et al, 1973). Compared with pullulanase, isoamylase has superior activity for debranching amylopectin (Hizukuri et al, 2006). Pullulanase hydrolyzes amylopectin slowly by exo-wise action, whereas isoamylase hydrolyzes both inner and outer branching linkages (Manners and Matheson, 1981; Yokobaya et al, 1973).

Depending on crystallization conditions such as solvent, chain length, concentration and temperature, SCA can organize into different crystalline types. Generally, a shorter chain length and a higher concentration of SCA and a higher crystallization temperature favor the formation of A- type crystallites, while the reverse conditions induce B- type crystallization (Buleon et al, 2007; Cai et al, 2010; Cai and Shi, 2010; Gidley and Bulpin, 1987; Helbert, 1993; Lebail et al, 1993; Pfannemuller, 1987; Planchot et al, 1997; Ring et al, 1987; Whittam et al, 1990; Williamson et al, 1992). The exact conditions to produce pure A- or B- crystalline products were different depending on the starting material used. For short chains prepared by extensive acid hydrolysis of native starches, the B-type crystalline structure was obtained by cooling the aqueous solution directly at a slow cooling rate, whereas the A-type polymorph could only be obtained by addition of water-ethanol mixture during cooling ( Helbert, 1993; Planchot et al, 1997; Ring et al, 1987; Whittam et al, 1990; Williamson et al, 1992). Pohn et al (2004) studied debranching of maltodextrins at 25% solids concentration by isoamylase. They found that the B-type network was produced during the first 12 h of debranching, followed by formation of the A-type lamellar crystals in the later reaction. Similar results were observed during debranching of a 25% solids concentration of waxy maize starch (Cai et al, 2010). Pfannemuller (1987) investigated the effects of chain length on the crystallization of pure short monodisperse amylose from aqueous solution. She reported that malto-oligomers of DP10-12 gave crystalline materials with the A-type X-ray diffraction pattern, chains of DP13 and above gave crystals with the B-type pattern, whereas chains with DP shorter than 10 did not crystallize. According to Gidely and



Bulpin (1987), the A-type crystals could be produced from debranched glycogen at 50% concentration by crystallization at 30°C, and the B-type structure could be obtained by crystallization at 30% or 40% aqueous solution at 15 °C.

### ***Characterization and digestibility of A- and B-type crystals***

The dissolution temperature of recrystallized SCA with the A-type structure has always been reported to be higher than that of its B-type counterpart (Cai et al, 2010; Cai and Shi, 2010; Planchot et al, 1997; Whittam et al, 1990; Williamson et al, 1992). However, the results of digestibility of the A- and B- type structures have yielded different results (Cai et al, 2010; Cai and Shi, 2010; Planchot et al, 1997; Williamson et al, 1992). Planchot et al (1997) prepared A- and B-type starch crystals from SCA obtained by extensive hydrolysis of native starches, and found that the A-type structure was more susceptible to  $\alpha$ -amylase hydrolysis than the B-type structure. Williamson et al (1992) prepared A- and B-type spherulite crystals from lintnerized potato starch, and observed that the B-type spherulites were more resistant to  $\alpha$ -amylase,  $\beta$ -amylase and glucoamylase-1 than the A-type spherulites. It is worth noting that the A- and B-spherulites prepared by Williamson et al (1992) and Planchot et al (1997) contained branch points. The B-type spherulites were crystallized in water whereas the A-type spherulites were produced in a water-ethanol mixture. According to Cai et al (2010), the A-type crystals formed from 25% solids SCA aqueous solution at 50 °C displayed higher resistant starch content than the B-type crystals prepared at 5% solids and 25 °C (Cai and Shi, 2010). The SCA used in those studies (Cai et al, 2010; Cai and Shi, 2010) was generated from debranched waxy starches and was confirmed to be linear. Therefore, the relationship between starch polymorphs and enzyme susceptibility is still not fully understood and requires further study.

### **Objectives**

It is known that B-type native starches are more resistant to digestion by alpha-amylase in the small intestine compared to A-type starch granules. But it is not clear whether the enzyme resistance of B-type starches is due to its B-type crystalline structure or the other structural features of starch granules. It is believed that the side chains of amylopectin are primarily responsible for the crystallinity of starch (Robin et al, 1974). In this study, waxy starches, which consist of ~ 100% amylopectin, were used as starting materials. The side chains of amylopectin

were released during debranching by isoamylase followed by assembling into the A- and B-type structures. Those A- and B-type starch crystals have the similar chain length distribution and highly pure crystallinity as native starches, thus represent the crystalline region of native starch granules and are good models to compare the digestibility of native starch granules. Our goals are to understand the structure and morphology of polymorphic crystalline solids obtained from debranched waxy starch, and to relate the crystalline polymorphs with their functional and nutritional properties.

Our research interest has focused on investigating starch molecular architecture during crystallization, structural formation of different types of crystals, and providing new insights into how these crystalline starches are digested by  $\alpha$ -amylases and glucoamylase. Specifically we want to establish how crystallization conditions influence the structure and morphology of starch crystals and then their susceptibility to digestion. This work could help understanding the molecular origins of resistant starch, and would be useful in designing better starch-based food ingredients with health benefits.

The specific objectives of this work were to (a) investigate the debranching and crystallization of waxy maize, waxy wheat, and waxy potato starches, (b) produce highly pure A- and B-type starch crystals with different morphologies, (c) examine the digestibility of starches with different crystalline structures and morphologies, and (d) establish the relationship between starch polymorphs and digestibility. Using combined advanced analytical techniques, we could study the crystallization of starch molecules in real time, characterize the resulting materials, and gain a thorough understanding of how starch molecules are assembled into different types of crystals and their impacts on the enzyme digestibility.

## References

- Biliaderis, C. G., & Galloway, G. (1989). Crystallization behavior of amylose-V complexes-structure property relationships. *Carbohydrate Research*, 189, 31-48.
- Bird, A. R., Lopez-Rubio, A., Shrestha, A. K., & Gidley, M. J. (2009). Resistant starch in Vitro and in Vivo: factors determining yield, structure, and physiological relevance. In Kasapis, S., Norton, I. T., & Ubbink, J. B. (Ed.). *Modern Biopolymer Science* (pp.449-510). Elsevier Inc.
- Bogracheva, T. Y., Morris, V. J., Ring, S. G., & Hedley, C. L. (1998). The granular structure of C-type pea starch and its role in gelatinization. *Biopolymers*, 45, 323-332.
- Buleon, A., Colonna, P., Planchot, V., & Ball, S. (1998). Starch granules : structure and biosynthesis. *International Journal of Biological Macromolecules*, 23, 85-112.
- Buleon, A., Veronese, G., & Putaux, J. L. (2007). Self-association and crystallization of amylose. *Australian Journal of Chemistry*, 60, 706-718.
- Cai, L., & Shi, Y-C. (2010). Structure and digestibility of crystalline short-chain amylose from debranched waxy wheat, waxy maize and waxy potato starches. *Carbohydrate Polymers*, 79, 1117-1123.
- Cai, L., Shi, Y-C., Rong, L., & Hsiao, B.S. (2010). Debranching and crystallization of waxy maize starch in relation to enzyme digestibility. *Carbohydrate Polymers*, 81, 385-393.
- Colonna, P., Leloup, V., & Buleon, A. (1992). Limiting factors of starch hydrolysis. *European Journal of Clinical Nutrition*. 46, Supply.2, S17-S32.
- Dreher, M. L., Dreher, C. J., & Berry, J. W. (1984). Starch digestibility of foods- A nutritional perspective. *Critical Reviews in Food Science and Nutrition*, 20, 47-71.
- Donald, A. M., Kato, K. L., Perry, P. A., & Waigh, T. A. (2001a). Scattering studies of the internal structure of starch granules. *Starch/Stärke*, 53, 504-512.
- Donald, A. M., Perry, P. A., & Waigh, T. A. (2001b). The impact of internal granule structure on processing and properties. In T.L. Barsby, A. M. Donald, & P. J. Frazier. (Ed.). *Starch: Advances in structure and functionality* (pp. 45-52). Cambridge, UK: The Royal Society of Chemistry.
- Evans, A., & Thompson, D. B. (2004). Resistance to alpha-amylase digestion in four native high-amylose maize starches. *Cereal Chemistry*, 81, 31-37.
- Fannon, E. J., Hauber, J. R., & BeMiller, N. J. (1992). Surface pores of starch granules. *Cereal Chemistry*, 69, 284-288.
- Gallant, D. J., Bouchet, B., & Baldwin, P. M. (1997). Microscopy of starch: Evidence of a new level of granule organization. *Carbohydrate Polymers*, 32, 177-191.
- Gallant, D.J., Bouchet, B., Buleon, A., & Perez, S. (1992). Physical characteristics of starch granules and susceptibility to enzymatic degradation. *European Journal of Clinical Nutrition*, 46, Suppl.2, S3-S16.
- Gallant, D., Guilbot, A., & Mercier, C. (1972). Electro-microscopy of starch granules modified by bacterial alpha-amylase. *Cereal Chemistry*, 49, 354-358.
- Gidley, M. J., & Bociek, S. M. (1985). Molecular-organization in starches-A C-13 CP MAS NMR- study. *Journal of the American Chemical Society*, 107, 7040-7044.
- Gidley, M. J., & Bulpin, P. V. (1987). Crystallization of malto-oligosaccharides as models of the crystalline forms of starch: minimum chain-length requirement for the formation of double helices. *Carbohydrate Research*, 161, 291-300.

- Gidley, M. J., & Bulpin, P. V. (1989). Aggregation of amylose in aqueous systems- the effect of chain-length on phase-behavior and aggregation kinetics. *Macromolecules*, 22, 341-346.
- Jane, J-L., Wong, K-S., & McPherson, E. A. (1997). Branch-structure difference in starches of A- and B-type X-ray patterns revealed by their Naegeli dextrans. *Carbohydrate Research*, 300, 219-227.
- Jiang, G., & Liu, Q. (2002). Characterization of residues from partially hydrolyzed potato and high amylose corn starches by pancreatic  $\alpha$ -amylase. *Starch/stärke*, 54, 527-533.
- Helbert, W., Chanzy, H., Planchot, V., Buleon, A., & Colonna, P. (1993). Morphological and structural features of amylose spherocrystals of A-type. *International Journal of Biological Macromolecules*, 15, 183-187.
- Helbert, W., Schulein, M., & Henrissat, B. (1996). Electron microscopic investigation of the diffusion of *Bacillus licheniformis*  $\alpha$ -amylase into corn starch granules. *International Journal of Biological Macromolecules*, 19, 165-169.
- Hizukuri, S., Abe, J., & Hanashiro, I. (2006). Starch: Analytical aspects. In A-C. Eliasson (Ed.). *Carbohydrates in food* (2nd ed., pp. 305-391). Boca Raton, FL: Taylor & Francis Group.
- Imberty, A., Chanzy, H., Perez, S., Buleon, A., & Tran, V. (1988). The double-helical nature of the crystalline part of A-starch. *Journal of Molecular Biology*, 201, 365-378.
- Imberty, A., & Perez, S. (1988). A revisit to the 3-dimensional structure of B-type starch. *Biopolymers*, 27, 1205-1221.
- Lauro, M., Poutanen, K., & Forssell, P. (2000). Effect of partial gelatinization and lipid addition on  $\alpha$ -amylolysis of barley starch granules. *Cereal Chemistry*, 77, 595-601.
- Lebail, P., Bizot, H., & Buleon, A. (1993). B-type to A-type phase-transition in short amylose chains. *Carbohydrate Polymers*, 21, 99-104.
- Lehmann, U.; & Robin, F. (2007). Slowly digestible starch-its structure and health implications: a review. *Trends in Food Science & Technology*, 18, 346-355.
- Manners, D. J. (1989). Recent developments in our understanding of amylopectin structure. *Carbohydrate Polymer*, 11, 87-112.
- Manners, D. J., & Matheson, N. K. (1981). The fine-structure of amylopectin. *Carbohydrate Research*, 90, 99-110.
- McCleary, B. V., & Monaghan, D. A. (2002). Measurement of resistant starch. *Journal of AOAC International*, 665-675.
- Noda, T., Takigawa, S., Matsuura-Endo, C., Kim, S-J., Hashimoto, N., Yamauchi, H., Hanashiro, I., & Takeda, Y. (2005). Physicochemical properties and amylopectin structures of large, small and extremely small potato starch granules. *Carbohydrate Polymers*, 60, 245-251.
- Pfannemuller, B. (1987). Influence of chain length of short monodisperse amyloses on the formation of A- and B-type X-ray diffraction patterns. *International Journal of Biological Macromolecules*, 9, 105-108.
- Planchot, V., Cononna, P., & Buleon, A. (1997). Enzymatic hydrolysis of  $\alpha$ -glucan crystallites. *Carbohydrate Research*, 298, 319-326.
- Planchot, V., Colonna, P., Gallant, D. J., & Bouchet, B. (1995). Extensive degradation of native starch granules by alpha-amylase from *Aspergillus fumigatus*. *Journal of Cereal Science*, 21, 163-171.
- Pohu, A., Planchot, V., Putaux, J. L., Colonna, P., & Buleon, A. (2004). Split crystallization during debranching of maltodextrins at high concentration by isoamylase. *Biomacromolecules*, 5, 1792-1798.

- Popov, D., Buleon, A., Burghammer, M., Chanzy, H., Montesanti, N., Putaux, J.-L., Potocki-Veronese, G., & Riekkel, C. (2009). Crystal structure of A-amylose: A revisit from synchrotron microdiffraction analysis of single crystals. *Macromolecules*, 42, 1167-1174.
- Potocki-Veronese, G., Putaux, J. L., Dupeyre, D., Albne, C., Remaud-Simeon, M., Monsan, P., & Buleon, A. (2005). Amylose synthesized in vitro by amylosucrase: Morphology, structure and properties. *Biomacromolecules*, 6, 1000-1011.
- Ring, S. G., Miles, M. J., Morris, V. J., Turner, R., & Colonna, P. (1987). Spherulitic crystallization of short chain amylose. *International Journal of Biological Macromolecules*, 9, 158-160.
- Robin, J. P., Mercier, C., Charbonn, R., & Guilbot, A. (1974). Lintnerized starches gel-filtration and enzymatic studies of insoluble residues from prolonged acid treatment of potato starch. *Cereal Chemistry*, 51, 389-406.
- Sarikaya, E., Higasa, T., Adachi, M., & Mikami, B. (2000). Comparison of degradation abilities of  $\alpha$ - and  $\beta$ - amylases on raw starch granules. *Process Biochemistry*, 35, 711-715.
- Shi, Y.-C., Capitani, T., Trzasko, P., & Jeffcoat, R. (1998). Molecular structure of a low-amylopectin starch and other high-amylose maize starches. *Journal of Cereal Science*, 27, 289-299.
- Srichuwong, S., Isono, N., Mishima, T., & Hisamatsu, M. (2005a). Structure of lintnerized starch is related to X-ray diffraction pattern and susceptibility to acid and enzyme hydrolysis of starch granules. *International Journal of Biological Macromolecules*, 37, 115-121.
- Srichuwong, S., Sunnarti, C. T., Mishima, T., Isono, N., & Hisamatsu, M. (2005b). Starches from different botanical sources I: Contribution of amylopectin fine structure to thermal properties and enzyme digestibility. *Carbohydrate Polymers*, 60, 529-538.
- Whittam, M. A., Noel, T. R., & Ring, S. G. (1990). Melting behavior of A-type and B-type crystalline starch. *International Journal of Biological Macromolecules*, 12, 359-362.
- Williamson, G., Belshaw, N. J., Self, D. J., Noel, T. R., Ring, S. G., Cairns, P., Morris, V. J., Clark, S. A., & Parker, M. L. (1992). Hydrolysis of A-type and B-type crystalline polymorphs of starch by Alpha-amylase, Beta-amylase and Glucoamylase-1. *Carbohydrate Polymers*, 18, 179-187.
- Takahashi, Y., Kumano, T., & Nishikawa, S. (2004). Crystal structure of B-amylose. *Macromolecules*, 37, 6827-6832.
- Tester, F. R.; Karkalas, J.; & Qi, X. (2004a). Starch-composition, fine structure and architecture. *Journal of Cereal Science*, 39, 151-165.
- Tester, F. R.; Karkalas, J.; & Qi, X. (2004b). Starch structure and digestibility enzyme-substrate relationship. *Worlds Poultry Science Journal*, 60,186-195.
- Tester, F. R.; Qi, X.; & Karkalas, J. (2006). Hydrolysis of native starches with amylases. *Animal Feed Science and Technology*, 130, 39-54.
- Yokobaya, K., Akai, H., Sugimoto, T., Hirao, M., Sugimotok, K., & Harada, T. (1973). Comparison of kinetic parameters of *Pseudomonas* isoamylase and *Aerobacter* pullulanase. *Biochimica et Biophysica Acta*, 293, 197-202.
- Zhang, G. Y., & Hamaker, B. R. (2009). Slowly digestible starch: concept, mechanism, and proposed extended glycemic index. *Critical Reviews in Food Science and Nutrioin*, 49, 852-867.
- Zhang, T., & Oates, C.G. (1999). Relationship between  $\alpha$ -amylase degradation and physico-chemical properties of sweet potato starches. *Food Chemistry*, 65, 157-163.

Zobel, H.F. (1988). Starch crystal transformations and their industrial importance. *Starch/ Stärke*, 40, 1-7.

## **Chapter 2 - Debranching and crystallization of waxy maize starch in relation to enzyme digestibility\***

### **Abstract**

Molecular and crystal structures as well as morphology during debranching and crystallization of waxy maize starch at a high solid content (25%, w/w) were investigated, and the results were related to the digestibility of debranched products. The starch was cooked at 115-120°C for 10 min, cooled to 50°C and debranched by isoamylase. After 1 h of debranching, wormlike objects with 5-10 nm width and ca. 30 nm length were observed by transmission electron microscopy. Further release of linear chains and crystallization led to assembly of semi-crystalline structures in the form of nano-particles and subsequent growth of nano-particles into large aggregates. After 24 h at 50°C, a debranched starch product with an A-type X-ray diffraction pattern, a high melting temperature (90°C to 140°C), and high resistant starch content (71.4%) was obtained. Small-angle X-ray scattering results indicated that all debranched products were surface fractal in a dry state (4% moisture) but had a mass fractal structure when hydrated (e.g., 45% moisture).

### **Introduction**

Starch debranching techniques have been extensively documented in patents and literature (Berry, 1986; Chiu et al., 1994; Chiu and Henley 1993; Chiu and Kasica 1995; Chiu and Mason 1998; Gonzalez-Soto et al, 2004, 2007; Guraya et al, 2001a, 2001b; Hizukuri et al, 2006; Kettlitz et al., 2000; Lehmann et al, 2002; Leong et al, 2007; Manners and Matheson, 1981; Onyango and Mutungi, 2008; Shin et al, 2004; Yokobaya et al, 1973). However, the debranching kinetics and structure changes during debranching have not been well studied. In this study, we investigated structural changes during debranching and crystallization of waxy maize starch at high concentration (25% solids). The specific objectives of this work were to (1) investigate the

---

\*Chapter 2 is published as a part of Cai, L. et al. (2010). *Carbohydrate Polymers*, 81, 385-393.

debranching and crystallization mechanism of waxy maize starch and (2) determine morphology, structure, and physicochemical properties of debranched products and impact on digestibility.

## **Materials and methods**

### ***Materials***

Waxy maize starch was obtained from National Starch LLC (Bridgewater, NJ, USA), and isoamylase (EC 3.2.1.68) from Hayashibara Biochemical Laboratories, Inc. (Okayama, Japan). The enzyme activity was  $1.41 \times 10^6$  IAU/g, and 1 IAU was defined as the amount of isoamylase that increased reducing-power absorbance of the reaction mixture by 0.008 in 30 min under the conditions of the isoamylase assay (FAO JECFA Monographs, 2007). All chemicals were reagent-grade.

### ***Debranching of starch***

Waxy maize starch (150 g, dry basis) was mixed with water to give a 25 wt% solids content. The slurry was adjusted to pH 4.0 by adding 0.5N HCl, cooked at 115-120°C in a Parr reactor with mixing (Parr Instrument, Moline, IL, USA) for 10 min, and cooled to 50°C. The debranching reaction was started by adding 0.5 wt% isoamylase based on the dry weight of starch. The mixture was kept at 50°C with stirring. At 1, 2, 4, 8, 16, and 24 h intervals after adding enzyme, sample slurries (about 40 mL) were taken, immediately frozen in a dry ice acetone bath, freeze-dried, and saved for analysis. The precipitates after 24 h of crystallization were filtered, washed with water, and dried in an oven at 40°C overnight. In separate experiments, after the starch was debranched and crystallized at 50°C for 24 h, the digestion mixture was cooled to 25°C and held for another 24 h to further increase the yield of crystallized product.

To determine the yield of crystallized product, an aliquot (1.0 mL) of starch slurry was taken and centrifuged ( $\times 13,226$  g) for 10 min. The carbohydrate concentration in the supernatant was determined with a portable refractometer (Fisher Scientific Inc., Pittsburgh, PA, USA). The blank reading was determined by the same procedure on uncooked starch slurry mixed with isoamylase. The level of precipitation of carbohydrate was calculated by reading difference. Each measurement was done in duplicate.



### ***Gel permeation chromatography (GPC)***

Each starch sample (4 mg) was mixed with dimethyl sulfoxide (DMSO) (4 mL) and stirred in a boiling water bath for 24 h. The sample was filtered through a 2  $\mu\text{m}$  filter and then injected by an autosampler into a PL-GPC 220 system (Polymer Laboratories Inc., Amherst, MA, USA) with three Phenogel columns (00H-0642-K0; 00H-0644-K0; 00H-0646-K0; Phenomenex Inc., Torrance, CA, USA), one guard column (03B-0290-K0, Phenomenex Inc., Torrance, CA, USA), and a differential refractive index detector. The eluenting solvent was 5 mM  $\text{NaNO}_3$  in DMSO, and the flow rate was 0.8 mL/min. The column oven temperature was controlled at 80°C. Standard dextrans (American Polymer Standards Co., Mentor, OH, USA) with different molecular weight (MW) were used for MW calibration.

### ***Scanning electron microscopy***

The isolated crystalline samples were coated with gold-palladium by using a sputter coater (Denton Vacuum, LLC., Moorestown, NJ) and viewed at 1000X magnification with a scanning electron microscope (S-3500N, Hitachi Science Systems, Ltd., Japan) operating at an accelerating voltage of 20 kV.

### ***Transmission Electron Microscopy (TEM)***

A drop of starch suspension was deposited on a 200 mesh copper Formvar/carbon-coated support film grid. Excessive liquid was wiped with filter paper. A drop of 2% uranyl acetate negative stain was added, and the suspension film was left to dry. The samples were observed and images were recorded with a Philips CM100 transmission electron microscope (FEI Company, Hillsboro, Oregon, USA) with 64,000 $\times$  magnification.

### ***Differential scanning calorimetry (DSC)***

A 25 wt% starch suspension in water was prepared and sealed in a DSC pan and analyzed with a TA Q5000 instrument (TA Instruments, New Castle, DE, USA). An empty pan was used as a reference. Samples were heated from 10°C to 160°C at 10°C/min. The onset ( $T_o$ ), peak ( $T_p$ ), and conclusion ( $T_c$ ) temperatures and enthalpy ( $\Delta H$ ) were calculated from the DSC endotherm (TA Instruments, New Castle, DE, USA). Experiments were conducted in duplicate.

### ***Synchrotron X-ray scattering and diffraction measurements***

Wide-angle X-ray diffraction (WAXD) and small-angle X-ray scattering (SAXS) experiments were carried out at the Advanced Polymers Beamline (X27C) in the National Synchrotron Light Source, Brookhaven National Laboratory, in Upton, NY. The details of the experimental setup at the X27C beamline have been reported elsewhere (Chen et al, 2006; Chen et al, 2007; Chu and Hsiao, 2001). The wavelength used was 0.1371 nm. The sample-to-detector distance was 155.6 mm for WAXD and 2018.5 mm for SAXS, respectively. A 2D MAR-CCD (MAR USA, Inc.) X-ray detector was used for data collection. In addition to native waxy maize starch (ca. 11% moisture) and freeze-dried debranched products (ca. 4% moisture), samples were mixed (hydrated) with water to form starch pastes (45% moisture) and examined by the WAXD and SAXS.

### ***In vitro digestion method***

The *in vitro* starch digestion profile was determined by a modified Englyst procedure (Englyst et al, 1992; Sang and Seib, 2006). Samples (~0.6 g) were mixed with guar gum (50 mg) and pepsin (50 mg) in 0.05 M hydrochloric acid (10 mL). Then, sodium acetate solution (0.25 M, 10 mL) and 30 glass beads (~8.4 g) were added. Guar gum (50 mg) in 0.1 M sodium acetate buffer (pH 5.2, 20 mL) and glucose standard solution (20 mL) were used as the blank and standard, respectively. After the enzyme (pancreatin and amyloglucosidase) solution (5 mL) was added, the mixture was shaken in a water bath (Models 25 and 50, Precision, Winchester, VA) at 37°C and 90 strokes/min. The enzyme activity of pancreatin from Sigma was  $12.9 \times 10^3$  Ceralpha Units/g of solid, and the Ceralpha Unit was defined as the amount of  $\alpha$ -amylase that releases 1  $\mu$ mol/min of *p*-nitrophenol at pH 5.4 and 40 °C from the non-reducing end-blocked *p*-nitrophenyl  $\alpha$ -glycoside of maltoheptose in the presence of excess glucoamylase and  $\alpha$ -glucosidase. The enzyme activity of amyloglucosidase from Sigma was 5000 Units/g of solid, and one unit was defined as liberating 1.0 mg of glucose from soluble starch in 3 min (1.85  $\mu$ mol/min) at pH 4.5 at 55 °C. The levels of  $\alpha$ -amylase and amyloglucosidase used in modified Englyst method were about  $14.5 \times 10^3$  Ceralpha Units/g starch and 150 Units/g starch, respectively.

At 20 and 120 min intervals, a 250  $\mu$ L aliquot of the mixture was taken and added into 66.6% ethanol solution (10 mL). After centrifugation, 100  $\mu$ L of supernatant was taken, and

glucose content was determined by a D-glucose assay procedure with a Megazyme glucose assay kit (Megazyme International Ireland Ltd, Wicklow, Ireland). Percentages of rapidly digestible starch (RDS), slowly digestible starch (SDS), and resistant (RS) were calculated by (% digestible starch at 20 min), (% digestible starch at 120 min - % digestible starch at 20 min) and (100% - % digestible starch at 120 min), respectively.

### ***Isolation of resistant starch***

At 120 min into the *in vitro* digestion method, the entire digest of ~ 25 mL was mixed with ethanol (100 mL). The sediment was collected by filtration and washed three times with distilled water. The residue was dried under room conditions and was called isolated resistant starch.

## **Results**

### ***Degree of debranching and Molecular weight distribution***

The molecular weight distribution of waxy maize starch at different debranching times is shown in **Figure 2.1**. For samples debranched at 1, 2, 4 and 8 h, three peaks were observed. Peaks 1 and 2 represent the unit chains released by debranching whereas Peak 3, ranged from about  $1.3 \times 10^4$  g/mol (Degree of polymerization, DP 80) to  $1 \times 10^6$  g/mol (DP 6,000), corresponds to branched molecules. Dividing the sum of areas of Peaks 1 and 2 by the total area of the 3 peaks gave the percentage of debranched starch at different debranching times (**Table 2.1**). From 1 to 24 h, Peaks 1 and 2, predominantly short linear chains (DP about 6-80), increased while Peak 3 decreased and disappeared at 16 h. Those short linear chains had similar molecular characteristics to amylose and were mainly linked by  $\alpha$ -1,4 linkage. Debranching of the starch started very rapidly after the isoamylase was added. Two-thirds of the debranching was achieved during the first hour. No changes were detected in the molecular weight distribution curve between 16 h and 24 h samples, indicating that the waxy maize starch was totally debranched within 16 h (**Table 2.1**).

### ***Crystallization and precipitation***

Crystallization occurred at the same time as the release of short-chain amylose (SCA, DP about 6-80) from amylopectin during debranching. The percentages of starch precipitate as a

function of debranching time are shown in **Figure 2.2A**. The amount of starch precipitate was initially low at 0-4 h, but increased significantly at 4-24 h. The precipitate accounted for about two-thirds of the weight of the initial starch after 24 h. If the temperature of the digestion mixture was cooled from 50°C to 25°C and held for another 24 h, the yield of precipitate increased to more than 90% (**Figure 2.2A**). The remarkable changes from the starch polymer solution at the beginning of debranching to the cloudy slurry after 24 h of crystallization at 50°C are depicted in **Figure 2.2B**. The aggregation and growth of crystallized SCA produced particles (**Figure 2.2C**) that could be recovered by filtration with a high yield.

The effects of incubation time on starch yield can be explained by the conformational changes of linear SCA during crystallization. On the molecular level, amylose chains in the aqueous solution are known to behave as random coils (Ring et al, 1985), along with some single helical structure, which could associate together and form double helices. The further association of double helices results in crystallites and aggregates of crystals. Therefore, coil-helix structure and formation of double helices from short linear chains appeared to predominate in the first 4 h, whereas crystallization and aggregation took place in the following stage.

### ***Morphology***

The morphology of waxy maize starch at different debranching times was analyzed by TEM. **Figure 2.3A** shows the morphology of waxy maize starch debranched at the first hour. The sample appeared to consist of wormlike objects with 5-10 nm width and 30-80 nm length. Aggregates (50-100 nm diameter) composed of semi-crystalline units were detected in the following hour (**Figure 2.3B**). After 4 h of debranching, particles with 5-30 nm diameter were evident, and double helices were probably aggregated (**Figure 2.3C**). Larger particles or a long-piece appearance of aggregates were observed after 8 h (**Figure 2.3D-F**). Therefore, the morphology of the SCA during crystallization had three steps: (1) association of starch chains into double helices and forming clustering, wormlike structure, (2) rearrangement of semi-crystalline units into nano-particles, and (3) growth of particles into large aggregates.

### ***Thermal properties***

The thermal properties of native waxy maize starch and the freeze-dried digests of waxy maize starch at different debranching times are shown in **Figure 2.4** and **Table 2.2**. Native starch was characterized by a sharp endothermic peak at about 65°C to 95°C with an enthalpy of 18.9

J/g. After debranching for 1, 2, and 4 h, a broad endothermic peak ranging from about 40°C to 100°C with enthalpy of 18.5, 18.3, and 20.6 J/g (**Figure 2.4** and **Table 2.2**), respectively, was observed, indicating that the materials solidifying at the early stage of debranching had weak crystalline structure and a large variation in crystal size and perfection.

Two endothermic peaks, one ranging from about 43 °C to 90 °C and the other ranging from about 99 °C and 138 °C, were observed in the sample debranched for 8 h. After 16 h, only one endothermic peak with melting temperature of about 115°C and enthalpy of about 20 J/g was detected. Moates et al. (1997) reported that the dissolution temperature of SCA crystallites increased from 57°C to 119°C with an increasing chain length in the range of 12 to 55 glucose units. In the present study, from 1 h to 24 h, a high percentage of short chains (Peak 1 in **Figure 2.1A**) released first and associated into weak crystals, and then more long chains (Peak 2 in **Figure 2.1A**) released with increasing debranching time and formed into crystals with high melting temperature. In addition, the long incubation time (24 h) at 50°C also facilitated the growth of crystals that required a high temperature to melt.

### *Synchrotron SAXS results*

**Figure 2.5A** and **B** shows SAXS patterns of native waxy maize starch and freeze-dried digests of waxy maize starch at different debranching times. As reported by Donald et al. (2001a, 2001b), the 9 nm lamellar peak of native waxy maize starch was absent in a dry state (**Figure 2.5A**) but appeared after hydration (**Figure 2.5B**). The presence of water molecules is thought to solvate the amorphous region containing branching points, which enables a decoupling between the main backbone of the amylopectin molecules and the side chains. The decoupling allows the side chains to be reconciled into order. However, no lamellar peaks were observed for debranched samples in dry or hydrated states in this study. This could be due to the lack of cluster structure of debranched samples. The released starch chains could be crystallized but lacked regularity between crystalline and amorphous regions.

The log-log plots of SAXS data of native waxy maize starch and freeze-dried digests of waxy maize starch debranched at different times are shown in **Figure 2.5C** and **D**. According to Suzuki et al (1997), the SAXS curves could be interpreted on the basis of fractals with the scattering power law:  $I \sim q^\alpha$ , where  $I$  is the scattering intensity and  $q$  is the scattering vector. The exponent  $\alpha$ , which can range from -1 to -4, relates to the fractal characteristics of the scattering

objectives. For  $-4 < \alpha < -3$ , the scattering source is classified as a surface fractal. The surface fractal dimension  $D_s = 6 + \alpha$ . For  $-3 < \alpha < -1$ , the scattering source is classified as a mass fractal. The mass fractal dimension  $D_m = -\alpha$ .

In **Figure 2.5C**, the slope  $\alpha$  of the straight lines in all curves was  $-4.0$ , which is a well-known behavior described by Porod's law (Porod, 1951). The  $\alpha$  value of samples after 1, 4 and 16 h of debranching was also  $-4.0$  (curves not shown). These results suggest that native starch and debranched samples were "surface fractal" in a dry state and that scattering was reflected from the surface or interface. The surface fractal dimension ( $D_s$ ) was 2.0 when  $\alpha = -4.0$ , indicating that the surface of native starch and debranched samples was smooth (Suzuki et al, 1997).

In contrast, all debranched samples when hydrated, had slope  $\alpha$  of around  $-2.0$  (**Figure 2.5D**), suggesting that hydrated starch aggregates were mass fractal and had self-similar structure in nature. When water molecules were present, they replaced the air around the starch molecules. Because the density of water was much closer to that of the starch than that of air, the scattering reflected the inner structure of starch rather than the surface structure. The mass fractal dimension ( $D_m$ ) was 2 for all hydrated, debranched samples. Using small-angle neutron scattering, Vallera et al. (1994) reported that amylose gels and sols had  $D_m$  of 2.6 and 2.0, respectively. It is interesting that the  $D_m$  of our hydrated debranched starches, which was 2.0, was close to that of amylose sols. The  $D_m$  value of our hydrated debranched starches was similar to that of gelatinized corn and potato starch, which was estimated to be 2.1 and 1.9, respectively (Suzuki et al, 1997).

In contrast to the hydrated debranched products, the hydrated native starch obeyed the power law at  $q$  value ranged from 0.06 to 0.2  $\text{nm}^{-1}$  with an exponent of  $\alpha = -3.7$ , which could still be interpreted as surface fractal structure. The surface of starch granules was too rigid and remained smooth in a hydrated state (Suzuki et al, 1997). The inner structure of starch granules was masked by the surface scattering.

### ***Synchrotron WAXD results***

**Figure 2.6** shows WAXD patterns of native waxy maize starch and waxy maize starch at different debranching times. In the dry state, the diffraction pattern of waxy maize starch debranched at 1, 2, and 4 h was unclear. An A-type crystalline structure was detected for native

waxy maize starch and 16 h and 24 h samples. In the hydrated state, a typical B-type structure with a peak around  $5^\circ$  ( $2\theta$ ) was observed for samples debranched for 1, 2, and 4 h. It seems that B-type crystallization was preferred during the first 8 h of incubation, followed by A-type crystallization between 16 and 24 h. This dual-stage crystallization phenomenon was also noted during the crystallization of debranched maltodextrin (Pohu et al, 2004a).

Using line-broadening analysis (Cairns et al, 1997), we estimated the size of crystallites in the native waxy maize starch and products debranched at different time (**Table 2.3**). At 1, 2, 4 h of debranching, the size of the crystallites was small ( $< 5$  nm in dry state), but dramatically increased to  $\sim 10$  nm in dry state (ca. 4% moisture) and  $\sim 12$  nm in hydrated state (45% moisture) after 8 h of debranching.

### *In vitro digestion profile*

**Table 2.4** shows the *in vitro* digestion profiles of native waxy maize starch, waxy maize starch at different debranching times, and isolated crystalline materials. Native waxy maize starch had a very low RS content ( $<5\%$ ). After debranching, RS content increased with time. The rate of increase in RS content was slow from 0 to 4 h but significantly increased from 4 to 24 h. After 24 h at  $50^\circ\text{C}$ , a product with 71.4% RS content was formed. The results confirmed the precipitate yield data (**Figure 2.2A**). The long incubation time resulted in thick, dense crystallites, which were characterized as resistant starch. After 24 h of crystallization, the isolated crystalline materials had a RS content of 86.9% (**Table 2.4**).

It is interesting to note that the changes of RDS and SDS content were not linear with debranching time. The SDS content decreased in the first hour of debranching but increased from 1 to 4 h. During the first 4 h of the reaction, the crystallized particles were small in size and weak in crystalline structure (**Figure 2.6** and **Table 2.3**). Alpha-amylase could digest these weak crystalline materials, but at a slow rate. After 4 h of reaction, aggregation and crystallization increased and the crystallized particles became thick and dense. Alpha-amylase has limited access to double helices in the crystalline phase, so RS was formed. Thus, RS formation could be characterized as the aggregation and arrangement of double helices from short linear chains in a crystalline structure. The differences in enzyme digestion behaviors among debranched waxy maize starches suggest that the debranching technique combined with controlled crystallization could be used to design the structure of starches with different digestibility.

### ***Molecular origin of RS***

After *in vitro* digestion, the MW distribution of waxy maize starch debranched at 24 h was slightly shifted (**Figure 2.1B**), suggesting that linear chains with a lower molecular weight is more susceptible to enzyme attack. The low MW linear chains (mostly DP <10) was too short to form the stable double helices (Gidley and Bulpin, 1987); thus, it failed to aggregate and was easily digestible. Lopez-Rubio et al. (2008) reported that the average characteristic dimension of RS crystals was ~ 5 nm, which corresponds to 2.2 helix turns, with ~13 glucose per helix. For waxy maize starch, the chain length (CL) distribution was peaked at DP 16 as determined by high-performance anion-exchange chromatography (Cai and Shi, 2010). The size of the crystallites in the final crystallized product was ~14.5 nm (**Table 2.3**). The nature of the RS product in this work was attributed to its dense crystalline structure and compact morphology. Pohu et al. (2004b) suggested an epitaxial growth of elementary crystalline A-type platelets for the origin of the  $\alpha$ -amylase resistance of debranched maltodextrin. The accessibility of double helices to  $\alpha$ -amylase was strongly limited by aggregation.

In this study, the RS product produced from the debranching of waxy maize starch had a relatively low DP which was assembled into a highly crystalline structure. In contrast, high amylose starch contains long linear molecules. Lopez-Rubio et al. (2008) noted a significant increase in molecular order and crystallinity when extruded high amylose starches were digested by  $\alpha$ -amylase and glucoamylase, suggesting that during the digestion process, amylose chains were rearranged into enzyme-resistant structures of higher crystallinity. In that case, two competing factors, the kinetics of enzyme hydrolysis and the kinetics of amylose retrogradation, determine the resistance to enzyme digestion of a specific processed starch (Lopez-Rubio et al, 2008).

### **Discussion**

There are two challenges when waxy maize starch is debranched at high solids content (25%, w/w). First, the slurry may become very viscous during gelatinization. In this study, a pressure cooker coupled with mechanical stirring was used to totally gelatinize the starch and perform the debranching reaction. Second, amylose can either precipitate or form a gel (network). When the amylose concentration is higher than 1.5%, amylose gels can be formed (Gidley, 1989). Therefore, conditions that led to crystallization instead of gelation were required. Increasing the



mobility of starch chains at 50°C helped to achieve this goal. With continuous stirring, the resulting products could be recovered by filtration, which made them practical for large-scale production.

Depending on CL, concentration, temperature and solvent used, amylose can be crystallized from solution to form gels, aggregates, precipitates, spherulites or lamellar crystals with A or B allomorphic type (Buleon et al, 2007). Combining debranching of starch with controlled crystallization provides a practical way of producing A- and B-type crystalline starches with different morphologies. In this study, the crystallization behaviors of debranched waxy maize starch were investigated in a concentrated solution (25%, w/w). After crystallization at 50°C, debranched starch with an A-type X-ray diffraction pattern and high RS content (71.4%) was obtained. In contrast, when a low starch concentration (5%, w/w) was used, debranching of waxy maize starch at 50°C followed by crystallization at 25°C resulted in crystalline short-chain amylose with a B-type X-ray pattern (Cai and Shi, 2010). Our results were in agreement with previous findings on debranched glycogen (Gidley and Bulpin, 1987) and amylopectin (Hizukuri, 1961) that A-type polymorph is favored by high concentration and high temperature. However, the exact solid concentration and crystallization temperature needed to produce A- or B-type polymorph were different for different materials. For instance, A-type crystals were produced from debranched glycogen by crystallization at 30°C with 50% solids (Gidley and Bulpin, 1987). The average CL of debranched glycogen was 11.2 (Gidley and Bulpin, 1987), much shorter than the debranched waxy maize starch (average CL 24.1) (Cai and Shi 2010). Indeed, CL is of primary importance in determining the type of polymorph formed during crystallization (Gidley and Bulpin, 1987; Hizukuri et al., 1983; Pfannemuller, 1987). Moreover, the yield of crystalline short-chain amylose increases as the CL increases (Cai and Shi, 2010). The yield of A-type crystalline debranched glycogen is 52% after crystallization at 30°C for 10-14 days (Gidley and Bulpin, 1987). In comparison, in this study, the yield of crystalline SCA was greater than 90% after debranching and crystallization of waxy maize starch at 50°C for 24 h followed by precipitation at 25° for 6 h (**Figure 2.2A**). The remarkable high yield and possible recovery by filtration make the large production of SCA from debranched waxy maize starch feasible.

## **Conclusions**

The simultaneous debranching of waxy maize starch and solidification of debranched products at a high solid content were investigated for the first time by combined analytical techniques. SCA crystallized upon release from amylopectin during debranching. A RS product with an A-type crystalline structure, high melting temperature (90°C to 140°C), and high RS content (71.4%) was obtained. The yield of the crystallized product was ca. 90% after the starch was completely debranched at 50°C and further precipitated at 25°C. Combining debranching techniques with controlled crystallization may be used to design the structure of starch with targeted digestibility. Further research is needed to determine health impact of starches with different digestibility.

## References

- Berry, C. S. (1986). Resistant starch- formation and measurement of starch that survives exhaustive digestion with amylolytic enzymes during the determination of dietary fiber. *Journal of Cereal Science*, 4, 301-314.
- Buleon, A., Veronese, G., & Putaux, J. L. (2007). Self-association and crystallization of amylose. *Australian Journal of Chemistry*, 60, 706-718.
- Cai, L., & Shi, Y-C. (2010). Structure and digestibility of crystalline short-chain amylose from debranched waxy wheat, waxy maize and waxy potato starches. *Carbohydrate Polymers*, 79, 1117-1123.
- Cairns, P., Bogracheva, T.Y., Ring, S.G., Hadley, C.L., & Morris, V.J. (1997). Determination of the polymorphic composition of smooth pea starch. *Carbohydrate Polymers*, 32, 275-282.
- Chen, X. M., Burge, C., Fang, D. F., Ruan, D., Zhang, L., Hsiao, B. S., & Chu, B. (2006). X-ray studies of regenerated cellulose fibers wet spun from cotton linter pulp in NaOH/thiourea aqueous solutions. *Polymer*, 47, 2839-2848.
- Chen, X. M., Burge, C., Wan, F., Zhang, J., Rong, L. X., Hsiao, B. S., Chu, B., Cai, J., & Zhang, L. (2007). Structure study of cellulose fibers wet-spun from environmentally friendly NaOH/urea aqueous solutions. *Biomacromolecules*, 8, 1918-1926.
- Chiu, C-W., & Henley, M. (1993). Foods opacified with debranched starch. US Patent Office, Pat. No. 5 194 282.
- Chiu, C-W., Henley, M., & Altieri, P. (1994). Process for making amylase resistant starch from high amylose starch. US Patent Office, Pat. No. 5 281 276.
- Chiu, C-W., & Kasica, J. J. (1995). Enzymatically debranched starches as tablet excipients. US Patent Office, Pat. No. 5 468 286.
- Chiu, C-W., & Mason, W. R. (1998). Method of replacing fats with short chain amylose. US Patent Office, Pat. No. 5 711 986.
- Chu, B., & Hsiao, B. S. (2001). Small-angle X-ray scattering of polymers. *Chemical Reviews*, 101, 1727-1762.
- Donald, A. M., Kato, K. L., Perry, P. A., & Waigh, T. A. (2001a). Scattering studies of the internal structure of starch granules. *Starch/Stärke*, 53, 504-512.
- Donald, A. M., Perry, P. A., & Waigh, T. A. (2001b). The impact of internal granule structure on processing and properties. In T.L. Barsby, A. M. Donald, & P. J. Frazier. *Starch: Advances in structure and functionality* (pp. 45-52). Cambridge, UK: The Royal Society of Chemistry.
- Englyst, H. N., Kingman, S. M., & Cummings, J. H. (1992). Classification and measurement of nutritionally important starch fractions. *European Journal of Clinical Nutrition*, 46, S33-S50.
- FAO JECFA Monographs (2007). Joint FAO/WHO expert committee on food additives. 4, 21-23.
- Gidley, M. J. (1989). Molecular mechanisms underlying amylose aggregation and gelation. *Macromolecules*, 22, 351-358.
- Gidley, M. J., & Bulpin, P. V. (1987). Crystallization of malto-oligosaccharides as models of the crystalline forms of starch: minimum chain-length requirement for the formation of double helices. *Carbohydrate Research*, 161, 291-300.

- Gonzalez-Soto, R. A., Agama-Acevedo, E., Solorza-Feria, J., Rendon-Villalobos, R., & Bello-Perez, L. A. (2004). Resistant starch made from banana starch by autoclaving and debranching. *Starch/ Stärke*, 56, 495-499.
- Gonzalez-Soto, R. A., Mora-Escobedo, R., Hernandez-Sanchez, H., Sanchez-Rivera, M., & Bello-Perez, L.A. (2007). The influence of time and storage temperature on resistant starch formation from autoclaved debranched banana starch. *Food Research International*, 40, 304-310.
- Guraya, H. S., James, C., & Champagne, E. T. (2001a). Effect of cooling and freezing on the digestibility of debranched rice starch and physical properties of the resulting material. *Starch/ Stärke*, 53, 64-74.
- Guraya, H. S., James, C., & Champagne, E. T. (2001b). Effect of enzyme concentration and storage temperature on the formation of slowly digestible starch from cooked debranched rice starch. *Starch/ Stärke*, 53, 131-139.
- Hizukuri, S. (1961). X-ray diffractometric studies on starches. VI. Crystalline types of amylopectin and effect of temperature and concentration of mother liquor on crystalline type. *Agricultural and Biological Chemistry*, 25, 45-49.
- Hizukuri, S., Abe, J., & Hanashiro, I. (2006). Starch: Analytical aspects. In A-C. Eliasson (Ed.). *Carbohydrates in food* (2nd ed., pp. 305-391). Boca Raton, FL: Taylor & Francis Group.
- Hizukuri, S., Kaneko, T., and Takeda, Y. (1983). Measurement of the chain length of amylopectin and its relevance to the origin of crystalline polymorphism of starch granules. *Biochimica et Biophysica Acta*, 760, 188-191.
- Kettlitz, B. W., Coppin, J. V. J-M., Roper, H. W. W., & Bornet, F. (2000). Highly fermentable resistant starch. US Patent Office, Pat. No. 6 043 229.
- Lehmann, U., Jacobasch, G., & Schmiedl, D. (2002). Characterization of resistant starch type III from banana (*Musa acuminata*). *Journal of Agricultural and Food Chemistry*, 50, 5236-5240.
- Leong, Y. H., Karim, A. A., & Norziah, M. H. (2007). Effect of pullulanase debranching of sago (*Metroxylon sagu*) starch at subgelatinization temperature on the yield of resistant starch. *Starch/ Stärke*, 59, 21-32.
- Lopez-Rubio, A., Flanagan, B. M., Shrestha, A. K., Gidley, M. J., & Gilbert, E. P. (2008). Molecular rearrangement of starch during in vitro digestion: towards a better understanding of enzyme resistant starch formation in processed starches. *Biomacromolecules*, 9, 1951-1958.
- Manners, D. J., & Matheson, N. K. (1981). The fine-structure of amylopectin. *Carbohydrate Research*, 90, 99-110.
- Moates, K. G., Noel, R. T., Parker, R., & Ring, G. S. (1997). The effect of chain length and solvent interactions on the dissolution of B-type crystalline polymorph of amylose in water. *Carbohydrate Research*, 298, 327-333.
- Onyango, C., & Mutungi, C. (2008). Synthesis and in vitro digestion of resistant starch type III from enzymatically hydrolysed cassava starch. *International Journal of Food Science & Technology*, 43, 1860-1865.
- Pfannemuller, B. (1987). Influence of chain length of short monodisperse amyloses on the formation of A- and B-type X-ray diffraction patterns. *International Journal of Biological Macromolecules*, 9, 105-108.

- Pohu, A., Planchot, V., Putaux, J. L., Colonna, P., & Buleon, A. (2004a). Split crystallization during debranching of maltodextrins at high concentration by isoamylase. *Biomacromolecules*, 5, 1792-1798.
- Pohu, A., Putaux, J. L., Planchot, V., Colonna, P., & Buleon, A. (2004b). Origin of the limited alpha-amylolysis of debranched maltodextrins crystallized in the A form: A TEM study on model substrates. *Biomacromolecules*, 5, 119-125.
- Porod, G. (1951). Die rontgenkleinwinkelstreuung von dichtgepackten kolloiden systemen 1. *Kolloid-Zeitschrift and Zeitschrift Fur Polymere*, 124, 83-114.
- Ring, S.G., Lanson, K.J., & Morris, V.J. (1985). Static and dynamic light-scattering studies of amylose solutions. *Macromolecules*, 18, 182-188.
- Sang, Y. J., & Seib, P. A. (2006). Resistant starches from amylose mutants of maize by simultaneous heat-moisture treatment and phosphorylation. *Carbohydrate Polymers*, 63, 167-175.
- Shin, S. I., Choi, H. J., Chung, K. M., Hamaker, B. R., Park, K. H., & Moon, T. W. (2004). Slowly digestible starch from debranched waxy sorghum starch: Preparation and properties. *Cereal Chemistry*, 81, 404-408.
- Suzuki, T., Chiba, A., & Yano, T. (1997). Interpretation of small angle X-ray scattering from starch on the basis of fractals. *Carbohydrate Polymers*, 34, 357-363.
- Vallera, A. M., Cruz, M.M., Ring, S., & Boue, F. (1994). The structure of amylose gels. *Journal of Physics-Condensed Matter*, 6, 311-320.
- Yokobaya, K., Akai, H., Sugimoto, T., Hirao, M., Sugimoto, K., & Harada, T. (1973). Comparison of kinetic parameters of *Pseudomonas* isoamylase and *Aerobacter* pullulanase. *Biochimica et Biophysica Acta*, 293, 197-202.

**Table 2.1 Percentage of debranched starch at different debranching times<sup>A</sup>**

Time (h)	1	2	4	8	16	24
Percentage of debranching (%)	68±2.8	75±1.4	80±2.0	89±1.8	100	100

<sup>A</sup> Mean ± standard deviation values are reported.

**Table 2.2 Thermal properties of native waxy maize starch and waxy maize starch debranched at different times as determined by differential scanning calorimetry<sup>A</sup>**

samples	Peak 1				Peak 2			
	T <sub>o</sub> (°C)	T <sub>p</sub> (°C)	T <sub>c</sub> (°C)	ΔH(J/g)	T <sub>o</sub> (°C)	T <sub>p</sub> (°C)	T <sub>c</sub> (°C)	ΔH(J/g)
native	64.3±0.3	73.5±0.1	94.6±0.1	18.9±0.1	-	-	-	-
1 h	42.3±0.1	73.4±1.9	86.9±0.6	18.5±0.2	-	-	-	-
2 h	44.4±1.2	69.6±1.1	90.1±0.4	18.3±0.3	-	-	-	-
4 h	42.7±0.1	73.6±0.3	99.5±0.5	20.6±0.1	-	-	-	-
8 h	43.3±0.1	68.5±3.1	89.7±2.2	10.9±0.1	99.3±2.1	114.4±1.4	137.8±0.4	8.3±0.0
16 h	-	-	-	-	92.9±0.5	113.6±0.9	138.7±0.4	19.2±0.4
24 h	-	-	-	-	92.3±0.3	114.0 ±0.2	141.8±0.5	20±0.2

<sup>A</sup> Mean ± standard deviation values are reported.

**Table 2.3 Average size of polymorph crystallites of native waxy maize starch and waxy maize starch debranched at different times as determined by wide-angle X-ray diffraction**

Samples	Size (nm)	
	Powder (ca. 4% moisture)	Hydrated (45% moisture)
Native starch <sup>a</sup>	8.1	9.4
Debranched		
1 h	3.8	9.7
2 h	4.0	8.8
4 h	4.8	8.5
8 h	10.3	12.4
16 h	9.5	14.8
24 h	9.8	14.5

<sup>a</sup> The moisture of native waxy maize starch powder was about 11%.



**Table 2.4 Levels of rapidly digestible starch (RDS), slowly digestible starch (SDS), and resistant starch (RS) content in native waxy maize starch, debranched waxy maize starch produced at different times at 50°C and isolated crystalline materials<sup>A</sup>**

Samples	RDS (%)	SDS (%)	RS (%)
Native starch	29±0.4	66.7±0.4	4.3±0.8
Debranched			
1h	59.8±0.3	32.9±1.4	7.3±1.7
2h	58.5±1.7	31.5±0.5	10±1.2
4h	43.5±0.3	38.9±0.6	17.6±0.9
8h	33.9±1.1	23.3±0.3	42.8±1.4
16h	25.1±0.4	8.3±0.9	66.6±0.5
24h	22.5±0.3	6.1±0.1	71.4±0.4
Isolated crystalline materials <sup>a</sup>	4.9±0	8.2±0.8	86.9±0.8

<sup>A</sup> Mean ± standard deviation values are reported.

<sup>a</sup> Isolated crystalline materials were obtained by filtering debranched waxy maize starch product after 24 h of crystallization and drying at 40°C in an oven over night.

**Figure 2.1** Molecular weight distribution of (A) waxy maize starch (25% solids) debranched and crystallized at 50°C at different times, and (B) waxy maize starch debranched and crystallized at 50°C for 24 h and its corresponding isolated resistant starch

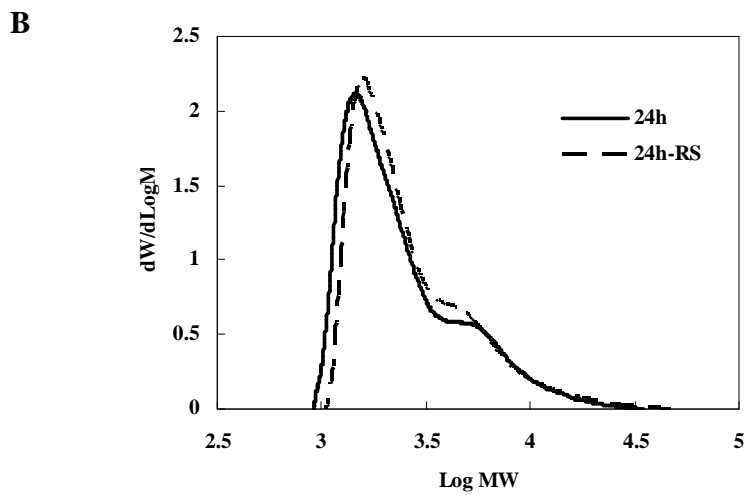
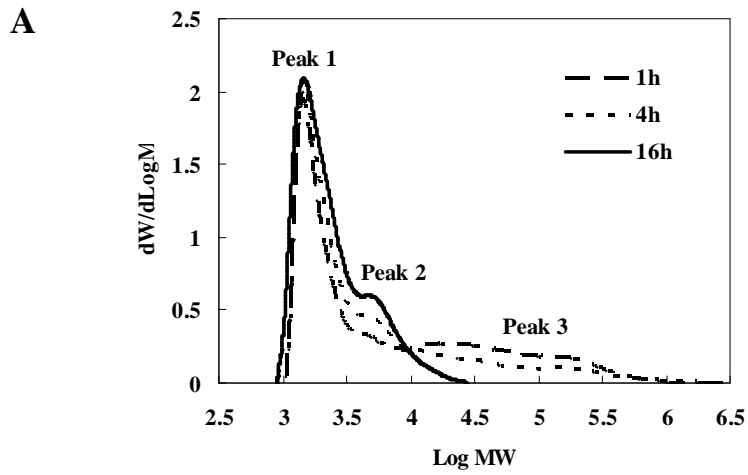


**Figure 2.2 (A) Yield of starch precipitate based on the weight of waxy maize starch at different debranching times; —◆— crystallization at 50°C; —■— crystallization at 25°C after the debranched starch was crystallized at 50°C for 24 h; (B) Starch polymer solution at the beginning of debranching and cloudy slurry after 24 h of crystallization at 50°C; and (C) SEM images of waxy maize starch debranched and crystallized at 50°C for 24 h recovered by filtration and drying in an oven at 40°C**

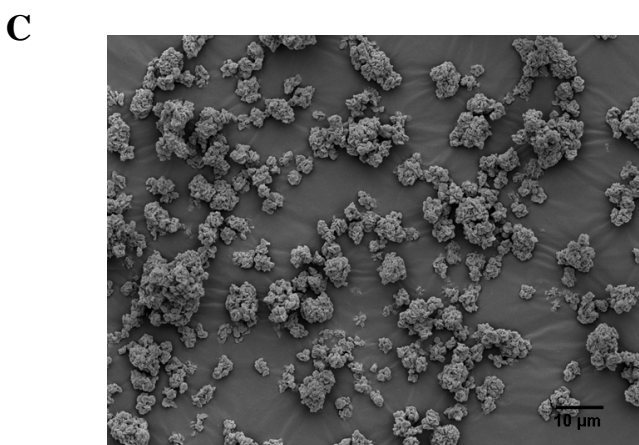
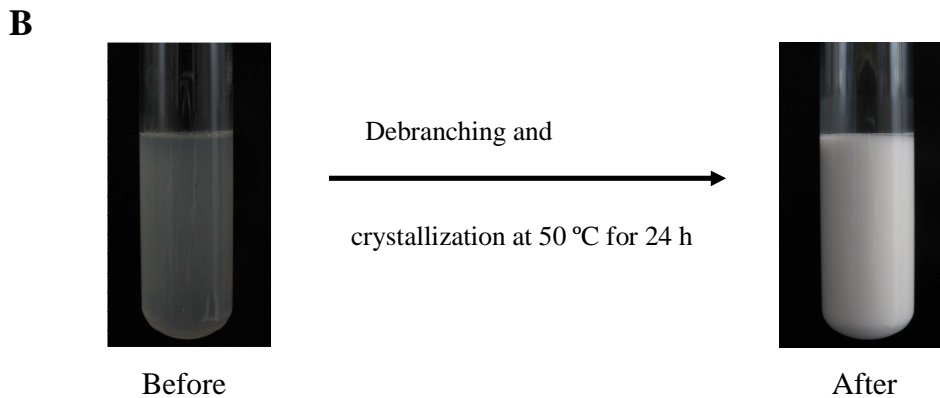
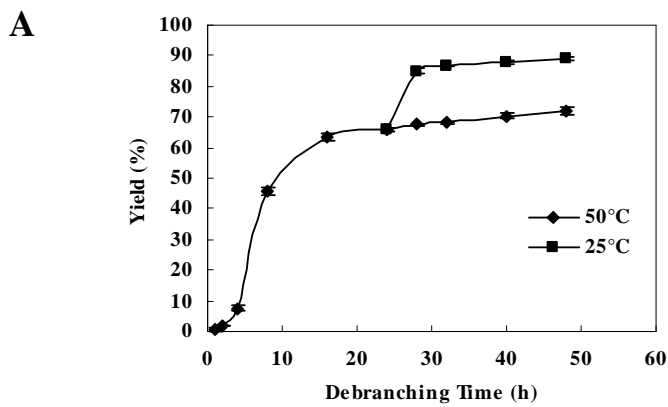


**Figure 2.3** Transmission electron microscopic images of waxy maize starch (25% solids) debranched at different times at 50°C: (A) 1 h, (B) 2 h, (C) 4 h, (D) 8 h, (E) 16 h, and (F) 24 h

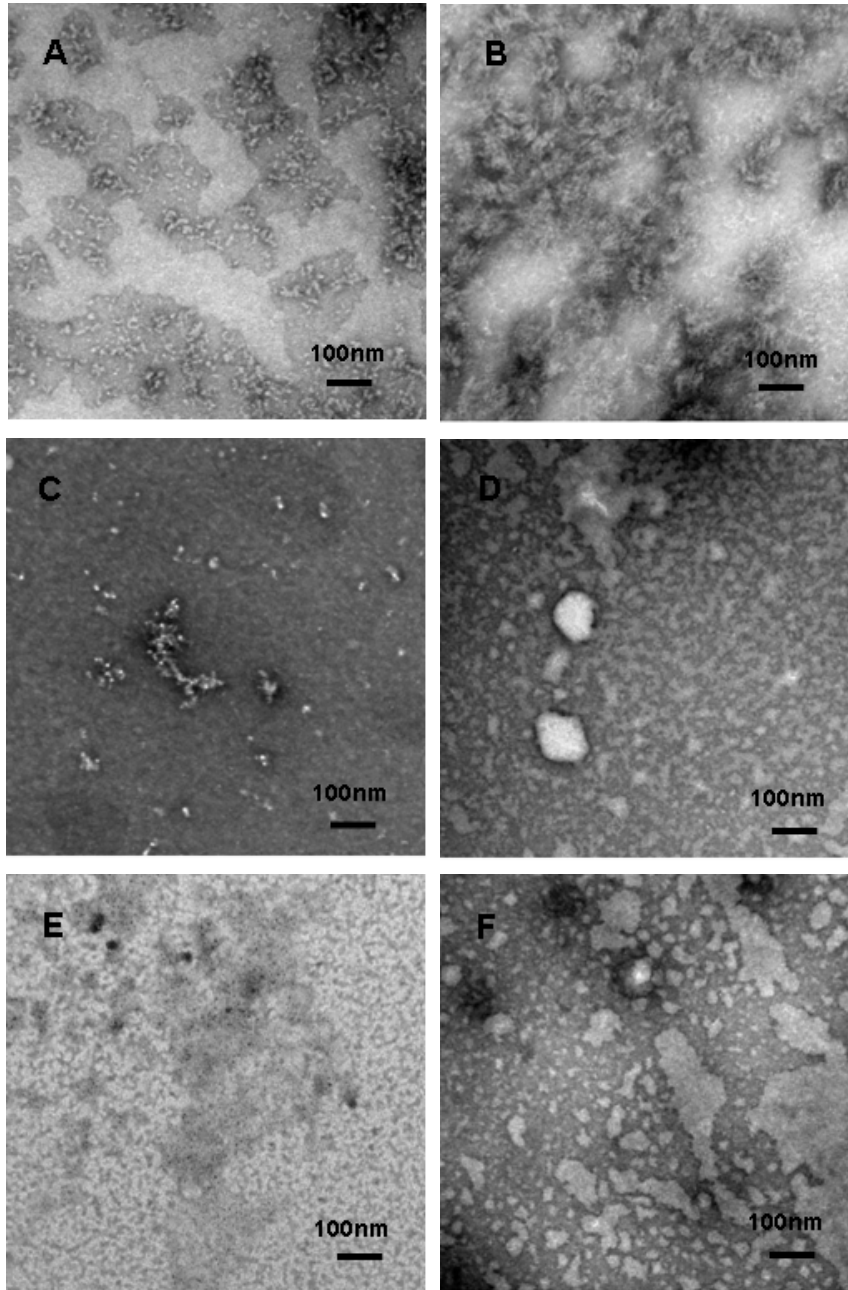


**Figure 2.4 Thermal properties of native waxy maize starch and waxy maize starch debranched at different times as determined by differential scanning calorimetry**

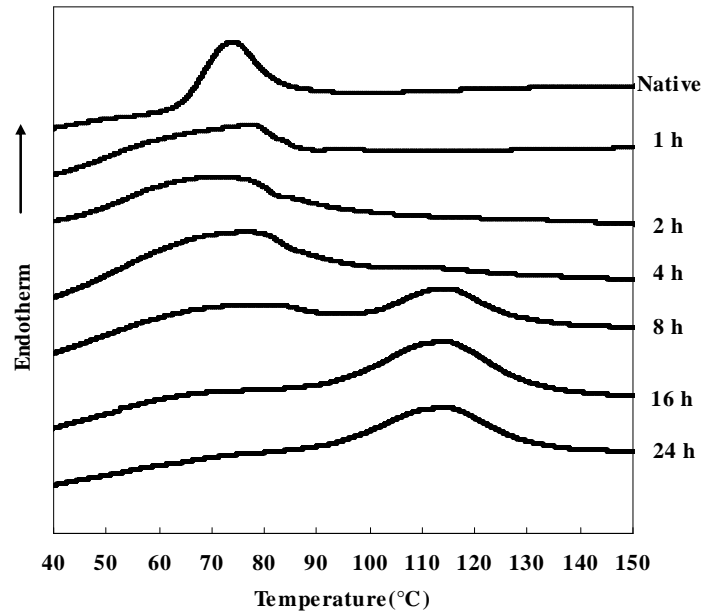
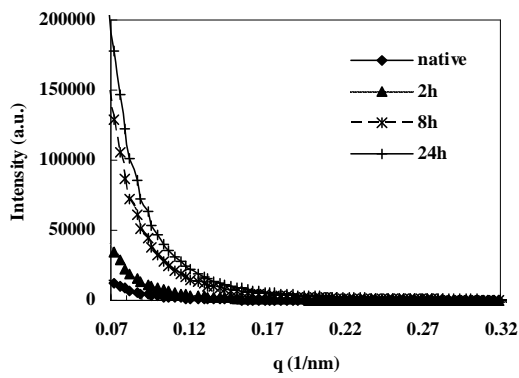
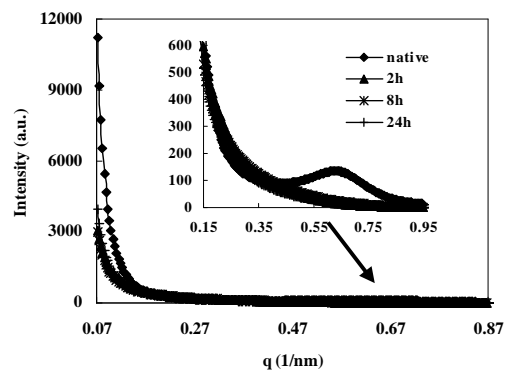


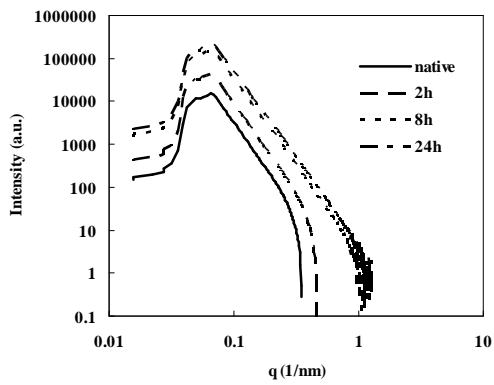
**Figure 2.5 Small-angle X-ray scattering of native waxy maize starch and freeze-dried digests of waxy maize starch debranched and crystallized at 50°C at different times with (A) 4% moisture (except that native starch was 11% moisture), (B) 45% moisture; (C) log-log plots, 4% moisture (except that native starch was 11% moisture) and (D) log-log plots, 45% moisture**



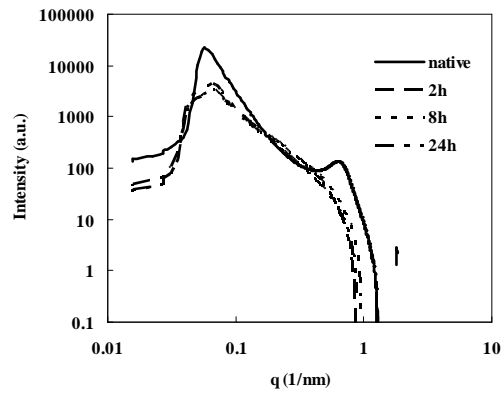
**A**



**B**

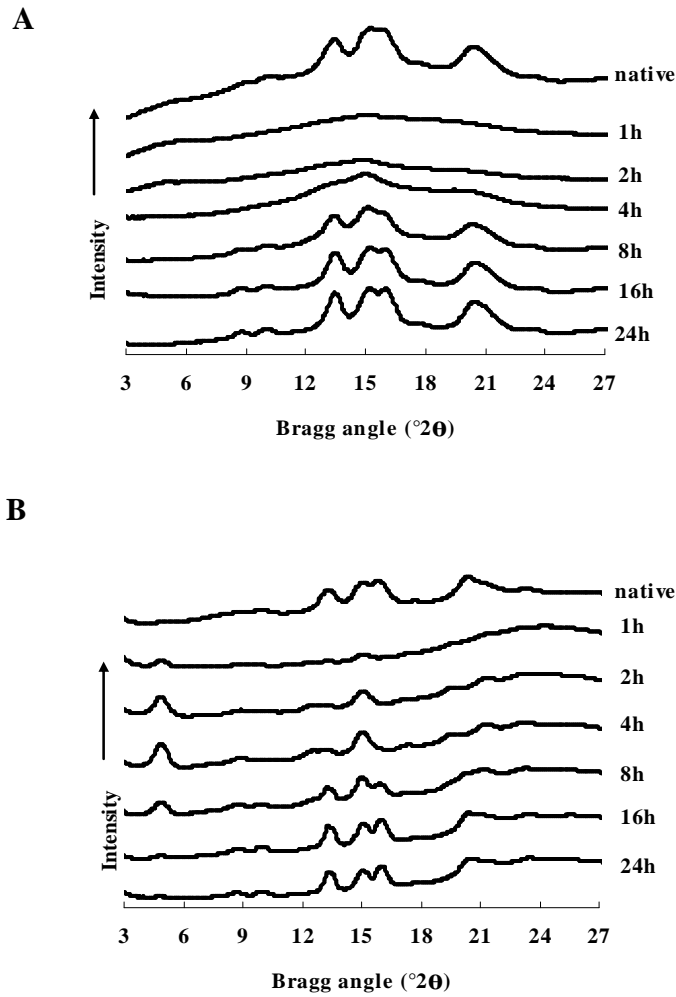


**C**



**D**

**Figure 2.6 Wide-angle X-ray diffraction of native waxy maize starch and freeze-dried digests of waxy maize starch debranched and crystallized at 50°C at different times with (A) 4% moisture (except that native starch was 11% moisture) and (B) 45% moisture**



## **Chapter 3 - Structure and digestibility of crystalline short-chain amylose from debranched waxy wheat, waxy maize and waxy potato starches\***

### **Abstract**

The structure and digestibility of crystalline short-chain amylose (CSCA) from debranched waxy wheat, waxy maize, and waxy potato starches were investigated and compared. The starches (5%, w/w) were cooked in acetate buffer (pH 4.0) and debranched by isoamylase at 50°C. After 24 h, the mixture was cooled and held at 25°C for another 24 h. Debranched waxy potato starch had a longer average chain length than debranched waxy wheat and waxy maize starches, resulting in a higher yield of crystallized product. All CSCA products displayed a B-type X-ray diffraction pattern, indicating that low solids concentration (5%) favored the formation of B-type crystals. CSCA from debranched waxy potato starch had a higher peak melting temperature (116.2°C) and higher resistant starch content (77.8%) than that from debranched waxy wheat and waxy maize starches, suggesting that waxy potato starch is a preferred starting material to prepare products with high resistant starch content by debranching and crystallization.

### **Introduction**

Starch, an abundant natural polysaccharide, normally consists of two types of  $\alpha$ -D-glucose polymers: amylose and amylopectin. Amylose is an essentially linear polymer with few branches, whereas amylopectin has a highly branched structure in which branch chains are linked to the linear chains by  $\alpha$ -(1, 6)-linkages (Hizukuri et al, 2006; Tester et al., 2004). Under specific conditions, amylopectin can be debranched in the presence of debranching enzymes (e.g. isoamylase and pullulanase). The chain length (CL) distribution of debranched amylopectin is highly related to its crystalline polymorphs (Hizukuri, 1985). In general, B-type starches have long branch chains of amylopectin, whereas A-type starches have a large amount of short chains

---

\*Chapter 3 is published as a part of Cai, L., & Shi, Y-C. (2010). *Carbohydrate Polymers*, 79, 1117-1123.



with a degree of polymerization (DP) of 6-12 (Hanashiro et al., 1996). The distinct branch CL distributions of amylopectin from A- and B- type starches affect their functional properties, such as gelatinization (Jane et al., 1999), retrogradation (Silverio et al., 2000), pasting properties (Jane and Chen, 1992; Srichuwong et al., 2005b), and acid and enzyme hydrolysis (Fredriksson et al., 2000; Srichuwong et al., 2005a).

Compared with waxy maize and waxy wheat (Chibbar and Chakraborty, 2005; Graybosch, 1998; Guan et al., 2009), waxy potato (Jeffcoat et al., 2002; Visser et al., 1997a, b) are relatively new and of great interest to the food and starch industries. However, the crystallization behaviors of debranched waxy wheat and waxy potato starches have not been reported. In contrast, waxy sorghum (Shin et al., 2004), waxy rice (Guraya et al., 2001a, b), and waxy maize (Berry, 1986; Miao et al., 2009; Shi et al., 2005a, b, 2006) starches have been debranched and crystallized to prepare slowly digestible starch (SDS) and resistant starch (RS). Waxy wheat and waxy maize starches are cereal starches with short branch chains and an A-type X-ray diffraction pattern whereas waxy potato starch contains long branch chains and displays a B-type pattern (McPherson and Jane, 1999). The objective of this work was to investigate the effects of CL and starch sources on the properties of short-chain amylose derived from waxy wheat, waxy maize, and waxy potato starches. The three starches were completely debranched and crystallized. The CL distributions, crystalline structure, thermal properties, and digestion behaviors of the crystalline short-chain amylose (CSCA) products were determined. This information will be useful for better designing starch-based food ingredients with improved health benefits.

## **Materials and methods**

### ***Materials***

Waxy wheat starch was isolated from hard waxy wheat flour as described by Guan et al. (2009). Waxy maize starch was obtained from National Starch Food Innovation (Bridgewater, NJ, USA). Waxy potato starch was provided by Penford Food Ingredients Company (Centennial, CO, USA). Isoamylase (EC 3.2.1.68) was obtained from Hayashibara Biochemical Laboratories, Inc. (Okayama, Japan) and had an enzyme activity of  $1.41 \times 10^6$  isoamylase activity units (IAU)/g. The enzyme activity was determined by incubating the enzyme with soluble waxy

maize starch as a substrate in the presence of iodine for 30 min at pH 3.5 and 40°C and measuring the absorbance of the reaction mixture at 610 nm (FAO JECFA Monographs, 2007). One IAU is defined as the amount of isoamylase that increased absorbance of the reaction mixture by 0.008 in 30 min under the conditions of the isoamylase assay.

### ***Debranching of starch and preparation of CSCA***

Starch (5 g, dry basis) was mixed with 95 mL acetic acid buffer (0.01 M, pH 4.0) in a sealed glass bottle and cooked in a boiling water bath with stirring for 1 h. After the mixture was cooled to 50°C, 1% isoamylase based on the dry weight of starch was added. The mixture was kept at 50°C with stirring. After 24 h, the mixture was cooled to 25°C and held for another 24 h to increase the yield of crystallites. The precipitates (CSCA products) were filtered, washed with water, and dried at 40°C in an oven overnight. The yield was calculated by dividing the weight of the precipitates over the weight of the starting starch.

In separate experiments, each starch was debranched as described above and the whole debranched product including solubles and precipitates was freeze-dried. To confirm that the starch was completely debranched, the freeze-dried debranched starch (20 mg) was weighed into a 10-mL vial, mixed with 2 mL of a mixture of DMSO and water (9:1, w/w), and cooked in a boiling water bath with magnetic stirring for 15 min. After the mixture was cooled to room temperature, acetic acid buffer (6.98 mL, 0.01 M, pH 4.0) and isoamylase (2 µL) were added (Shi et al, 1998). The mixture was kept at 50°C with stirring for 24h. After that, 2 mL of the mixture was taken and mixed with 2 mL DMSO, and analyzed by GPC.

### ***Gel permeation chromatography (GPC)***

The details of GPC were previously described in Chapter 2.

### ***High-performance anion-exchange chromatograph (HPAEC)***

CL distributions of debranched waxy starches and CSCA products were quantitatively analyzed using a HPAEC (Dionex ICS-3000, Dionex Corp., Sunnyvale, CA, USA) equipped with a pulsed amperometric detector, a guard column, a CarboPac<sup>TM</sup> PA1 analytical column and an AS-DV autosampler. The eluents were prepared as described previously (Shi and Seib, 1992). Eluent A was 150mM NaOH and eluent B was 150mM NaOH containing 500mM sodium acetate. The gradient program was as followed: 40% of eluent B at 0 min, 50% at 2min, 60% at

10min, and 80% at 40min. The separations were carried out at 25°C with a flow rate of 1 mL/min. The concentration of debranched starches and CSCA products was 2 mg/mL in 1 M NaOH solution. Maltohexaose and maltoheptaose (Sigma-Aldrich, Inc., St.Louis, MO, USA) were used as standards.

### ***Average CL determination***

Average CL was determined by the Nelson/Somogyi reducing sugar method (Nelson, 1944; Robyt and Whelan, 1968; Somogyi, 1952). Because the CSCA products could not be completely dissolved in boiling water, each starch sample was dissolved in 1.25 N sodium hydroxide, neutralized by hydrochloride acid, and analyzed for reducing sugar.

### ***Wide-angle X-ray diffraction***

X-ray diffraction was conducted with a Philips X-ray diffractometer with Cu-Ka radiation at 35 kV and 20 mA, a theta-compensating slit, and a diffracted beam monochromator. The moisture of all samples was adjusted to about 18% in a sealed dessicator at room temperature before analysis. The diffractograms were recorded between 2 and 35° (2 $\theta$ ). Relative crystallinity was estimated by the ratio of the peak areas to the total diffractogram area (Komiya and Nara, 1986).

### ***Differential scanning calorimetry (DSC)***

The parameters of DSC and sample scanning program were described in Chapter 2.

### ***In vitro digestion method***

The *in vitro* digestion test was determined by a modified Englyst procedure that was described in Chapter 2.

### ***Statistical analysis***

Data were analyzed by an analysis of variance (ANOVA) procedure with Tukey's studentized range (HSD) test using SAS version 9.1 (SAS Institute Inc., Cary, NC, USA). Mean values from the duplicated experiments were reported.

## Results and discussion

### *Molecular weight distribution by GPC*

The molecular weight (MW) distributions of debranched waxy wheat, waxy maize, waxy potato starches and their CSCA products as determined by GPC are shown in **Figure 3.1**. A bimodal distribution of low and high MW peaks, designated Peak 1 and Peak 2 respectively, was observed for all debranched starches and CSCA products. The area and percentage of each peak were calculated and reported in **Table 3.1**. Waxy wheat starch had a large proportion of the low MW fraction (i.e. short side chains in amylopectin) (**Figure 3.1A**). Debranched waxy wheat and waxy maize starches had a similar ratio of area of Peak 1 to Peak 2, In contrast, debranched waxy potato starch had a distinct MW distribution (**Figure 3.1A**), and the proportion of the low MW fraction was much lower compared with debranched waxy wheat and waxy maize starches (**Table 3.1**). These results are consistent with the fact that side chains of amylopectin in a B-type starch are longer than those in A-type starch (Hanashiro et al., 1996; Hizukuri, 1985; Jane et al., 1999).

Compared with parent debranched starches, the MW distribution curves of all CSCA products shifted to higher molecular weight (**Figure 3.1B**) and the proportion of the low MW fraction (Peak 1) decreased (**Table 3.1**). CSCA products from debranched waxy wheat and waxy maize starches showed a similar MW distribution, whereas CSCA product from debranched waxy potato starch had a distinct MW distribution (**Figure 3.1B**) and a small proportion of the low MW fraction (**Table 3.1**).

To confirm that the three waxy starches were completely debranched, the freeze-dried whole debranched starch samples were further debranched by isoamylase. No change in MW distribution was observed (data not shown), indicating that the whole debranched starch molecules were linear.

### *CL distribution*

The CL distributions of debranched starches and their CSCA products as determined by HPAEC are shown on **Figure 3.2**. The debranched waxy wheat starch had a higher proportion of chains with DP 6-19 and a lower proportion of chains with DP 20-67 than its CSCA product (**Figure 3.2A**). Similar trend was observed for debranched waxy maize and waxy potato starches

and their corresponding CSCA products (**Figure 3.2B** and **C**). These results suggested that the chain length of the CSCA products were longer than that of their parent debranched starches. This increase in chain length of CSCA was attributed to the preferential crystallization and precipitation of long chains. According to Gidely and Bulpin (1987), the minimum CL required to form starch double helices is 10. During debranching and crystallization, a fraction of low molecular amylose (mostly DP < 10) was too short to form the stable double helices and remained in the solution. In this study, the CL distribution of the CSCA was peaked at around DP 16 (**Figure 3.2**).

### *Yield and average CL*

The yields and average CLs of debranched starches and their corresponding CSCA products are listed in **Table 3.2**. Debranched waxy potato starch gave a higher yield (72.6%) than debranched waxy wheat (58.7%) and waxy maize (60.7%) starches. The average CLs of debranched waxy wheat, waxy maize, and waxy potato starches were 21.8, 24.1, and 32.1 glucose units, respectively. Our results suggested that B-type starch with a longer CL yield more CSCA than A-type starches. Using amylose with different average DPs ranging from 40 to 610, Eerlingen et al (1993) reported that the yield of enzyme RS was correlated with the DP of amylose. However, the isolated RS fractions consisted of short chains (average DP between 19 and 26) and were independent of the CL of the starting amylose used.

The average CLs of CSCA products from debranched waxy wheat, waxy maize, and waxy potato starches were 28.1, 29.2, and 35.5 glucose units, respectively, larger than those of the whole starches. The results were in agreement with the MW distribution (**Figure 3.1** and **Table 3.1**) and CL distribution (**Figure 3.2**) data.

### *Crystalline structure*

Native waxy wheat and waxy maize starches showed the A-type crystalline structure, whereas waxy potato starch displayed the B-type X-ray diffraction pattern (**Figure 3.3**). The degree of crystallinity of all three native starches was around 40%. Among the three CSCA products, the one produced from debranched waxy potato starch gave a stronger peak at  $2\theta$  of  $5^\circ$  and the two peaks between  $13-15^\circ$   $2\theta$  were better resolved (**Figure 3.3**), suggesting that long chains form a stronger crystalline structure more readily than short chains.

After debranching and crystallization, a typical B-type structure was observed for all CSCA products. The results followed the general “rules” of short-chain amylose crystallization, namely, shorter CL, higher concentration, and higher temperature favor the formation of A-type crystallites, whereas the reverse conditions induce B-type crystallization (Buleon et al., 2007; Gidley and Bulpin, 1987; Lebail et al., 1993; Pfannemuller, 1987; Ring et al., 1987; Whittam et al., 1990). In this study, a dilute starting concentration (5% solid) was used, which led to the formation of B-type crystalline structure. In another study, short-chain amylose from debranched waxy maize starch formed an A-type crystalline structure when debranched at 25% solids and crystallized at 50°C (Cai et al, 2010). Continued research is being conducted to investigate the debranching and crystallization of these waxy starches at a high solid content and to manipulate temperature, CL, and starch solid content to produce highly pure A- and B-type crystallites and then determine their digestibility (**Chapter 5**).

### ***Thermal properties***

Native waxy wheat, waxy maize, and waxy potato starches were characterized with a sharp endotherm peak at 67.8, 73.5, and 70.4°C and an enthalpy of 15.6, 18.9, and 18.3 J/g, respectively (**Figure 3.4** and **Table 3.3**). An endothermic peak that ranged from 80°C to 140°C was observed for all three CSCA products, revealing the formation of crystalline structure during the starch debranching. The large melting temperature range was due to the broad chain length distributions in the CSCA products. In a study by Moates et al. (1997), the dissolution temperature of short-chain amylose crystals increased from 57°C to 119°C with increasing CL from 12 to 55 residues. In the present study, the average CL of the CSCA products from waxy wheat, waxy maize and waxy potato starches was 28.1, 29.2 and 35.5, respectively (**Table 3.2**). The CSCA from debranched waxy potato starch displayed a higher peak melting temperature (116.2°C) than those from debranched waxy wheat (99.7°C) and waxy maize (99.9°C) starches (**Table 3.3**). The difference in melting properties was due to the longer chains generated from debranched waxy potato starch, which formed stronger double helices than the shorter chains in debranched waxy wheat and waxy maize starches.

### ***In vitro digestion***

The *in vitro* digestion profiles of waxy wheat, waxy maize, and waxy potato starches and their corresponding CSCA products are given in **Table 3.4**. Native waxy wheat starch and waxy

maize starch had high RDS (33.1% and 29.0%, respectively) and low RS content (0.4% and 4.3%, respectively). In contrast, native waxy potato starch contained very low RDS (1.2%) and high RS content (88.5%). It is well known that native normal potato starch and high amylose maize starches, both having B-type X-ray diffraction patterns, are more resistant to  $\alpha$ -amylase digestion than those starches with an A-type pattern (Dreher et al., 1984; Evans and Thompson, 2004; Gallant et al., 1997; Gerard et al., 2001; McCleary and Monaghan, 2002; Oates, 1997). In the present study, it was observed again that native waxy potato starch, which had a B-type X-ray diffraction pattern, was more resistant to enzyme digestion than cereal waxy starches with an A-type pattern. The underlying reasons of the above observations, however, are still not well understood. Gallant et al. (1997) noted that granules of normal potato starch and high-amylose maize starch appear to have a thick peripheral layer of large stacked “blocklets”. The enzyme resistance of these B-type starches may be linked to their large blocklet size. The “blocklets” comprises of both crystalline and amorphous lamellae of amylopectin that are organized in larger, more or less spherical structures. However, as pointed out by Gallant et al. (1997), wrinkled pea starch has a smaller blocklet size than smooth pea, but it is more resistant to enzyme digestion (Gallant et al 1992), indicating that other factors besides blocklet size determine the resistance to  $\alpha$ -amylase. Zhang et al. (2006) suggested that the pores and channels in waxy and normal cereal starches are large enough for enzymes to enter into the starch granules and allow enzymes to digest starch granules in a side-by-side mechanism. B-type starches without pores are more resistant to enzyme digestion. In addition, waxy wheat and waxy maize starches had a high level of SDS content (**Table 3.4**). The supramolecular A-type crystalline structure, including both the crystalline lamellae and the amorphous lamellae, has been linked to the slowly digestion property of A-type cereal starches (Zhang et al., 2006).

Comparing the digestibility of the native starches and the CSCA products (**Table 3.4**) reveals interesting results. The CSCA products from debranched waxy wheat and waxy maize starches contained a much higher RS content (67.7% and 68.1%, respectively) than the native cereal starches, which were not resistant to enzyme digestion. In the case of waxy potato starch, both native waxy potato starch and its CSCA product had high RS content but they belong to different types of RS (Englyst et al., 1992) and have different thermal stability (**Figure 3.4** and **Table 3.3**). Native potato granular starch is classified as a type 2 RS whereas CSCA has no granular structure and is considered a type 3 (cooked and crystallized) RS product. The enzyme

resistance was due to the granular structure in native waxy potato starch but largely attributed to the dense crystalline structure in the CSCA products. It is known that even though native normal potato starch has greater than 70% RS content, its RS content is reduced to less than 1% after boiling (Evans and Thompson, 2004). Similarly results would be expected for waxy potato starch because its gelatinization temperature was below 90°C and the granular structure would be lost during cooking. In contrast, the CSCA from waxy potato starch had a much higher peak melting temperature (116.2°C), suggesting that the product would have better thermal stability and more potential applications because of its high melting temperature (**Figure 3.4** and **Table 3.3**).

Among the three CSCA products, the one from debranched waxy potato starch had the lowest RDS content and highest RS content (**Table 3.4**). Those results were consistent with the yield and chain length data (**Table 3.2**), indicating that double helices formed from longer chains were more resistant to enzyme digestion.

Lopez-Rubio et al (2008) reported that the average characteristic dimension of the RS crystals was about  $\approx 5$  nm, suggesting that enzyme resistant crystals are formed from chains with a maximum DP of  $\approx 13$  for double helices (2.2 helix turns) with potential amorphous fringed ends. In this study, the CL distribution of the CSCA was peaked at around DP 16 (**Figure 3.2**). As a result, a highly dense crystalline structure was formed and became resistant to enzyme digestion.

## Conclusions

CSCA prepared from debranched waxy wheat, waxy maize, and waxy potato starches were studied and compared for the first time in this study. Waxy potato starch is the preferred starch to make a product with high RS content by debranching and crystallization. Debranched waxy potato starch had a higher average CL than debranched waxy wheat and waxy maize starches, which resulted in a higher yield of crystallized product with stronger crystalline structure, higher peak melting temperature, and higher RS content. These differences suggest that the double helices formed from the longer chains in waxy potato starch are stronger, more resistant to enzyme hydrolysis, and have better thermal stability.



## References

- Berry, C. S. (1986). Resistant starch-formation and measurement of starch that survives exhaustive digestion with amylolytic enzymes during the determination of dietary fiber. *Journal of Cereal Science*, 4, 301-314.
- Buleon, A., Veronese, G., & Putaux, J. L. (2007). Self-association and crystallization of amylose. *Australian Journal of Chemistry*, 60, 706-718.
- Cai, L., Shi, Y-C., Rong, L., & Hsiao, B.S. (2010). Debranching and crystallization of waxy maize starch in relation to enzyme digestibility. *Carbohydrate Polymers*, 81, 385-393.
- Chibbar, R. N., & Chakraborty, M. (2005). Characteristics and uses of waxy wheat. *Cereal Foods World*, 50, 121-126.
- Dreher, M. L., Dreher, C. J., & Berry, J. W. (1984). Starch digestibility of foods- A nutritional perspective. *Critical Reviews in Food Science and Nutrition*, 20, 47-71.
- Eerlingen, R. C., Deceuninck, M., & Delcour, J. A. (1993). Enzyme-resistant starch. II. Influence of amylose chain length on resistant starch formation. *Cereal Chemistry*, 70, 345-350.
- Englyst, H. N., Kingman, S. M., & Cummings, J. H. (1992). Classification and measurement of nutritionally important starch fractions. *European Journal of Clinical Nutrition*, 46, S33-S50.
- Evans, A., & Thompson, D. A. (2004). Resistance to  $\alpha$ -amylase digestion in four native high-amylose maize starches. *Cereal Chemistry*, 81, 31-37.
- FAO JECFA Monographs (2007). Joint FAO/WHO expert committee on food additives. 4, 21-23.
- Fredriksson, H., Bjorck, I., Andersson, R., Liljeberg, H., Silverio, J., Eliasson, A-C., & Aman, P. (2000). Studies on  $\alpha$ -amylase degradation of retrograded starch gels from waxy maize and high-amylopectin potato. *Carbohydrate Polymers*, 43, 81-87.
- Gallant, D. J., Bouchet, B., & Baldwin, P. M. (1997). Microscopy of starch: Evidence of a new level of granule organization. *Carbohydrate Polymers*, 32, 177-191.
- Gallant, D. J., Bouchet, B., Buleon, A., & Perez, S. (1992). Physical characteristics of starch granules and susceptibility to enzymatic degradation. *European Journal of Clinical Nutrition*, 46(Suppl.2), S3-S16.
- Gerard, C., Colonna, P., & Buleon, A. (2001). Amylolysis of maize mutant starches. *Journal of the Science of Food and Agriculture*, 81, 1281-1287.
- Gidley, M. J., & Bulpin, P. V. (1987). Crystallization of malto-oligosaccharides as models of the crystalline forms of starch: minimum chain-length requirement for the formation of double helices. *Carbohydrate Research*, 161, 291-300.
- Graybosch, R. A. (1998). Waxy wheats: Origin, properties and prospects. *Trends in Food Science & Technology*, 9,135-142.
- Guan, L., Seib, P. A., Graybosch, R. A., Bean, S., & Shi, Y.-C. (2009). Dough rheology and wet milling of hard waxy wheat flours. *Journal of Agricultural and Food Chemistry*, 57, 7030-7038.
- Guraya, H. S., James, C., & Champagne, E. T. (2001a). Effect of cooling and freezing on the digestibility of debranched rice starch and physical properties of the resulting material. *Starch/ Stärke*, 53, 64-74.
- Guraya, H. S., James, C., & Champagne, E. T. (2001b). Effect of enzyme concentration and storage temperature on the formation of slowly digestible starch from cooked debranched rice starch. *Starch/ Stärke*, 53, 131-139.

- Hanashiro, I., Abe, J., & Hizukuri, S. (1996). A periodic distribution of the chain length of amylopectin as revealed by high-performance anion-exchange chromatography. *Carbohydrate Research*, 283,151-159.
- Hizukuri, S. (1985). Relationship between the distribution of the chain-length of amylopectin and the crystalline-structure of starch granules. *Carbohydrate Research*, 141, 295-306.
- Hizukuri, S., Abe, J., & Hanashiro, I. (2006). Starch: Analytical aspects. In A-C. Eliasson (Ed.). *Carbohydrates in food* (2nd ed., pp. 305-391). Boca Raton, FL: Taylor & Francis Group.
- Jane, J., & Chen, J. F. (1992). Effect of amylose molecular size and amylopectin branch chain length on paste properties of starch. *Cereal Chemistry*, 69, 60-65.
- Jane, J., Chen, Y. Y., Lee, L. F., McPherson, A. E., Wong, K. S., Radosavljevic, M., & Kasemsuwan, T. (1999). Effects of amylopectin branch chain length and amylose content on the gelatinization and pasting properties of starch. *Cereal Chemistry*, 76, 629-637.
- Jeffcoat, R., Mason, W. R., Emling, J. L., & Chiu, C.-W. (2002). Food viscosity modification by using hydroxypropylated waxy potato distarch phosphate. *US Patent Office*, Pat. No. 6 488 980.
- Komiya, T., & Nara, S. (1986). Changes in crystallinity and gelatinization phenomena of potato starch by acid treatment. *Starch/Stärke*, 38, 9-13.
- Lebail, P., Bizot, H., & Buleon, A. (1993). B-type to A-type phase-transition in short amylose chains. *Carbohydrate Polymers*, 21, 99-104.
- Lopez-Rubio, A., Flanagan, B. M., Shrestha, A. K., Gidley, M. J., & Gilbert, E. P. (2008). Molecular rearrangement of starch during in vitro digestion: towards a better understanding of enzyme resistant starch formation in processed starches. *Biomacromolecules*, 9, 1951-1958.
- McCleary, B. V., & Monaghan, D. A. (2002). Measurement of resistant starch. *Journal of AOAC International* , 85, 665-675.
- McPherson, A. E., & Jane, J. (1999). Comparison of waxy potato with other root and tuber starches. *Carbohydrate Polymers*, 40, 57-70.
- Miao, M., Bo, J., & Zhang, T. (2009). Effect of pullulanase debranching and recrystallization on structure and digestibility of waxy maize starch. *Carbohydrate Polymers*, 76, 214-221.
- Moates, K. G., Noel, R. T., Parker, R., & Ring, G. S. (1997). The effect of chain length and solvent interactions on the dissolution of B-type crystalline polymorph of amylose in water. *Carbohydrate Research*, 298, 327-333.
- Nelson, N. (1944). A photometric adaptation of the Somogyi method for the determination of glucose. *Journal of Biological Chemistry*, 153, 375-380.
- Oates, C. G. (1997). Towards an understanding of starch granule structure and hydrolysis. *Trends in Food Science & Technology*, 8, 375-382.
- Pfannemuller, B. (1987). Influence of chain length of short monodisperse amyloses on the formation of A- and B-type X-ray diffraction patterns. *International Journal of Biological Macromolecules*, 9, 105-108.
- Ring, S. G., Miles, M. J., Morris, V. J., Turner, R., & Colonna, P. (1987). Spherulitic crystallization of short chain amylose. *International Journal of Biological Macromolecules*, 9, 158-160.
- Robyt, J. F., & Whelan, W. J. (1968). The alpha-amylases. In J. A. Radley (Ed.). *Starch and its derivatives* (pp. 432-433). Chapman & Hall Ltd, London.

- Shi, Y.-C., Capitani, T., Trzasko, P., & Jeffcoat, R. (1998). Molecular structure of a low-amylopectin starch and other high-amylose maize starches. *Journal of Cereal Science*, *27*, 289-299.
- Shi, Y.-C., Cui, X. M., Birkett, A. G., & Thatcher, M. (2005a). Slowly digestible starch product. *US Patent Office*, Pat. No. 6 890 571.
- Shi, Y.-C., Cui, X. M., Birkett, A. G., & Thatcher, M. (2005b). Slowly digestible starch product. *US Patent Office*, Pat. No. 6 929 817.
- Shi, Y.-C., Cui, X. M., Birkett, A. G., & Thatcher, M. (2006). Resistant starch prepared by isoamylase debranching of low amylose starch. *US Patent Office*, Pat. No. 7 081 261.
- Shi, Y.-C., & Seib, P. A. (1992). The structure of four waxy starches related to gelatinization and retrogradation. *Carbohydrate Research*, *227*, 131-145.
- Shin, S. I., Choi, H. J., Chung, K. M., Hamaker, B. R., Park, K. H., & Moon, T. W. (2004). Slowly digestible starch from debranched waxy sorghum starch: Preparation and properties. *Cereal Chemistry*, *81*, 404-408.
- Silverio, J., Fredriksson, H., Andersson, R., Eliasson, A. C., & Aman, P. (2000). The effect of temperature cycling on the amylopectin retrogradation of starches with different amylopectin unit-chain length distribution. *Carbohydrate Polymers*, *42*, 175-184.
- Srichuwong, S., Sunarti, T. C., Mishima, T., Isono, N., & Hisamatsu, M. (2005a). Starch from different botanical sources I: Contribution of amylopectin fine structure to thermal properties and enzyme digestibility. *Carbohydrate Polymers*, *60*, 529-538.
- Srichuwong, S., Sunarti, T. C., Mishima, T., Isono, N., & Hisamatsu, M. (2005b). Starch from different botanical sources II: Contribution of starch structure to swelling and pasting properties. *Carbohydrate Polymers*, *62*, 25-34.
- Somogyi, M. (1952). Notes on sugar determination. *Journal of Biological Chemistry*, *195*, 19-23.
- Tester, F. R.; Karkalas, J.; & Qi, X. (2004). Starch-composition, fine structure and architecture. *Journal of Cereal Science*, *39*, 151-165.
- Visser, R. G. F., Suurs, L. C. J. M., Bruinenberg, P. M., Bleeker, I., & Jacobsen, E. (1997a). Comparison between amylose-free and amylose containing potato starches. *Starch/Stärke*, *49*, 438-443.
- Visser, R. G. F., Suurs, L. C. J. M., Steeneken, P. A. M., & Jacobsen, E. (1997b). Some physicochemical properties of amylose-free potato starch. *Starch/Stärke*, *49*, 443-448.
- Whittam, M. A., Noel, T. R., & Ring, S. G. (1990). Melting behavior of A-type and B-type crystalline starch. *International Journal of Biological Macromolecules*, *12*, 359-362.
- Zhang, G., Ao, Z., & Hamaker, B. R. (2006). Slow digestion property of native cereal starches. *Biomacromolecules*, *7*, 3259-3266.

**Table 3.1 Molecular weight distributions of debranched waxy wheat, waxy maize, waxy potato starches and their crystalline short-chain amylose (CSCA) products**

Starch samples	Waxy wheat		Waxy maize		Waxy potato	
	Peak 1	Peak 2	Peak 1	Peak 2	Peak 1	Peak 2
Peak area (%)						
Debranched starch	79.8	20.2	74.2	25.8	56.5	43.5
CSCA	63.9	36.1	64.4	35.6	45.6	54.4
DP <sub>Max</sub> <sup>a</sup>						
Debranched starch	8		9		10	35
CSCA	13		11		12	35

<sup>a</sup>DP<sub>max</sub> = degree of polymerization at the peak.

**Table 3.2 Yields and average chain lengths (CL) of debranched waxy wheat, waxy maize, waxy potato starches and their corresponding crystalline short-chain amylose (CSCA) products<sup>A, B</sup>**

Debranched Starch samples	Average CL (whole starch)	Average CL (CSCA products)	Yield of CSCA (%)
Waxy wheat starch	21.8 <sup>b</sup>	28.1 <sup>b</sup>	58.7 <sup>b</sup>
Waxy maize starch	24.1 <sup>b</sup>	29.2 <sup>b</sup>	60.7 <sup>b</sup>
Waxy potato starch	32.1 <sup>a</sup>	35.5 <sup>a</sup>	72.6 <sup>a</sup>

<sup>A</sup> Yield of CSCA (%) =  $(W_{\text{Precipitate}} / W_{\text{Starch}}) \times 100$ .

<sup>B</sup> Values with the same letter in the same column are not significantly different ( $p < 0.05$ ).

**Table 3.3 Thermal properties of waxy wheat, waxy maize, waxy potato starches and debranched crystalline short-chain amylose (CSCA) products as determined by differential scanning calorimetry <sup>A, B</sup>**

Samples	Native starches				CSCA products			
	T <sub>o</sub> (°C)	T <sub>p</sub> (°C)	To(°C)	ΔH(J/g)	T <sub>o</sub> (°C)	T <sub>p</sub> (°C)	T <sub>c</sub> (°C)	ΔH(J/g)
Waxy wheat	59.7 <sup>c</sup>	67.8 <sup>c</sup>	92.9 <sup>b</sup>	15.6 <sup>b</sup>	83.4 <sup>a</sup>	99.7 <sup>b</sup>	136.4 <sup>a</sup>	18.3 <sup>b</sup>
Waxy maize	64.3 <sup>a</sup>	73.5 <sup>a</sup>	94.6 <sup>a</sup>	18.9 <sup>a</sup>	76.7 <sup>b</sup>	99.9 <sup>b</sup>	135.9 <sup>a</sup>	18.6 <sup>ab</sup>
Waxy potato	62.5 <sup>b</sup>	70.4 <sup>b</sup>	89.1 <sup>c</sup>	18.3 <sup>a</sup>	80.8 <sup>ab</sup>	116.2 <sup>a</sup>	133.8 <sup>a</sup>	19.2 <sup>a</sup>

<sup>A</sup> The ratio of sample (dry basis) and water was 1:3.

<sup>B</sup> Values with the same letter in the same column are not significantly different ( $p < 0.05$ ).

**Table 3.4 Levels of rapidly digestible starch (RDS), slowly digestible starch (SDS), and resistant starch (RS) in waxy wheat, waxy maize, waxy potato starches and debranched crystalline short-chain amylose (CSCA) products<sup>A, B</sup>**

Samples	Native starches			CSCA products		
	RDS (%)	SDS (%)	RS (%)	RDS (%)	SDS (%)	RS (%)
Waxy wheat starch	33.1 <sup>a</sup>	66.5 <sup>a</sup>	0.4 <sup>c</sup>	18.6 <sup>a</sup>	13.7 <sup>a</sup>	67.7 <sup>b</sup>
Waxy maize starch	29.0 <sup>a</sup>	66.7 <sup>a</sup>	4.3 <sup>b</sup>	17.5 <sup>a</sup>	14.4 <sup>a</sup>	68.1 <sup>b</sup>
Waxy potato starch	1.2 <sup>b</sup>	10.3 <sup>b</sup>	88.5 <sup>a</sup>	13.5 <sup>b</sup>	8.7 <sup>b</sup>	77.8 <sup>a</sup>

<sup>A</sup> RS% = 100% - RDS% - SDS%.

<sup>B</sup> Values with the same letter in the same column are not significantly different ( $p < 0.05$ ).

**Figure 3.1** Molecular weight distributions of (A) debranched waxy wheat, waxy maize, and waxy potato starches; (B) crystalline short-chain amylose (CSCA) products from debranched waxy wheat, waxy maize and waxy potato starches

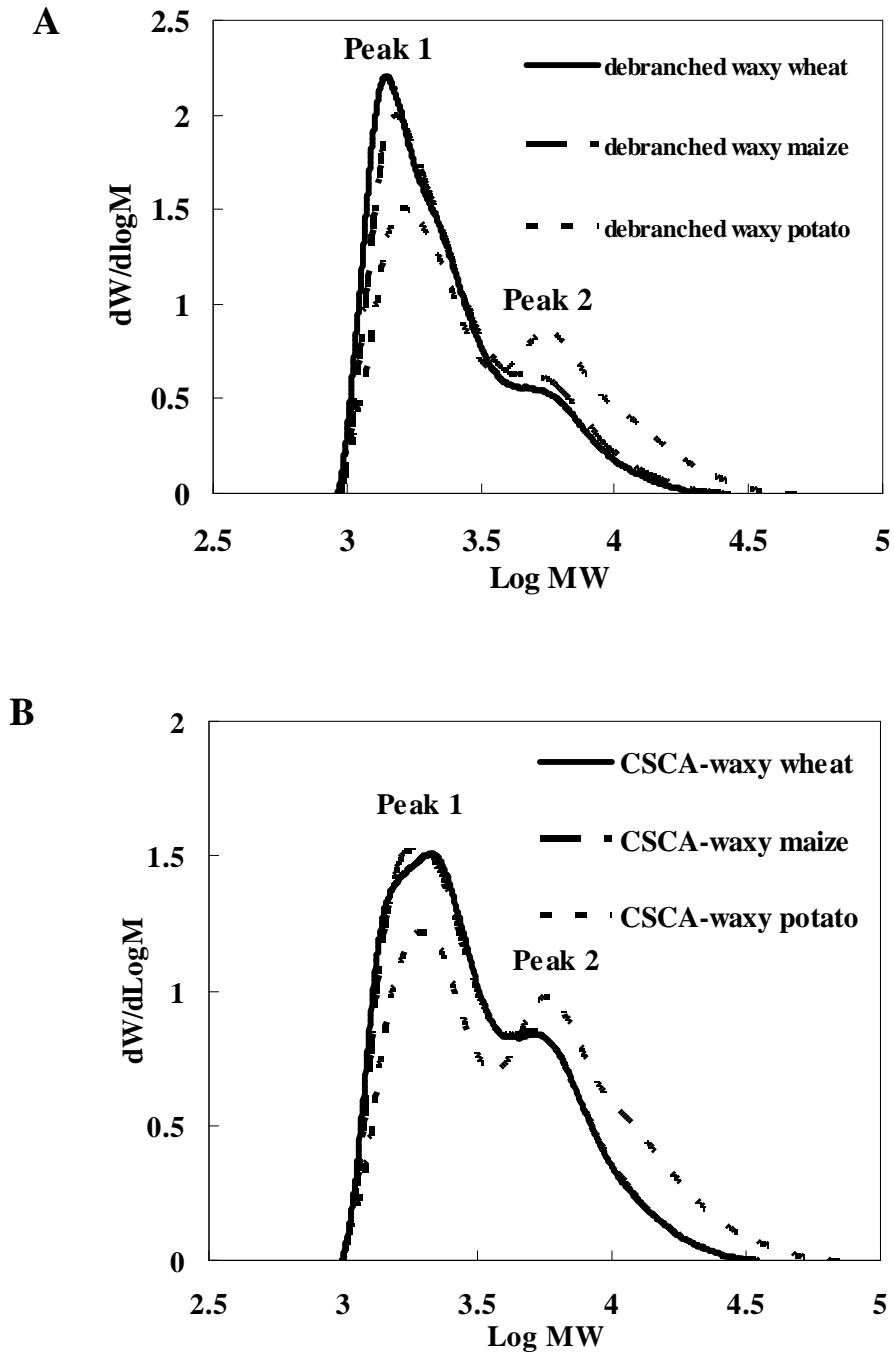




**Figure 3.2** Chain length distributions of (A) debranched waxy wheat starch and its CSCA product; (B) debranched waxy maize starch and its CSCA product; (C) debranched waxy potato starch and its CSCA product

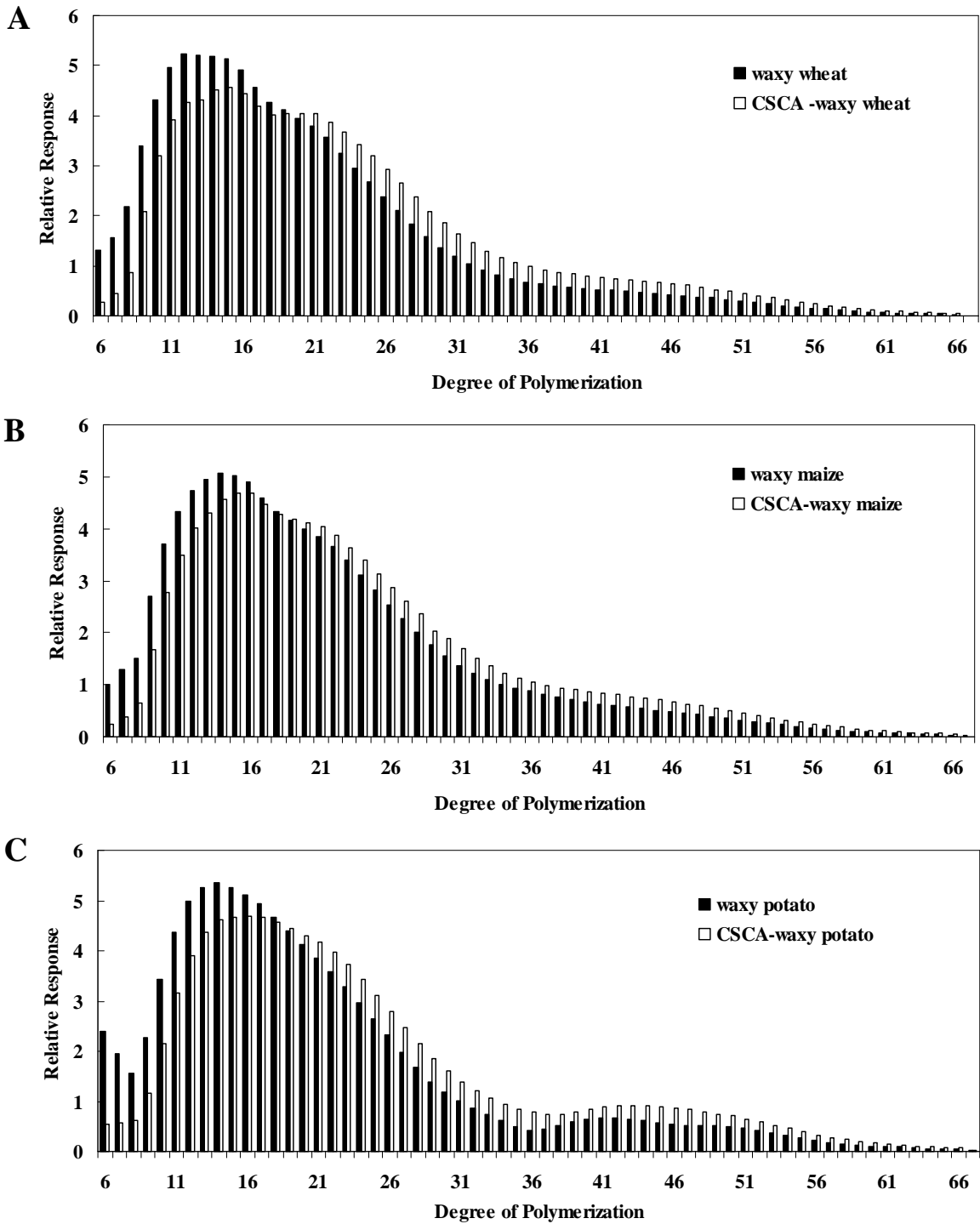


**Figure 3.3 X-ray diffraction patterns of waxy wheat, waxy maize, waxy potato starches and debranched crystalline short-chain amylose (CSCA) products**

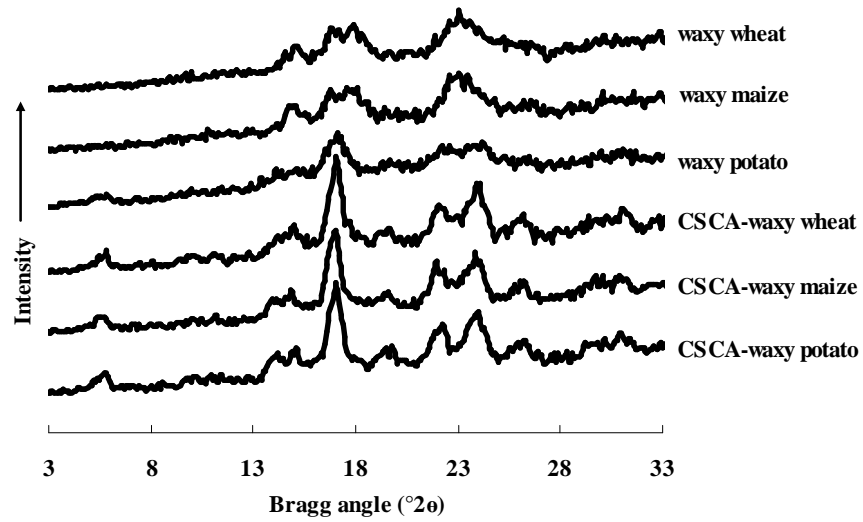
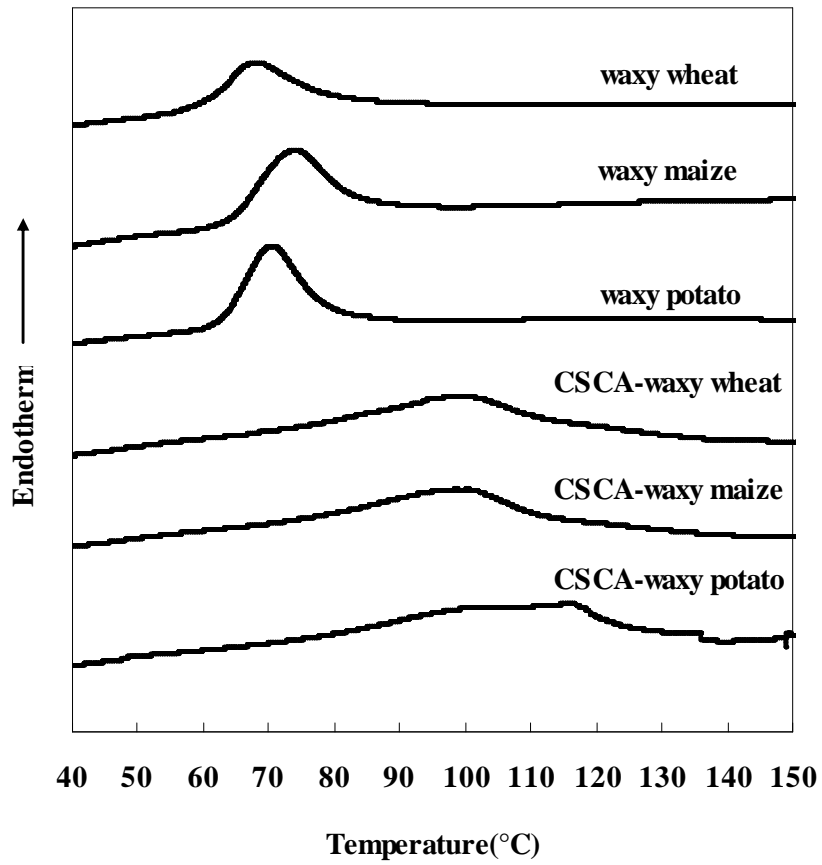


**Figure 3.4** Differential scanning calorimetry thermograms of waxy wheat, waxy maize, waxy potato starches and debranched crystalline short-chain amylose (CSCA) products



## **Chapter 4 - Study on melting and crystallization of short-chain amylose by *in situ* synchrotron wide-angle X-ray diffraction**

### **Abstract**

*In-situ* melting and crystallization of short-chain amylose (SCA) from debranched waxy starches were investigated by synchrotron wide-angle X-ray diffraction (WAXD). Amorphous SCA was prepared by dissolving completely debranched waxy wheat, waxy maize and waxy potato starches into alkaline solution and neutralized by hydrochloric acid. When hydrated with about 50% water at 25°C, all amorphous SCA crystallized immediately and gave a B-type X-ray diffraction pattern. The hydrated SCA paste was heated from 25 to 100°C at 10°C/min, held for 5min, and cooled to 25°C at 10°C/min. The whole heating and cooling process was monitored by WAXD. The SCA from debranched waxy potato starch had higher average chain length, higher melting temperature, but relatively lower crystallinity upon hydration. It was not completely melted at 100°C and remained its original B-type polymorph during rapid cooling. In contrast, the SCA from debranched waxy wheat and waxy maize starch had a large portion of low molecular weight fraction, a higher crystallinity upon hydration but a lower melting temperature. These differences suggest that amylopectin short chains crystallized more readily but their crystals were weaker than those of long chains. After the SCA from waxy wheat and waxy maize starches was melted, it reformed into an A-type polymorph under rapid cooling. The thermal properties as determined by differential scanning calorimetry showed that the A-type polymorph of debranched waxy wheat and waxy maize starches had a higher melting temperature (ca. 120°C) than their B-type structure (ca. 90°C).

### **Introduction**

Wide-angle X-ray diffraction (WAXD) using synchrotron radiation has been developed as a tool for analysis of polymers (Riekkel and Davies, 2005). This method has advantages over the conventional WAXD such as high intensity of radiation and short acquisition time, and enables experiments under real-time conditions (Ezquerria et al, 2009). Synchrotron WAXD has been applied to study ultrastructure of starch (Buleon et al, 1998), gelatinization behaviors (Gebhardt et al, 2007), and amylose-lipid interactions (Derycke et al, 2005). Monitoring structural changes of starch during heat treatment (Cagiao et al, 2004), and allomorphic

transition of native starch and amylose spherocrystals (Nishiyama et al, 2010) by using *in situ* synchrotron WAXD were also reported.

In present work, melting and crystallization of short-chain  $\alpha$ -glucans from debranched waxy wheat, waxy maize and waxy potato starches were investigated in real time by synchrotron WAXD. Waxy wheat, waxy maize and waxy potato starches have different unit chain length distributions (Cai and Shi, 2010). The objectives were to study effects of crystallization temperature and chain length on the dynamic changes of SCA polymorphs and gain insight into the mechanism of starch retrogradation.

## **Materials and methods**

### ***Materials***

Waxy wheat starch was isolated from hard waxy wheat flour as described by Guan et al. (2009). Waxy maize starch was provided by National Starch LLC (Bridgewater, NJ, USA). Waxy potato starch was obtained from Penford Food Ingredients Company (Centennial, CO, USA). Isoamylase (EC 3.2.1.68, enzyme activity:  $1.41 \times 10^6$  IAU/g, 1 IAU is defined as the amount of isoamylase that increased absorbance of the reaction mixture by 0.008 in 30 min under the conditions of the isoamylase assay) was obtained from Hayashibara Biochemical Laboratories, Inc. (Okayama, Japan).

### ***Starch debranching and preparation of SCA***

Starch (5 g, dry basis) was mixed with 95 mL acetic acid buffer (0.01 M, pH 4.0) in a sealed glass bottle and cooked in a boiling water bath with stirring for 1 h. After the mixture was cooled to 50°C, 1% isoamylase based on the dry weight of starch was added. The mixture was kept at 50°C with stirring. After 24 h, the mixture was freeze-dried and saved as SCA product. This product was confirmed to be linear and completely debranched (Cai and Shi, 2010).

### ***Preparation of amorphous SCA***

SCA (0.5g, db) was dissolved in 5 mL 1M NaOH solution and neutralized by 5 mL 1M HCL acid. The mixture was slowly added into 150 mL ethanol with continuous stirring. The beaker was put into the refrigerator overnight to facilitate the precipitation. After centrifuge three times, the supernatant was decanted and the precipitate was collected and vacuum dried. The

dried amorphous SCA was then gently ground with a pestle and mortar. In order to prove that salts have no effects on the products, 5 mL 1M NaOH was neutralized by 5 mL 1M HCl, and added to 150 mL ethanol with continuous stirring, and stored at 4°C, no precipitation was observed.

### ***Synchrotron WAXD***

Synchrotron WAXD experiment was carried out at the Advanced Polymers Beamline (X27C) in the National Synchrotron Light Source, Brookhaven National Laboratory, in Upton, NY. The details of the experimental setup at the X27C beamline have been reported elsewhere (Chen et al, 2006; Chen et al, 2007; Chu and Hsiao, 2001). The wavelength used was 0.1371 nm. The sample-to-detector distance was 94.8 mm. A 2D MAR-CCD X-ray detector (MAR USA, Inc., Norwood, NJ, USA) was used for data collection.

Amorphous SCA was mixed with water to make ca.50% solids. The mixture was put into a sample holder, sealed and placed into a hot stage (Instec Inc., Boulder, CO, USA). The sample was heated from 25 to 100°C at 10°C/min, held at 100°C for 5min, and cooled from 100°C to 25°C at 10°C/min. The *in-situ* melting and crystallization was monitored by using synchrotron WAXD. No weight changes were observed for the sample before and after heating, indicating that no moisture was lost during the experiment.

The relative crystallinity of samples was estimated by the ratio of the peak areas to the total diffractogram area (Komiya and Nara, 1986). By using X-ray line-broadening technique (Cairns et al, 1997), the approximate average size (D) in nm of crystallites in samples was calculated from Scherrer formula:  $D = 0.9\lambda/\beta/\cos\theta$ , where  $\lambda$  is wavelength used;  $\beta$  is peak broadening given by full width at half maximum in radians of diffraction peak minus full width at half maximum in radians of a peak from a standard sample;  $\theta$  is half of angular position of peak in radians.

### ***Differential scanning calorimetry (DSC)***

Amorphous SCA suspension in water (50% solids) was prepared and sealed in a DSC pan and analyzed with a TA Q200 instrument (TA Instruments, New Castle, DE, USA). Samples were heated from 10°C to 160°C at 10°C /min to study the melting behavior. To study the crystallization of SCA during cooling, samples were heated from 10 to 100 °C at 10 °C/min, held at 100 °C for 5 min, cooled from 100 °C to 10 °C at 10 °C/min, and rescanned from 10 to 160 °C

at 10 °C/min. An empty pan was used as a reference. The onset ( $T_o$ ), peak ( $T_p$ ), and conclusion ( $T_c$ ) temperatures and enthalpy ( $\Delta H$ ) were calculated from the DSC endotherm (TA Instruments, New Castle, DE, USA). All experiments were conducted in duplicates.

## Results

### *Synchrotron WAXD of powder and hydrated SCA*

The synchrotron WAXD results of powder and hydrated SCA from debranched waxy starches are shown in **Figure 4.1**. In the powder state, all SCA from debranched waxy starches showed amorphous X-ray diffraction pattern, indicating that the crystalline structure of SCA was completely disrupted after dissolving in the alkaline solution; however, all SCA gave a typical B-type diffraction pattern when hydrated with about 50% water (**Figure 4.1**). This phenomenon was attributed to the rapid crystallization of SCA. Comparing to rigid long-chain amylose and amylopectin with highly branched architecture, SCA has greater mobility and could associate together immediately to form the double helices, especially under such a high solids concentration condition (50%). At the low temperature (25°C), B-type rather than the A-type structure was formed.

Interestingly, SCA from debranched waxy wheat and waxy maize starches had a higher crystallinity (58.7% and 55.6%, respectively) and a larger average crystal size (11.5 and 10.9 nm, respectively), as compared to SCA from debranched waxy potato starch, which had a lower crystallinity of 53% and a smaller average crystal size of 10.4 nm (**Table 4.1**). This result was related with the chain length (CL) of SCA. The average CLs of debranched waxy wheat, waxy maize, and waxy potato starches were 21.8, 24.1, and 32.1 glucose units, respectively (Cai and Shi, 2010). Debranched waxy wheat and waxy maize starches contained larger portion of low molecular weight fraction than debranched waxy potato starch. Small chains possess higher mobility than large chains, and could have a greater interaction with each other, resulting in more crystalline materials.

### *Melting and crystallization of SCA from waxy starches*

#### *Waxy wheat starch*

The dynamic synchrotron WAXD results of SCA from debranched waxy wheat starch during heating and cooling is given on **Figure 4.2**. The peaks of B-type X-ray diffraction pattern remained intact between 25 to 60°C, but started to weaken from 70°C, and almost disappeared at 100°C (**Figure 4.2A**). During cooling (**Figure 4.2B**), a weak A-type diffraction pattern was observed at 100°C and became evident with the decrease in temperature. Notably, a small residual peak occurred around  $2\theta$  of 5°, which is mostly characteristic of B-type structure pattern. One explanation for this is that the original B-type polymorph was not completely melted. Another hypothesis is that a small amount of B-type polymorph accompanied with the formation of A-type polymorph, but this residue structure did not affect the predominant A-type structure of SCA formed during cooling.

#### ***Waxy maize starch***

Similarly, the B-type polymorph of SCA of debranched waxy maize starch was disrupted above 70 °C, and almost melted at 100°C (**Figure 4.3A**). An A-type diffraction pattern was detected at 100°C and became clear when temperature decreased (**Figure 4.3B**). Unlike the SCA from debranched waxy wheat starch, the small peak of SCA from debranched waxy maize starch around 5° $2\theta$  was stronger and better resolved during cooling, suggesting that a little B-type structure was accompanied by A-type structure during cooling.

#### ***Waxy potato starch***

**Figure 4.4** shows the dynamic synchrotron WAXD results of SCA from debranched waxy potato starch during heating and cooling. The crystallinity of SCA started to decrease above 70°C, but most B-type polymorph was retained at 100°C (**Figure 4.4A**). The hydrated SCA from debranched waxy potato starch appeared to have a lower degree of crystallinity (**Table 4.1, Figure 4.1C**), but was more resistant to heat than those from debranched waxy wheat and waxy maize starches (**Figure 4.2A and 4.3A**). The difference suggested that long chains, despite their lower mobility, could form more stable double helices and be more resistant to thermal heating.

Unlike debranched waxy wheat and waxy maize starches, the original B-type X-ray diffraction pattern remained in SCA from debranched waxy potato starch and no significant structural change was observed during cooling (**Figure 4.4B**). Notably, those melted SCA, although in small amount, were not rearranged into A-type (or B-type) structure as expected.



There are two possible explanations for this phenomenon: (1) The remaining B-type structures may act as nuclei, and those melted chains can associate into double helices, but present in the amorphous region; and (2) the remaining B-type structures may act as barriers to inhibit the formation of B-type structure from free SCA, since the formation of B-type polymorph is a reversible equilibrium (kinetic event). It is hard to prove which explanation is good at current point.

### *Thermal properties of SCA from waxy starches*

Interestingly, a broad melting endotherm and a broad exothermic peak were observed when directly heating samples from 10 to 160°C (**Table 4.2 and Figure 4.5**). The broadness of the curves indicated that SCA samples had a large variation in crystal size and perfection. The melting peak of SCA from debranched waxy wheat, waxy maize and waxy potato starches was centered at 87.3, 87.3 and 91.0°C, respectively, whereas the crystallization peak was centered at 118.9, 119.3 and 121.5°C, respectively. Similar phenomena in amylose-lipid complexes were observed by Biliaderis et al (1985), who proposed that two thermal events were involved: melting of the original crystallites and recrystallization during heating. Thus, one possible explanation for our results was that part of the SCA melted at a lower temperature (~55-105°C), but readily recrystallized at a higher temperature (~105-150°C). Debranched waxy wheat and waxy maize starch melted around 100°C with a higher enthalpy (~13.5 J/g), whereas debranched waxy potato starch was disassociated at slightly higher temperature (~105°C) with a lower enthalpy of 10.6 J/g (**Table 4.2 and Figure 4.5**). This observation was consistent with the WAXD results that debranched waxy wheat and waxy maize starch had a higher crystallinity but almost completely melted at 100°C, whereas debranched waxy potato starch showed a lower crystallinity and was not completely melted at 100°C (**Table 4.1, Figures 4.1-4.4**). Because the moisture used in DSC study was 50%, limited hydration of the sample could have affected the thermal behaviors of SCA. To eliminate this impact, debranched waxy starches (adjusted to a moisture of 75%) were heated from 10 to 160°C at 10°C/min; similar results were observed (**Figure 4.5**), indicating that the melting followed by the immediate crystallization during heating was the nature of SCA, not because of the low water content used (50%).

To further understand the recrystallization observed by WAXD, SCA from debranched waxy wheat, waxy maize, and waxy potato starches was heated to 100 °C, cooled and rescanned

by DSC (**Table 4.3 and Figure 4.5**). All debranched waxy starches displayed an onset melting temperature of 60-70°C when heated from 10 to 100°C at 10°C/min, which was in agreement with the synchrotron WAXD data, indicating that the materials started melting around 70°C. The enthalpy of debranched waxy wheat, waxy maize and waxy potato starches was 8.9, 8.4 and 7.6 J/g, respectively. After cooling from 100°C at 10°C/min, an endotherm with a melting temperature ranged from about 100°C to 150°C was observed at the second scan for all debranched waxy starches. The enthalpy of debranched waxy wheat, waxy maize and waxy potato starches was 13.0, 15.7 and 17.2 J/g, respectively. The shift of melting peak from lower temperature to higher temperature after cooling debranched waxy wheat and waxy maize starches at 10°C/min could be explained by the crystallization behaviors of SCA. Based on the synchrotron WAXD data (**Figure 4.2 and 4.3**), an A-type structure was formed during cooling melted B-type structure of debranched waxy wheat and waxy maize starches. SCA with A-type structure was reported to have a higher melting temperature than those with B-type polymorph (Cai et al, 2010; Cai and Shi, 2010; Planchot et al, 1997; Whittam et al, 1990; Williamson et al, 1992). In this study, the peak melting temperature of A-type structure of debranched waxy wheat starch was 119°C compared to 87.9°C of B-type structure. Similarly, the melting peaks of A-type and B-type structure of debranched waxy maize starch were centered at 128.1°C and 87.2°C, respectively; however, the debranched waxy potato starch was an exception. After cooling, the remained B-type structure was centered at around 134.1°C, which may be attributed to its longer chain length and stronger double helices.

Our data showed that SCA could crystallize during either cooling (WAXD and DSC results) or heating (DSC results). Due to safety concerns, the temperature was not heated above 100°C in our WAXD experiments; therefore, no information was available regarding the polymorph of the recrystallized materials above 100°C. Further studies are needed to heat samples to higher temperatures in a sealed pressure cell and elucidate the mechanism behind such changes.

## Discussion

Compared to complex architecture of amylopectin, SCA is a short linear segment of  $\alpha$ -1,4-glucans and may retrograde into crystalline structure more readily (Cai et al, 2010). Depending on crystallization conditions such as solvent, chain length, concentration and temperature, SCA

could be rearranged as different crystalline types (Buleon et al, 2007; Cai et al, 2010; Cai and Shi, 2010; Gidley and Bulpin, 1987; Lebail et al, 1993; Pfannemuller, 1987; Planchot et al, 1997; Ring et al, 1987; Whittam et al, 1990; Williamson et al, 1992). Generally, shorter chain length, higher concentration and higher temperature favor the formation of A- type crystallites, whereas the reverse situations induce B- type crystallization. The main differences between A- and B-structure are the packing of double helices (monoclinic and hexagonal arrangement, respectively) and the water amount (8 and 36 water molecules, respectively) in the crystal unit cell (Imberty et al, 1988; Imberty and Perez, 1988; Takahashi et al, 2004; Popov et al, 2009).

In this study, we observed formation of A-type polymorph from a melted B-type crystalline structure. **Figure 4.6** depicts the melting and crystallization of SCA studied using synchrotron WAXD. The A-structure was formed from the rapid cooling of a hot solution of SCA from high temperature, whereas B-structure was obtained with hydration of amorphous SCA at low temperature. The A-type structure was suggested to be a thermodynamic product whereas the B-type polymorph is a kinetic event (Gidley, 1987). Thus, A-type structure is favored at high temperature and is more thermal stable than the B-type polymorph.

Crystallization or retrogradation of starch is important in bakery products such as bread staling. After baking, starch is partially gelatinized and formed B-type crystalline structure during staling (Ribotta et al, 2004); however, the starch crystal polymorph formed upon retrogradation is largely dependent on the conditions at which the recrystallization proceeds and the storage time of retrogradation. Obtaining A-type rather than B-type polymorph after retrogradation is possible. Lionetto et al (2005) studied the retrogradation of concentrated wheat starch systems. They observed that wheat starch extrudates (both 37% and 51% water content) predominantly crystallized into the A-polymorph after stored at 25 °C for 7 days. Ottenhof et al (2005) compared the retrogradation behaviors of extruded waxy maize, wheat and potato starches with intermediate water content (34%). After about 3 days of storage at 25°C, waxy maize and wheat starch essentially crystallized to the A-type polymorph while potato starch crystallized into the B-type polymorph. Bello-Perez et al (2005) found that extruded banana starch retrograded from its native mixture of A- and B-type polymorphs to the A-type polymorph after stored at 25 °C and at 30% water content. Eerlingen et al (1993) prepared enzyme resistant starch (RS) by incubation of autoclaved wheat starch at different temperatures. RS formed at 100 °C showed A-type X-ray diffraction pattern, whereas B-type polymorph was observed for RS

incubated at 0 or 68 °C. According to Farhat et al (2001), extruded potato starch retrograded to B-type, C-type (mixture of pure A- and B- polymorph) and A-type polymorphs, when stored at 22 °C, 40 °C and 60 °C respectively, at 35% moisture content. Investigating the possibility of holding bakery products at high storage temperature long enough or cooling rapidly from high temperature after baking to induce an A-type structure would be interesting, as would determining the texture and digestibility of the products with an A-type X-ray diffraction pattern.

## **Conclusions**

Melting and crystallization of SCA were investigated for the first time by synchrotron WAXD *in-situ*. All amorphous SCA from debranched waxy starches immediately crystallized into B-type polymorph when hydrated (moisture content ca.50%) at 25°C. SCA from debranched waxy potato starch with higher average chain length showed a relatively low crystallinity and a higher melting temperature; it did not completely melt at 100°C and its original B-type polymorph remained during rapid cooling. In contrast, SCA from debranched waxy wheat and waxy maize starch contained a large portion of low molecular weight fractions, thus had a higher crystallinity and a lower melting temperature. When melted, it could predominantly reform into an A-type polymorph under rapid cooling. The reformed A-type polymorph of debranched waxy wheat and waxy maize starches had a higher melting temperature (ca. 120°C) than their original B-type structure (ca.90°C).

## References

- Bello-Perez, L. A., Ottenhof, M. A., Agama-Acevedo, E., & Farhat, I. A. (2005). Effect of storage time on the retrogradation of banana starch extrudate. *Journal of agricultural and food chemistry*, 53, 1081-1086.
- Biliaderis, C.G., Page, C. M., Slade, L., & Sirett, R. R. (1985). Thermal behavior of amylose-lipid complexes. *Carbohydrate Polymers*, 5, 367-389.
- Buleon, A., Gerard, C., Riekkel, C., Vuong, R., & Chanzy, H. (1998). Details of crystalline ultrastructure of C-starch granules revealed by synchrotron microfocus mapping. *Macromolecules*, 31, 6605-6610.
- Buleon, A., Veronese, G., & Putaux, J. L. (2007). Self-association and crystallization of amylose. *Australian Journal of Chemistry*, 60, 706-718.
- Cagiao, M. E., Rueda, D. R., Bayer, R. K., & Calleja, F. J.B. (2004). Structural changes of injection molded starch during heat treatment in water atmosphere: simultaneous wide and small-angle X-ray scattering study. *Journal of Applied Polymer Science*, 93, 301-309.
- Cairns, P., Bogracheva, T.Y., Ring, S.G., Hadley, C.L., & Morris, V.J. (1997). Determination of the polymorphic composition of smooth pea starch. *Carbohydrate Polymers*, 32, 275-282.
- Cai, L., & Shi, Y-C. (2010). Structure and digestibility of crystalline short-chain amylose from debranched waxy wheat, waxy maize and waxy potato starches. *Carbohydrate Polymers*, 79, 1117-1123.
- Cai, L., Shi, Y-C., Rong, L., & Hsiao, B.S. (2010). Debranching and crystallization of waxy maize starch in relation to enzyme digestibility. *Carbohydrate Polymers*, 81, 385-393.
- Chen, X. M., Burge, C., Fang, D. F., Ruan, D., Zhang, L., Hsiao, B. S., & Chu, B. (2006). X-ray studies of regenerated cellulose fibers wet spun from cotton linter pulp in NaOH/thiourea aqueous solutions. *Polymer*, 47, 2839-2848.
- Chen, X. M., Burge, C., Wan, F., Zhang, J., Rong, L. X., Hsiao, B. S., Chu, B., Cai, J., & Zhang, L. (2007). Structure study of cellulose fibers wet-spun from environmentally friendly NaOH/urea aqueous solutions. *Biomacromolecules*, 8, 1918-1926.
- Chu, B., & Hsiao, B. S. (2001). Small-angle X-ray scattering of polymers. *Chemical Reviews*, 101, 1727-1761.
- Derycke, V., Vandeputte, G. E., Vermeylen, R., De Man, W., & Goderis, B. et al. (2005). Starch gelatinization and amylose-lipid interactions during rice parboiling investigated by temperature resolved wide angle X-ray scattering and differential scanning calorimetry. *Journal of Cereal Science*, 42, 334-343.
- Ezquerria, T. A., Garcia-Gutierrez, M. C., Nogales, A., & Gomez, M. (2009). Applications of synchrotron light to scattering and diffraction in materials and life sciences. *Lecture notes in physics 776*. Springer- Verlag Berlin Heidelberg.
- Eerlingen, R. C., Crombez, M., & Delcour, J. A. (1993). Enzyme-resistant starch. I. Quantitative and qualitative influence of incubation time and temperature of autoclaved starch on resistant starch formation. *Cereal Chemistry*, 70, 339-344.
- Farhat, I. A., Protzmann, J., Becker, A., Valles-Pamies, B., Neale, R., & Hill, S. E. (2001). Effect of the extent of conversion and retrogradation on the digestibility of potato starch. *Starch/Stärke*, 53, 431-436.
- Gebhardt, R., Hanfland, M., Mezouar, M., & Riekkel, C. (2007). High-pressure potato starch granule gelatinization: Synchrotron radiation Micro-SAXS/WAXS using a diamond anvil cell. *Biomacromolecules*, 8, 2092-2097.

- Gidley, M. J. (1987). Factors affecting the crystalline type (AC) of native starches and model compounds- A rationalization of observed effects in terms of polymorphic structures. *Carbohydrate Research*, 161, 301-304.
- Gidley, M. J., & Bulpin, P. V. (1987). Crystallization of malto-oligosaccharides as models of the crystalline forms of starch: minimum chain-length requirement for the formation of double helices. *Carbohydrate Research*, 161, 291-300.
- Guan, L., Seib, P. A., Graybosch, R. A., Bean, S., & Shi, Y.-C. (2009). Dough rheology and wet milling of hard waxy wheat flours. *Journal of Agricultural and Food Chemistry*, 57, 7030-7038.
- Imberty, A., Chanzy, H., Perez, S., Buleon, A., & Tran, V. (1988). The double-helical nature of the crystalline part of A-starch. *Journal of Molecular Biology*, 201, 365-378.
- Imberty, A., & Perez, S. (1988). A revisit to the 3-dimensional structure of B-type starch. *Biopolymers*, 27, 1205-1221.
- Lebail, P., Bizot, H., & Buleon, A. (1993). B-type to A-type phase-transition in short amylose chains. *Carbohydrate Polymers*, 21, 99-104.
- Lionetto, F., Maffezzoli, A., Ottenhof, M-A., Farhat, I. A., & Mitchell, J. R. (2005). The retrogradation of concentrated wheat starch systems. *Starch/ Stärke*, 57, 16-24.
- Komiya, T., & Nara, S. (1986). Changes in crystallinity and gelatinization phenomena of potato starch by acid treatment. *Starch/Stärke*, 38, 9-13.
- Nishiyama, Y., Putaux, J. I., Montesanti, N., Hazemann, J. L., & Rochas, C. (2010). B→A allomorphic transition in native starch and amylose spherocrystals monitored by in situ synchrotron X-ray diffraction. *Biomacromolecules*, 11, 76-87.
- Ottenhof, M-A., Hill, S.E., & Farhat, I. A. (2005). Comparative study of the retrogradation of intermediate water content waxy maize, wheat and potato starches. *Journal of agricultural and food chemistry*, 53, 631-638.
- Pfannemuller, B. (1987). Influence of chain length of short monodisperse amyloses on the formation of A- and B-type X-ray diffraction patterns. *International Journal of Biological Macromolecules*, 9, 105-108.
- Planchot, V., Cononna, P., & Buleon, A. (1997). Enzymatic hydrolysis of  $\alpha$ -glucan crystallites. *Carbohydrate Research*, 298, 319-326.
- Popov, D. ; Buleon, A. ; Burghammer, M., Chanzy, H., Montesanti, N., Putaux, J.-L., Potocki-Veronese, G., & Riekkel, C. (2009). Crystal structure of A-amylose: A revisit from synchrotron microdiffraction analysis of single crystals. *Macromolecules*, 42, 1167-1174.
- Ribotta, P. D., Cuffini, S., Leon, A. E., & Anon, M. C. (2004). The staling of bread: an X-ray diffraction study. *European Food Research and Technology*, 218, 219-223.
- Riekkel, C., & Davies, R. J. (2005). Applications of synchrotron radiation micro-focus techniques to the study of polymer and biopolymer fibers. *Current Opinion in Colloid & Interface Science*, 9, 396-403.
- Ring, S. G., Miles, M. J., Morris, V. J., Turner, R., & Colonna, P. (1987). Spherulitic crystallization of short chain amylose. *International Journal of Biological Macromolecules*, 9, 158-160.
- Takahashi, Y., Kumano, T., & Nishikawa, S. (2004). Crystal structure of B-amylose. *Macromolecules*, 37, 6827-6832.
- Whittam, M.A., Noel, T.R., & Ring, S.G. (1990). Melting behavior of A-type and B-type crystalline starch. *International journal of biological macromolecules*, 12, 359-362.

Williamson, G., Belshaw, N. J., Self, D. J., Noel, T. R., Ring, S. G., Cairns, P., Morris, V. J., Clark, S. A., & Parker, M. L. (1992). Hydrolysis of A-type and B-type crystalline polymorphs of starch by Alpha-amylase, Beta-amylase and Glucoamylase-1. *Carbohydrate Polymers*, 18, 179-187.

**Table 4.1 Relative crystallinity and approximate average size of polymorph crystallites of short-chain amylose from debranched waxy wheat starch, debranched waxy maize starch and debranched waxy potato starch as determined by synchrotron wide-angle X-ray diffraction<sup>A, B</sup>**

Samples	Relative Crystallinity (%)	Average size of crystallites (nm)
Debranched waxy wheat	58.7±0.3	11.5±0.3
Debranched waxy maize	55.6±0.1	10.9±0.1
Debranched waxy potato	53.0±1.0	10.4±0.1

<sup>A</sup> The relative crystallinity was estimated by the ratio of the peak areas to the total diffractogram area (Komiya and Nara, 1986).

<sup>B</sup> The approximate average crystal size was calculated by using X-ray line-broadening technique (Cairns et al, 1997).



**Table 4.2 Melting and crystallization of short-chain amylose from debranched waxy wheat starch, debranched waxy maize starch and debranched waxy potato starch as determined by differential scanning calorimetry <sup>A, B</sup>**

Samples	Melting Peak				Crystallization Peak			
	T <sub>o</sub> (°C)	T <sub>p</sub> (°C)	To(°C)	ΔH(J/g)	T <sub>o</sub> (°C)	T <sub>p</sub> (°C)	To(°C)	ΔH(J/g)
Debranched waxy wheat	52.7±0.6	87.3±1.5	100.7±0.9	13.4±0.8	103.6±0.6	118.9±0.8	144.3±1.7	15.1±0.2
Debranched waxy maize	54.0±0.9	87.3±0.7	101.3±1.3	13.5±0.1	103.9±1.0	119.3±1.7	148.4±1.2	15.0±0.6
Debranched waxy potato	59.2±0.5	91.0±0.2	104.3±0.6	10.6±0.4	106.0±0.3	121.5±0.8	148.8±0.3	15.2±0.6

<sup>A</sup> The ratio of sample (dry basis) and water was 1:1. The samples were heated from 10 to 160°C at 10°C/min.

<sup>B</sup> Mean ± standard deviation values are reported.

**Table 4.3 Thermal properties of short-chain amylose from debranched waxy wheat starch, debranched waxy maize starch and debranched waxy potato starch as determined by differential scanning calorimetry <sup>A, B</sup>**

Samples	First Scan				Second Scan			
	T <sub>o</sub> (°C)	T <sub>p</sub> (°C)	To(°C)	ΔH(J/g)	T <sub>o</sub> (°C)	T <sub>p</sub> (°C)	To(°C)	ΔH(J/g)
Debranched waxy wheat	62.5±0.8	87.9±0.4	97.9±0.3	8.9±0.5	101.4±0.8	119±0.5	148.2±1.2	13.0±0.4
Debranched waxy maize	63.7±0.2	87.2±0.6	98.8±0.1	8.4±0.3	105.1±1.0	128.1±0.9	153.5±0.6	15.7±0.3
Debranched waxy potato	69.4±0.7	86.6±1.1	97.9±0.2	7.6±0.7	101.5±0.2	134.1±0.4	151±0.9	17.2±0.7

<sup>A</sup> First scan was heated from 10 to 100°C at 10°C/min, and second scan was heated from 10 to 160°C at 10°C/min, after heating from 10 to 100°C at 10°C/min, holding at 100°C for 5min, and cooling from 100°C to 10°C at 10°C/min. The ratio of sample (dry basis) and water was 1:1.

<sup>B</sup> Mean ± standard deviation values are reported.

**Figure 4.1** Synchrotron wide-angle X-ray diffraction of short-chain amylose (as is and hydrated) from (A) waxy wheat starch; (B) waxy maize starch; and (C) waxy potato starch

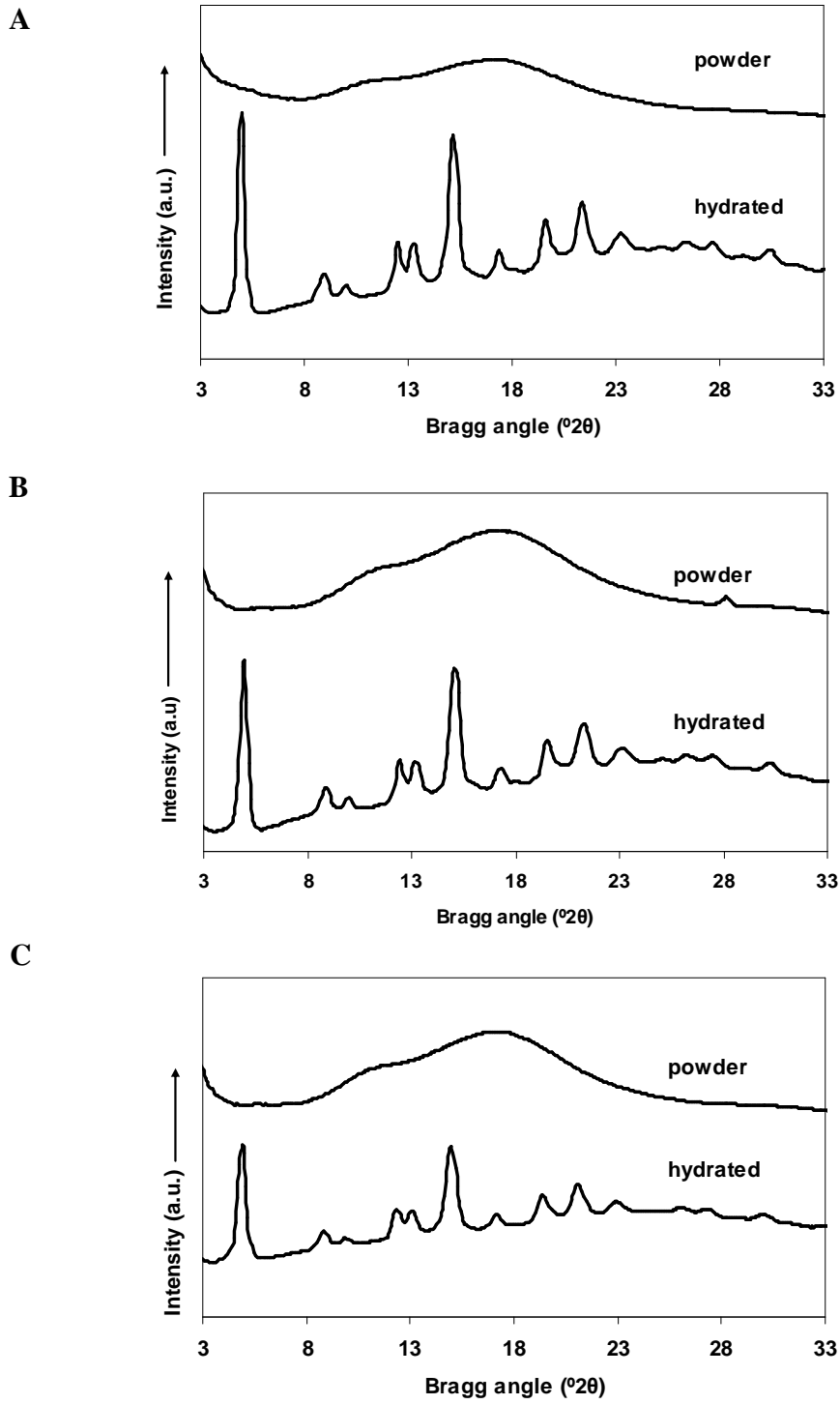


**Figure 4.2** Dynamic synchrotron wide-angle X-ray diffraction results of short-chain amylose from debranched waxy wheat starch during (A) heating and (B) cooling

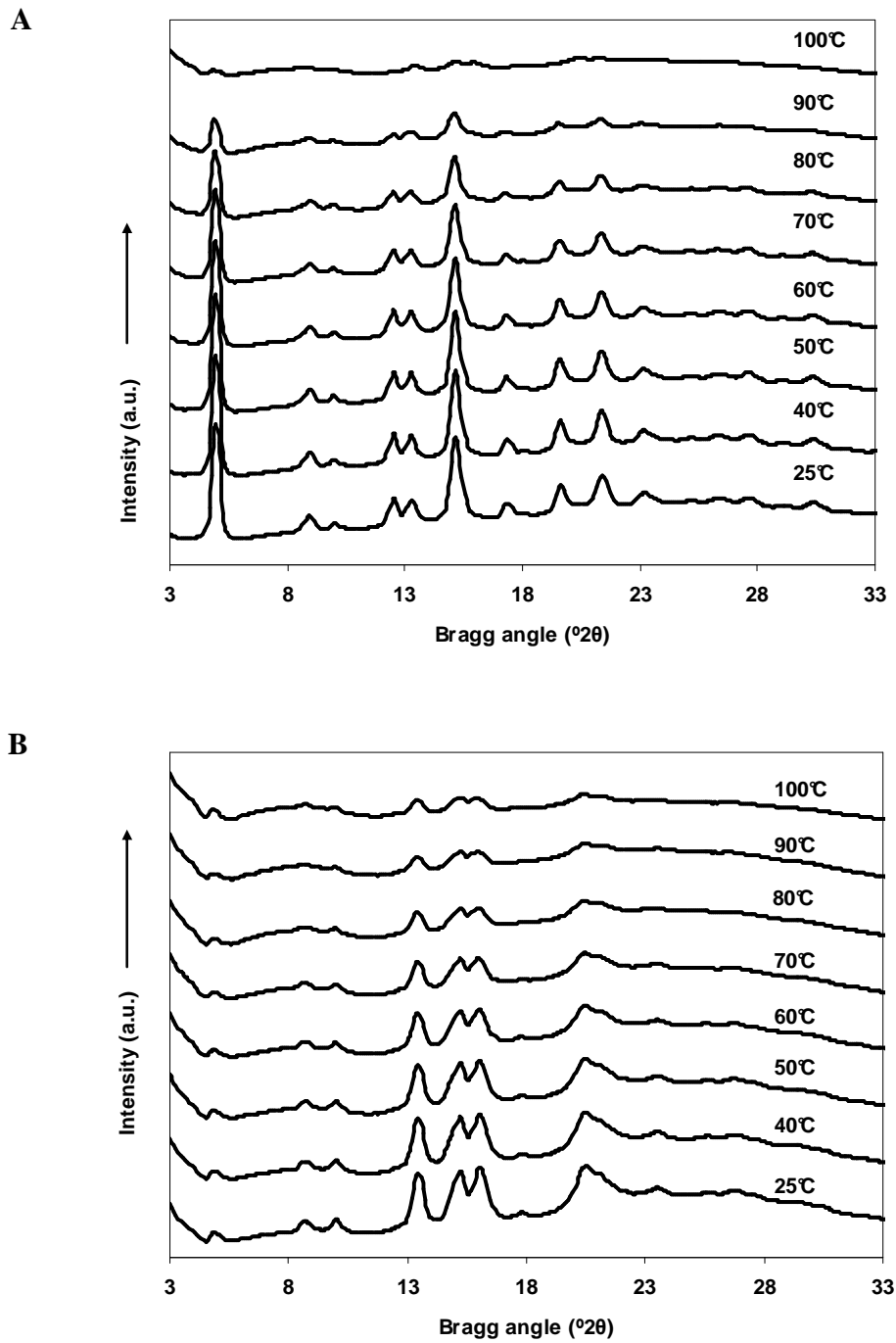


**Figure 4.3** Dynamic synchrotron wide-angle X-ray diffraction results of short-chain amylose from waxy maize starch during (A) heating and (B) cooling

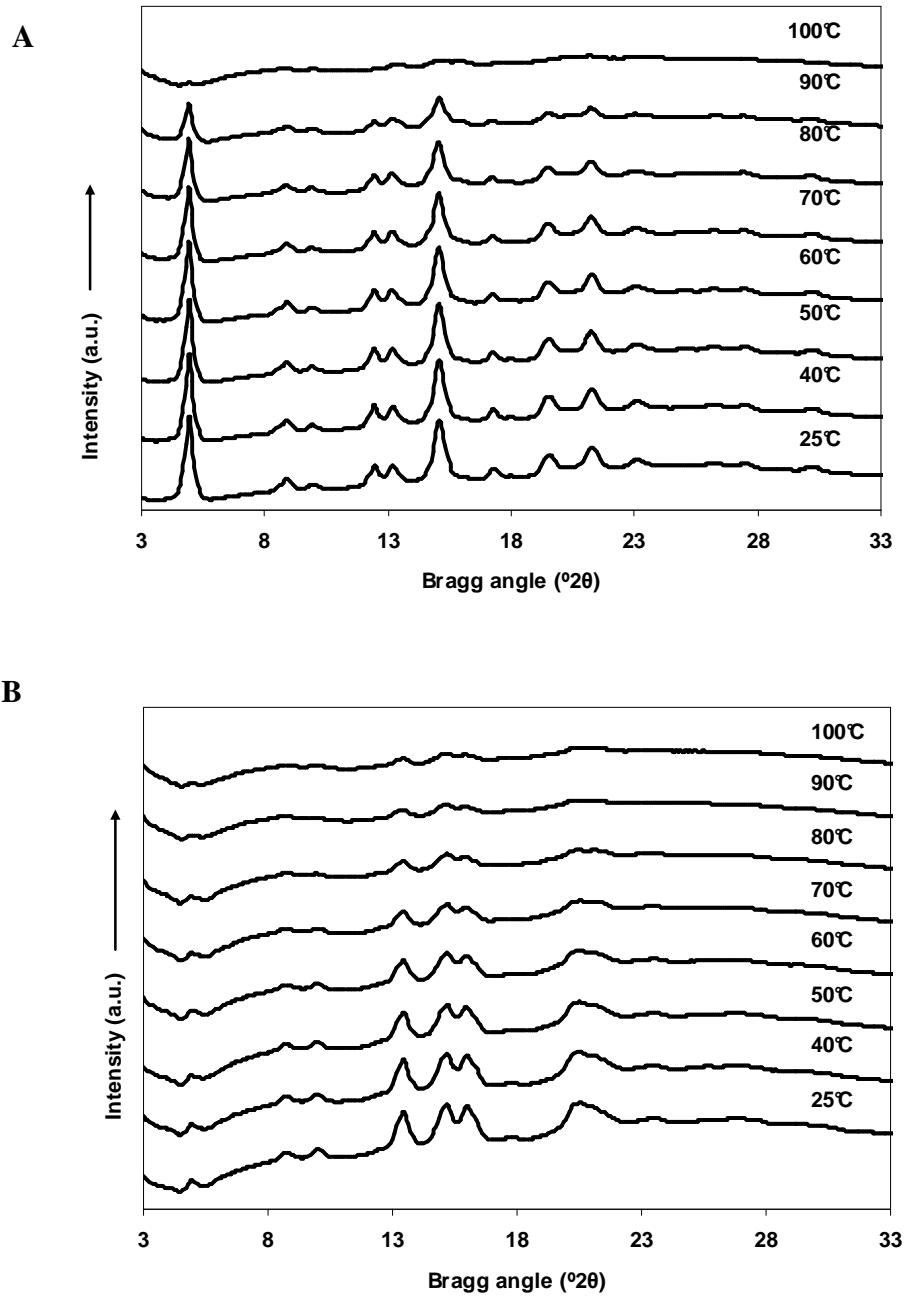
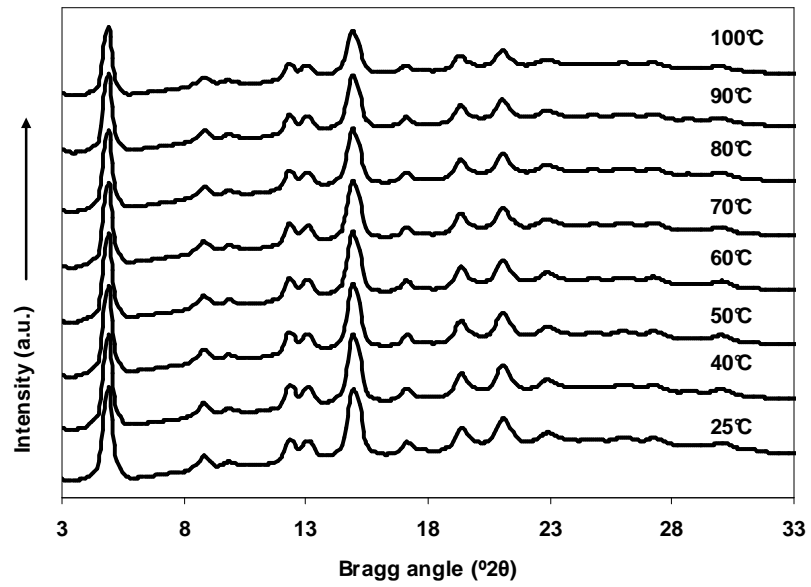


**Figure 4.4 Dynamic synchrotron wide-angle X-ray diffraction results of short-chain amylose from waxy potato starch during (A) heating and (B) cooling**

**A**



**B**

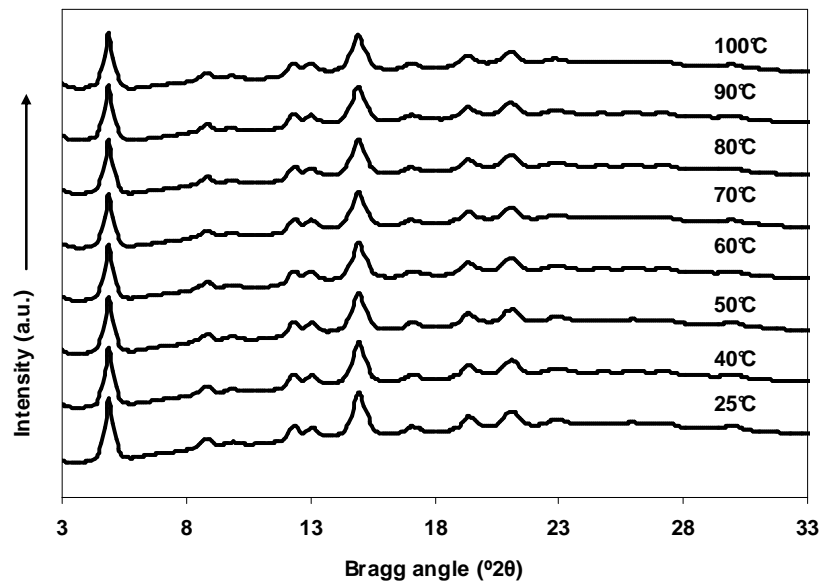


**Figure 4.5 Thermal properties of short-chain amylose from (A) debranched waxy wheat starch, (B) debranched waxy maize starch and (C) debranched waxy potato starch as determined by differential scanning calorimetry: (a) Samples (50% moisture) were heated from 10 to 160°C at 10°C/min; (b) Samples (75% moisture) were heated from 10 to 160°C at 10°C/min; (c) Samples (50% moisture) were heated from 10 to 100°C at 10°C/min; and (d) Samples (50% moisture) were heated from 10 to 160°C at 10°C/min, after heating from 10 to 100°C at 10°C/min, holding at 100°C for 5min, and cooling from 100°C to 10°C at 10°C/min**

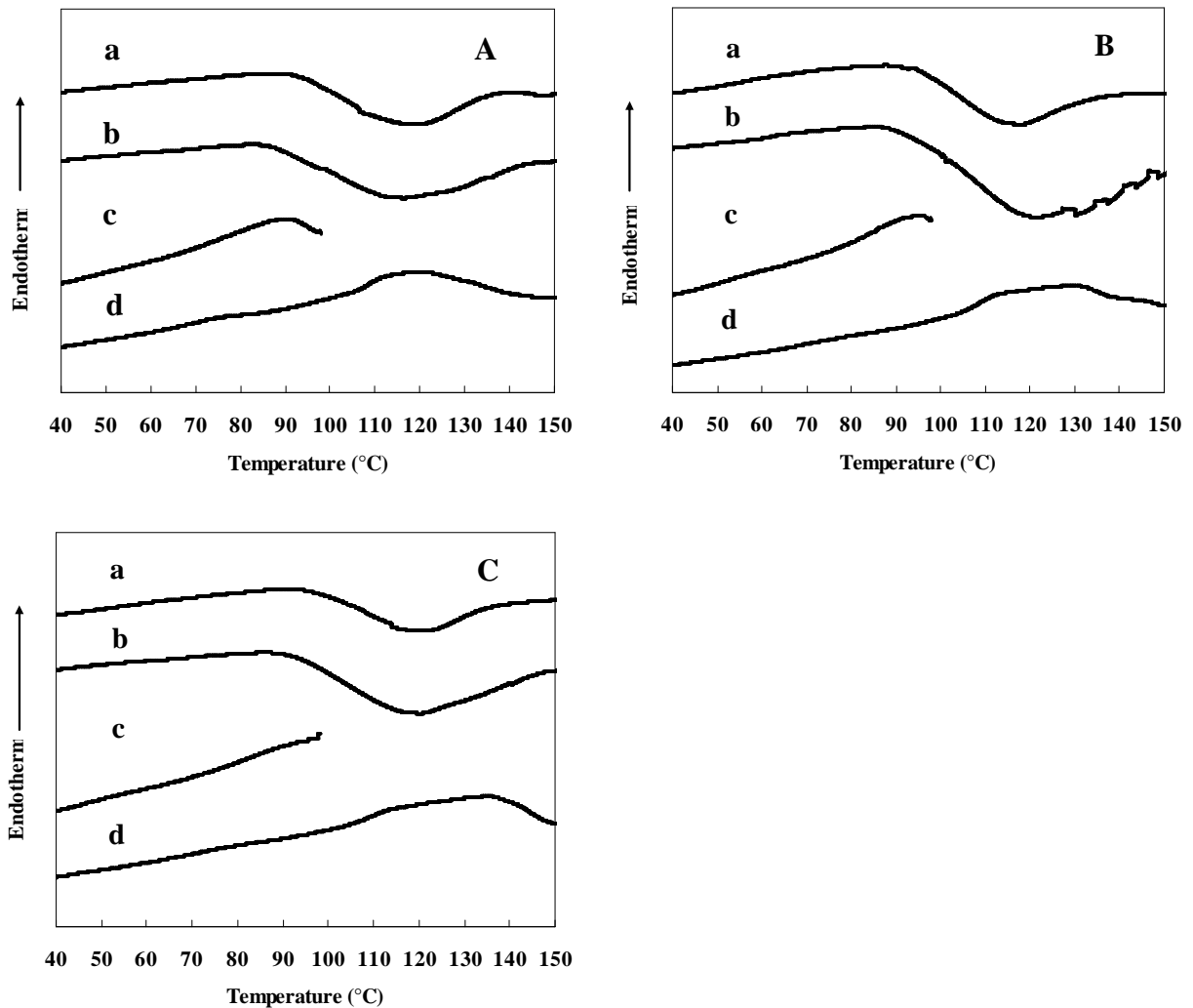
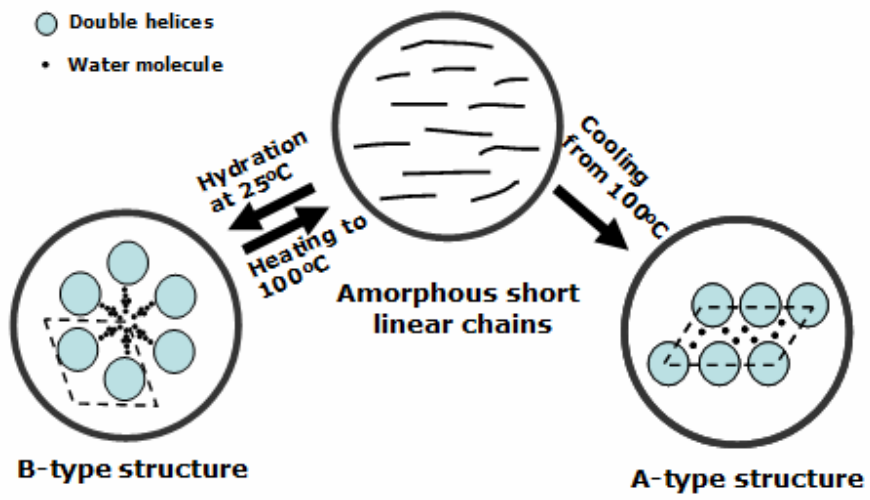


**Figure 4.6** The diagram of melting and crystallization of short-chain amylose studied by using synchrotron wide-angle X-ray diffraction





## **Chapter 5 - Manipulation of A- and B-type crystals from short-chain amylose in relation to their digestibility**

### **Abstract**

Starch is the most important source of food energy. It is well known that native starches with a B-type X-ray diffraction pattern are more resistant to alpha-amylase digestion than those starches with an A-type X-ray pattern, but the underlying mechanism is not well understood. It is not clear whether the enzyme resistance of B-type starch is due to its B-type crystalline structure or the other structural features in starch granules. The objective of this study was to compare the structure and enzyme digestibility of highly pure A- and B-type starch crystals, and understand the roles of crystalline types in starch digestibility. Highly pure A- and B-type starch crystals were prepared from short linear  $\alpha$ -glucans (short-chain amylose) generated from completely debranched waxy starches by manipulating the processing conditions such as starch solids concentration, crystallization temperature and chain length. High concentration, high temperature and short chain length favored the formation of the A-type structure, whereas reverse conditions resulted in the B-type polymorph. Digestion results using a mixture of  $\alpha$ -amylase and glucoamylase showed that the A-type crystals were more resistant to enzyme digestion than the B-type crystals. The A-type crystalline product obtained upon debranching 25% waxy maize starch at 50°C for 24 h gave 16.6% digestion after 3 h, whereas the B-type crystals produced by debranching 5% waxy maize starch at 50°C for 24 h followed by holding at 25°C for another 24 h had 38.9% digested after 3 h. The A-type crystals had a higher melting temperature than the B-type crystals as determined by differential scanning calorimetry. Annealing increased the peak melting temperature of the B-type crystals, making it similar to that of the A-type crystals, but did not improve the enzyme resistance of the B-type crystals. The possible reason for these results was due to more condensed packing pattern of double helices in A-type crystallites. Our observations are opposite to the fact that B-type native starches are more enzyme resistant. It seems that the crystalline types are not the key factor that controls the digestibility of native starch granules. The resistance of native starches with a B-type X-ray diffraction pattern is probably attributed to the other structural features in starch granules.

## Introduction

Native starches with a B-type X-ray diffraction pattern are known to be more resistant to alpha-amylase digestion than those starches with an A-type X-ray pattern (Dreher et al 1984; Gallant et al, 1972; Gallant et al 1997; Jane et al, 1997; McCleary and Monaghan 2002; Planchot et al, 1995; Srichuwong et al, 2005a, b); however, whether the enzyme resistance of B-type starch is due to its B-type crystalline structure or the other structural features of starch granules is unclear.

Studies that compare enzyme digestibility of pure A- and B-type crystals are limited. Williamson et al (1992) and Planchot et al (1997) prepared A- and B-type spherulite crystal from lintnerized potato starch and found that B-type spherulites were more resistant to  $\alpha$ -amylase than A-type spherulites. In contrast, Cai et al (2010) observed that the A-type crystals formed from 25% solids SCA solution at 50 °C had higher resistant starch (RS) content than the B-type crystals prepared at 5% solids and 25 °C (Cai and Shi, 2010).

In this study, both highly pure A- and B-type starch crystals were prepared from short linear chains (short-chain amylose, SCA) generated from completely debranched waxy starches in an aqueous environment. The overall objective was to compare the structure and enzyme digestibility of highly pure A- and B-type starch crystals and to understand the roles of crystalline types in starch digestibility. Our specific goals were to (1) prepare highly crystalline materials with A- and B-type polymorphs by manipulating the processing conditions such as starch solids concentration, crystallization temperature, and chain length (starch sources), (2) characterize the properties and digestibility of the resulting materials, and (3) relate the starch polymorphs to enzyme digestion.

## Materials and methods

Waxy maize starch was gained from National Starch LLC (Bridgewater, NJ, USA), waxy potato starch was provided by Penford Food Ingredients Company (Centennial, CO, USA) and isoamylase (EC 3.2.1.68) was obtained from Hayashibara Biochemical Laboratories, Inc. (Okayama, Japan). The enzyme activity was  $1.41 \times 10^6$  IAU/g, where 1 IAU of activity was defined as the amount of isoamylase that increased reducing-power absorbance of the reaction mixture by 0.008 in 30 min under the conditions of the isoamylase assay (FAO JECFA Monographs, 2007). All chemicals were reagent-grade.

### ***Manipulation of A- and B- type crystals from short-chain amylose (SCA)***

Three approaches were used to produce A- and B-type starch crystals from SCA (**Figure 5.1**). The first approach was to use different solids concentrations of starch. Three different solids levels (5%, 15% and 25%) were used. To debranch starch, waxy maize starch was mixed with acetic acid buffer (0.01M, pH4.0) in a pressure bottle and heated in a boiling water bath with stirring for 30 min followed by heating at 120°C in an oven for 30 min. After the mixture was cooled to 50°C, the debranching reaction was started by adding 1% isoamylase based on the dry weight of starch. For the 25% solids sample, the precipitates were filtered after 24 h of debranching reaction. For the 5% and 15% solids samples, the mixture was reacted at 50°C for 24 h, then cooled to 25°C and held for another 24 h. The precipitates were filtered, washed with water, dried in an oven at 40°C overnight, and ground by a mortar and pestle.

The second approach to favor A- or B-type crystals was to manipulate the crystallization temperatures. Waxy maize starch (25% solids concentration) was debranched for 24h as described above. Then, the mixture was heated at 140 °C in an oven for 1 h to completely melt the crystals. The clear solution was held at 4, 25 or 50°C for 24 h to induce crystallization. The precipitates were filtered, washed with water, dried in an oven at 40°C overnight, and ground by a pestle and mortar.

The third approach to prepare A- or B- type crystals was to use SCA with different chain lengths (CL). Waxy potato starch (25% solids concentration), which has longer unit chains than waxy maize starch, was debranched for 24h as described above, then, the precipitates were filtered, washed with water, dried in an oven at 40°C overnight, and ground with a mortar and pestle. The yield of all crystallized product was determined as previously described in **Chapter 2**.

To compare the results in the literature, the SCA from debranched waxy maize starch was used to prepare A- and B-type crystals by the method of Planchot et al (1997).

### ***Annealing of starch crystals***

Immediately after debranching for 24 h, waxy potato starch slurry (25% solids) was annealed at 100 °C in a water bath for 4 h with continuous stirring. The mixture was filtered, dried at 40 °C in an oven overnight, and saved for further digestion analysis.

### ***Gel permeation chromatography (GPC)***

The starch samples were examined by GPC as previously described in Chapter 2.

### ***Scanning electron microscopy (SEM)***

The morphology of starch samples were viewed by SEM as previously described in Chapter 2.

### ***Particle size distribution***

Crystalline samples of SCA were suspended in aqueous 1% sodium azide, and after sonication, several drops of the suspension were added into a Beckman Coulter LS 13 320 Laser Diffraction Size Analyzer (Beckman Coulter, Inc. Brea, CA, USA) equipped with the universal liquid module. Each sample was measured twice.

### ***Wide-angle X-ray diffraction***

Wide-angle X-ray diffraction was conducted as previously described in Chapter 3.

### ***In vitro digestion method***

The *in vitro* starch digestion profile was determined by a modified Englyst procedure (Englyst et al, 1992; Sang and Seib, 2006) as previously described in Chapter 2.

## **Results and Discussion**

### ***Formation of A- and B- starch crystals***

Wide-angle X-ray diffraction patterns of SCA prepared from different approaches are shown in **Figure 5.2**. All samples displayed a diffraction pattern with sharp peaks that were associated with a crystalline structure. A highly pure A-type crystal was obtained by debranching and crystallization of 25% solids waxy maize starch at 50 °C for 24 h. Debranching 5 % solids waxy maize starch and crystallization at 50 °C for 24 h followed by holding at 25 °C for another 24 h resulted in a B-type polymorph. A mixture of A- and B-type starch crystal was observed for 15% solids sample (**Figure 5.2A**). At the same starch concentration (25% solids), an amorphous sample of SCA was transformed into A-type starch crystals at 50 °C, whereas B-type crystalline materials were formed at 4 or 25 °C (**Figure 5.2B**). In contrast with waxy maize starch (**Figure 5.2A**), 25% solids waxy potato starch debranched and crystallized at 50 °C showed the B-type X-

ray diffraction pattern (**Figure 5.3C**). Our results agree with the general findings that higher solids and crystallization temperature, and lower chain length favor the formation of A-type crystallites, and the reverse conditions induce B-type crystallization (Buleon et al, 2007; Cai et al, 2010; Cai and Shi, 2010; Gidley and Bulpin, 1987; Helbert, 1993; Lebail et al, 1993; Pfannemuller, 1987; Planchot et al, 1997; Ring et al, 1987; Whittam et al, 1990; Williamson et al, 1992).

The underlying mechanism of these phenomena can be explained as follows. According to Gidley (1987), the A-type crystal is a thermodynamic product and the B-type structure is a kinetic product. A thermodynamic product is formed by an equilibrium reaction through an intermediate stage to form a stable structure of low free energy, whereas a kinetic event involves a rapid precipitation of a less stable, less perfect structure. At a high temperature, thermodynamic products are favored. The B-type structure may form temporarily, but this structure is not stable and melts to form the more stable A-type structure (Cai et al, 2010; Pohn et al, 2004). At high concentrations of SCA, more double helices can be generated, which favor the A-type structure because it has a denser packing pattern of double helices. For SCA with a long average CL, the double helices formed will be larger and tend to rapidly precipitate from solution to yield the less stable and imperfect B-type crystalline product.

The yields of A- and B-type starch crystals are listed in **Table 5.1**. Debranching 5% solids waxy maize starch at 50 °C for 24 h gave no precipitate, but 59.2% crystalline material was obtained after holding the mixture at 25 °C for another 24 h. Debranching 15% and 25% solids waxy maize starch at 50 °C for 24 h yielded 33% and 65.8% precipitates, respectively, and 77.4% and 89.8% products, respectively, after holding at 25 °C for another 24 h. Cooling debranched waxy maize starch that has been preheated to 140 °C for 1 h to 4, 25, and 50 °C for 24 h generated 90.4, 88.0, and 72.4% starch crystals, respectively. The yield of waxy potato starch debranched at 50°C for 24 h was 72.8%. The results showed that yield was increased as solids concentration and chain length increased, and as crystallization temperature decreased. The high yields of crystalline SCA indicated their great potential for industry applications.

### ***Molecular weight distribution of A- and B- starch crystals***

The molecular weight distributions of A- and B- starch crystals are presented in **Figure 5.3**. A bimodal distribution with a low molecular weight peak and a high molecular weight peak

was observed for all samples. Crystals prepared from 25% solids had a higher proportion of low molecular weight fraction than those from 5% solids (**Figure 5.3A**). Molecules with short chains seem favored to crystallize at higher solids concentration. At the same solids concentration, the distribution pattern of SCA crystallized at 4, 25 and 50 °C was essentially the same (**Figure 5.3B**). Compared to samples prepared from debranched waxy maize starch, those generated from debranched waxy potato starch had a higher percentage of large molecular weight molecules (**Figure 5.3C**). The average CL of waxy maize and waxy potato starch was 24.1 and 32.1 glucose units, respectively (Cai and Shi, 2010).

### ***Morphology and particle size distribution of A- and B- starch crystals***

All A- and B- starch crystals contained particles with a coarse surface and irregular shape (**Figures 5.4-5.6**). No starch granules were observed in the micrograph, suggesting that the granular structure has been completely disrupted and that a new crystalline structure was formed. Small isolated particles (<1µm) along with large pieces of particle clusters (>10µm) existed in the same sample, revealing a wide distribution of particle size in the samples. The observations were in agreement with particle size distribution results, as shown in **Figures 5.7-5.9**. The average particle sizes of SCA prepared from debranched waxy maize starch at 5, 15 and 25% solids were 9, 7.4 and 4.7 µm respectively. The average dimension of SCA particles produced from debranched waxy maize starch at 4, 25, and 50 °C were 8.9, 10.1 and 13.5 µm, respectively (**Table 5.1**). There was no correlation between the particle size and the *in vitro* digestibility of A- and B-type starch crystals discussed below.

### ***Thermal properties of A- and B- starch crystals***

The thermal properties of A- and B-type starch crystals are given in **Figure 5.10** and **Tables 5.2-5.4**. The B-type starch crystals obtained from 5% solids showed an endotherm with a melting temperature ranging from 67 to 104 °C and an enthalpy of 15.9J/g, whereas the A-type starch crystals displayed a melting peak ranging from 98 to 140 °C with an enthalpy of 20.5 J/g. For samples prepared from 15% solids, two endotherms with a low melting peak and a high melting peak were observed, reflecting the presence of a mixture of A- and B-type structure (**Figure 5.10A** and **Table 5.2**). Under the same concentration of 25% solids, the A-type structure prepared at a higher temperature had a higher melting temperature than the B-type polymorph formed at lower temperatures (**Figure 5.10B** and **Table 5.3**).

The melting temperature of recrystallized SCA in excess water with the A-type structure was always reported to be higher than that of its B-type counterpart (Cai et al, 2010; Cai and Shi, 2010; Planchot et al, 1997; Whittam et al, 1990; Williamson et al, 1992). With the same B-type polymorph, crystals generated from debranched waxy potato starch displayed a higher peak melting temperature (**Figure 5.10C** and **Table 5.4**). This phenomenon could be explained by stronger double helices formed from debranched waxy potato starch with longer unit chains than that in debranched waxy maize starch (Cai and Shi, 2010).

Due to the concern that less thermal stability of B-type structure may result into its high susceptibility to the digestive enzymes, which was discussed in the next section, the debranched waxy potato starch was annealed to achieve a higher melting peak centered around 120 °C, similar as that of A-type structure (**Figure 5.10** and **Table 5.4**). This annealed sample retained predominant B-type X-ray diffraction pattern (**Figure 5.2C**), similar molecular weight distribution (**Figure 5.3C**), morphology (**Figure 5.6**) and particle size distribution (**Figure 5.9**), thus was used as samples with the B-type structure and improved thermal stability to compare the digestibility with that of A-type crystals.

### ***In vitro digestibility of A- and B- starch crystals***

The rate and extent of hydrolysis of A- and B- type starch crystals by a mixture of  $\alpha$ -amylase and glucoamylase is shown in **Figure 5.11**. The A-type crystals prepared from 25% solids displayed a lower digestibility than the C-type crystals and the B-type crystals prepared from 15% and 5% solids, respectively (**Figure 5.11A**). The A-type crystalline product obtained from debranching of 25% waxy maize starch at 50°C for 24 h gave 16.6% digestibility after 3 h incubation. In contrast, the B-type crystals obtained by debranching 5% waxy maize starch at 50°C for 24 h followed by holding at 25°C for another 24 h, gave 38.9% digestion after 3 h incubation. Similarly, A-type crystals crystallized at 50 °C had a lower hydrolysis extent (28.0% digested after 3 h hydrolysis) than B-type crystals formed at 4 and 25 °C (41.7% and 44.5% hydrolysis after 3 h digestion respectively, **Figure 5.11B**). The B-type crystals formed from debranched waxy potato starch with higher CL were less resistant to enzyme digestion (27.6% hydrolyzed after 3 h digestion) than the A-type crystals prepared from debranched waxy maize starch (**Figure 5.11A** and **C**). Our results suggested that the A-type crystals prepared from linear SCA were always more resistant to the enzyme digestion than their B-type counterparts.

On the molecular level, A- and B-type starch crystals differ in the packing pattern of double helices (monoclinic and hexagonal geometry, respectively) and the number of water molecules (8 and 36, respectively) in the crystal unit cell (Imberty et al, 1988; Imberty and Perez, 1988; Popov et al, 2009; Takahashi et al, 2004). Thus, the A-type structure is comprised of a denser and tighter structure than the B-type structure (**Figure 5.12**). This feature may inhibit the access of enzyme to the starch molecules and reduce the hydrolysis.

The B-type crystals had a lower melting temperature in excess water than A-type crystals (**Figure 5.10** and **Tables 5.2-5.4**). Was the high digestibility of B-type crystals due to their low thermal stability and imperfect crystals? To eliminate this effect, debranched waxy maize starch with a B-type structure (5% solids debranched at 50 °C for 24 h and held at 25 °C for another 24 h) was annealed at 60 °C and 80 °C respectively to increase its thermal stability; however, the peak melting temperature of the sample was increased only slightly from 87 °C to 90.6 °C after annealing at 60 °C for 8 h. Upon annealing at 80 °C, the sample displayed a peak melting temperature of 98.0 °C, but with a significantly decreased enthalpy of 4.1J/g. Debranched waxy maize starch with a B-type polymorph was concluded to have a weak crystalline structure that was difficult to strengthen by annealing.

Thus, the crystallized B-type polymorph with a relatively high melting temperature of 104.3 °C obtained from debranched waxy potato starch, was used as starting materials. After annealing, the B-type crystals had a similar peak melting temperature compared with the A-type crystals (119.6 °C vs. 117.9 °C); however, the B-type crystals exhibited an increase in its extent of hydrolysis rather than a decrease (**Figure 5.11C**). These results provide evidence that annealing did not improve the enzyme resistance of the B-type structure, and that its relatively high enzyme susceptibility was largely dependent on its polymorphic structure rather than its thermal stability.

Our results conflict with the observations on the digestibility of A- and B-type crystals in the literature. Planchot et al (1997) prepared A- and B-type starch crystals from lintnerized starch and found that the A-type structure was more susceptible to the  $\alpha$ -amylase hydrolysis. Williamson et al (1992) reported that the B-type crystalline starch was more resistant to  $\alpha$ -amylase,  $\beta$ -amylase and glucoamylase 1. Notably, those authors prepared A- and B-type starch crystals using mild acid-treated potato starch. Their crystalline solids contained  $\alpha$ -1,6 branch points and a mixture of linear and branched polymers. The B-type starch crystals were prepared



by cooling the solution of acid-treated starch at a slow rate, whereas the A-type crystals were crystallized from an ethanol-water mixture. To explain the differences, SCA generated from debranched waxy maize starch was used as starting material to prepare A- and B-type crystals by the same procedures described by Planchot et al (1997). Surprisingly, the A-type crystals from debranched waxy maize starch were still more enzyme-resistant than their corresponding B-type crystals. The A-type structure gave only 22.9% hydrolysis in 3h, compared with 33.4% for the B-type structure (**Figure 5.11D**). The different starting materials to prepare the model crystals may have led to the opposite digestion results.

In the case of native starches, cereal starches (mostly A-type X-ray diffraction pattern) are always found to have higher digestibility than tuber starches and high amylose starches with B-type X-ray diffraction pattern (Dreher et al 1984; Gallant et al, 1972; Gallant et al 1997; Jane et al, 1997; McCleary and Monaghan 2002; Planchot et al, 1995; Srichuwong et al, 2005a, b), but the A-type starch crystals were found to be more enzyme resistant than the B-type crystals in this study. Thus, the crystalline structure seems not to be the key factor that affects the digestibility of native starch granules. The resistance of native starches with the B-type X-ray diffraction pattern is probably attributed to the other structural features of starch granules.

## Conclusions

The A-type crystalline SCA could be formed at high concentration, high temperature and short CL, while the B-type polymorph was produced at low concentration, low temperature and long CL. Digestion results with a mixture of  $\alpha$ -amylase and glucoamylase showed that the A-type structure was more resistant to enzyme digestion than its B-type counterpart. The A-type crystalline products had a higher melting temperature in excess water than the B-type as determined by DSC. Annealing increased the peak melting temperature of the B-type crystals made from waxy potato starch, making it similar to that of the A-type crystals; however, the annealed B-type crystals did not have improved enzyme resistance. The higher enzyme resistance of the A-type structure was probably due to its denser packing pattern of double helices. Our observations are in striking contrast to the fact that the B-type native starches are more enzyme resistant. It seems that the A- and B- type crystalline structure is not the key factor that impacts the digestibility of native starch granules. The resistance of native starch with the B-

type X-ray diffraction pattern is probably attributable to the surface features and other organizational structure of starch granules.

## References

- Buleon, A., Veronese, G., & Putaux, J. L. (2007). Self-association and crystallization of amylose. *Australian Journal of Chemistry*, 60, 706-718.
- Cai, L., & Shi, Y-C. (2010). Structure and digestibility of crystalline short-chain amylose from debranched waxy wheat, waxy maize and waxy potato starches. *Carbohydrate Polymers*, 79, 1117-1123.
- Cai, L., Shi, Y-C., Rong, L., & Hsiao, B.S. (2010). Debranching and crystallization of waxy maize starch in relation to enzyme digestibility. *Carbohydrate Polymers*, 81, 385-393.
- Dreher, M. L., Dreher, C. J., & Berry, J. W. (1984). Starch digestibility of foods- A nutritional perspective. *Critical Reviews in Food Science and Nutrition*, 20, 47-71.
- Englyst, H. N., Kingman, S. M., & Cummings, J. H. (1992). Classification and measurement of nutritionally important starch fractions. *European Journal of Clinical Nutrition*, 46, S33-S50.
- FAO JECFA Monographs (2007). Joint FAO/WHO expert committee on food additives. 4, 21-23.
- Gallant, D. J., Bouchet, B., & Baldwin, P. M. (1997). Microscopy of starch: Evidence of a new level of granule organization. *Carbohydrate Polymers*, 32, 177-191.
- Gallant, D., Guilbot, A., & Mercier, C. (1972). Electro-microscopy of starch granules modified by bacterial alpha-amylase. *Cereal Chemistry*, 49, 354-358.
- Gidley, M. J. (1987). Factors affecting the crystalline type (AC) of native starches and model compounds- A rationalization of observed effects in terms of polymorphic structures. *Carbohydrate Research*, 161, 301-304.
- Gidley, M. J., & Bulpin, P. V. (1987). Crystallization of malto-oligosaccharides as models of the crystalline forms of starch: minimum chain-length requirement for the formation of double helices. *Carbohydrate Research*, 161, 291-300.
- Helbert, W., Chanzy, H., Planchot, V., Buleon, A., & Colonna, P. (1993). Morphological and structural features of amylose spherocrystals of A-type. *International Journal of Biological Macromolecules*, 15, 183-187.
- Imberty, A., Chanzy, H., Perez, S., Buleon, A., & Tran, V. (1988). The double-helical nature of the crystalline part of A-starch. *Journal of Molecular Biology*, 201, 365-378.
- Imberty, A., & Perez, S. (1988). A revisit to the 3-dimensional structure of B-type starch. *Biopolymers*, 27, 1205-1221.
- Jane, J-L., Wong, K-S., & McPherson, E. A. (1997). Branch-structure difference in starches of A- and B-type X-ray patterns revealed by their Naegeli dextrans. *Carbohydrate Research*, 300, 219-227.
- Lebail, P., Bizot, H., & Buleon, A. (1993). B-type to A-type phase-transition in short amylose chains. *Carbohydrate Polymers*, 21, 99-104.
- McCleary, B. V., & Monaghan, D. A. (2002). Measurement of resistant starch. *Journal of AOAC International*, 665-675.
- Pfannemuller, B. (1987). Influence of chain length of short monodisperse amyloses on the formation of A- and B-type X-ray diffraction patterns. *International Journal of Biological Macromolecules*, 9, 105-108.
- Planchot, V., Cononna, P., & Buleon, A. (1997). Enzymatic hydrolysis of  $\alpha$ -glucan crystallites. *Carbohydrate Research*, 298, 319-326.

- Planchot, V., Colonna, P., Gallant, D. J., & Bouchet, B. (1995). Extensive degradation of native starch granules by alpha-amylase from *Aspergillus fumigatus*. *Journal of Cereal Science*, 21, 163-171.
- Pohu, A., Planchot, V., Putaux, J. L., Colonna, P., & Buleon, A. (2004). Split crystallization during debranching of maltodextrins at high concentration by isoamylase. *Biomacromolecules*, 5, 1792-1798.
- Popov, D., Buleon, A., Burghammer, M., Chanzy, H., Montesanti, N., Putaux, J.-L., Potocki-Veronese, G., & Riekkel, C. (2009). Crystal structure of A-amylose: A revisit from synchrotron microdiffraction analysis of single crystals. *Macromolecules*, 42, 1167-1174.
- Ring, S. G., Miles, M. J., Morris, V. J., Turner, R., & Colonna, P. (1987). Spherulitic crystallization of short chain amylose. *International Journal of Biological Macromolecules*, 9, 158-160.
- Sang, Y. J., & Seib, P. A. (2006). Resistant starches from amylose mutants of maize by simultaneous heat-moisture treatment and phosphorylation. *Carbohydrate Polymers*, 63, 167-175.
- Srichuwong, S., Isono, N., Mishima, T., & Hisamatsu, M. (2005a). Structure of lintnerized starch is related to X-ray diffraction pattern and susceptibility to acid and enzyme hydrolysis of starch granules. *International Journal of Biological Macromolecules*, 37, 115-121.
- Srichuwong, S., Sunnarti, C. T., Mishima, T., Isono, N., & Hisamatsu, M. (2005b). Starches from different botanical sources I: Contribution of amylopectin fine structure to thermal properties and enzyme digestibility. *Carbohydrate Polymers*, 60, 529-538.
- Takahashi, Y., Kumano, T., & Nishikawa, S. (2004). Crystal structure of B-amylose. *Macromolecules*, 37, 6827-6832.
- Whittam, M. A., Noel, T. R., & Ring, S. G. (1990). Melting behavior of A-type and B-type crystalline starch. *International Journal of Biological Macromolecules*, 12, 359-362.
- Williamson, G., Belshaw, N. J., Self, D. J., Noel, T. R., Ring, S. G., Cairns, P., Morris, V. J., Clark, S. A., & Parker, M. L. (1992). Hydrolysis of A-type and B-type crystalline polymorphs of starch by Alpha-amylase, Beta-amylase and Glucoamylase-1. *Carbohydrate Polymers*, 18, 179-187.

**Table 5.1 Yields and average particle size of crystalline short-chain amylose products prepared by different approaches**

a. Effect of solids concentration <sup>A</sup>

Solids (%)	5	15	25
Yield (%)	0.0 <sup>a</sup>	32.0±0.4 <sup>a</sup>	65.8±0.8 <sup>a</sup>
	59.2±1.4 <sup>b</sup>	77.4±0.5 <sup>b</sup>	89.8±0.3 <sup>b</sup>
Average particle size (µm)	9.0±0.4 <sup>b</sup>	7.4±0.3 <sup>b</sup>	4.7±0.1 <sup>a</sup>

<sup>A</sup> Mean ± standard deviation values are reported.

<sup>a</sup> Waxy maize starch was debranched at 50°C for 24h.

<sup>b</sup> Waxy maize starch was debranched at 50°C for 24h, followed by holding at 25°C for another 24h.

b. Effect of crystallization temperature <sup>A, B</sup>

Crystallization temperature (°C)	4	25	50
Yield (%)	90.4±1.1	88.0±0.8	72.4±0.6
Average particle size (µm)	8.9±0.3	10.1±0.4	13.5±0.5

<sup>A</sup> Mean ± standard deviation values are reported.

<sup>B</sup> Waxy maize starch (25% solids) was debranched at 50°C for 24h, then heated to 140°C for 1h and crystallized at different temperatures.

c. Effect of chain length <sup>A, B</sup>

Average chain length (Glucose units)	Waxy maize starch	Waxy potato starch
	24	32
Yield (%)	65.8±0.8	72.8±1.4
Average particle size (µm)	4.7±0.1	15.9±0.1

<sup>A</sup> Mean ± standard deviation values are reported.

<sup>B</sup> Starch (25% solids) was debranched and crystallized at 50°C for 24h.

**Table 5.2 Thermal properties of short-chain amylose prepared at different solids concentration of debranched waxy maize starch as determined by differential scanning calorimetry <sup>A</sup>**

Solids (%)	Peak 1				Peak 2			
	T <sub>o</sub> (°C)	T <sub>p</sub> (°C)	T <sub>c</sub> (°C)	ΔH(J/g)	T <sub>o</sub> (°C)	T <sub>p</sub> (°C)	T <sub>c</sub> (°C)	ΔH(J/g)
5	67.4±0.5	87±0.1	104±0.6	15.9±0.1	-	-	-	-
15	76.6±0.1	95.9±0	110.4±0.8	12.7±0.5	115.5±0.2	127.3±0.5	140.4±0.4	3.15±0.1
25	-	-	-	-	97.6±0.8	117.9±0.8	139.5±0.9	20.5±1.2

<sup>A</sup> Mean ± standard deviation values are reported.

**Table 5.3 Thermal properties of short-chain amylose prepared at different crystallization temperature of debranched waxy maize starch as determined by differential scanning calorimetry <sup>A</sup>**

Crystallization Temperature (°C)	T <sub>o</sub> (°C)	T <sub>p</sub> (°C)	T <sub>c</sub> (°C)	ΔH(J/g)
4	63.8±0.4	92.1±0.4	108.2±0.6	17.2±0.2
25	68.3±0.9	89.4±1.2	108.2±0.4	18.7±0.1
50	99±1.3	115.9±1.1	140.3±0.3	19.5±0.7

<sup>A</sup> Mean ± standard deviation values are reported.

**Table 5.4 Thermal properties of short-chain amylose prepared from debranched waxy potato starch before and after annealing<sup>A</sup>**

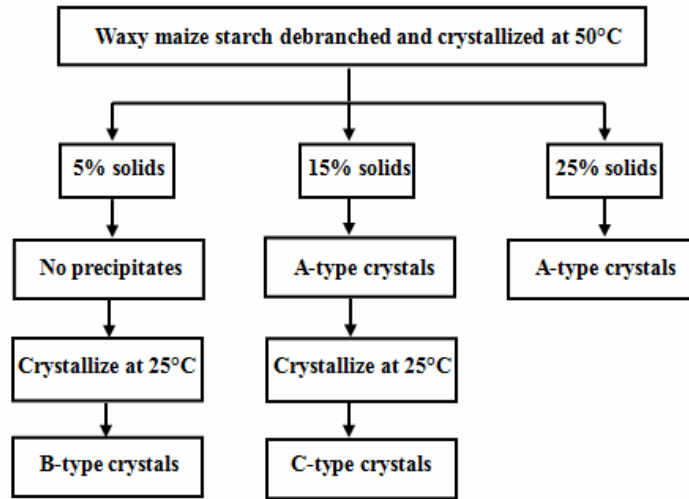
Debranched waxy potato starch	T <sub>o</sub> (°C)	T <sub>p</sub> (°C)	T <sub>c</sub> (°C)	ΔH(J/g)
Before Annealing	83.8±0.7	104.3±0.1	123.4±0.8	20.0±0.3
After Annealing	83.5±0.6	119.6±0.6	143.0±0.4	16.8±0.8

<sup>A</sup> Mean ± standard deviation values are reported.

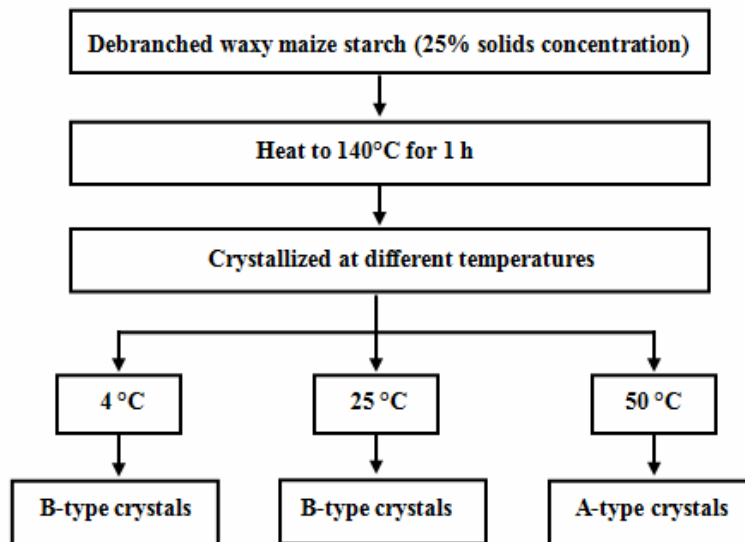


**Figure 5.1 Production of A- and B-type crystals from short-chain amylose by changing (A) starch solids; (B) crystallization temperature; and (C) chain length**

**A**



**B**



**C**

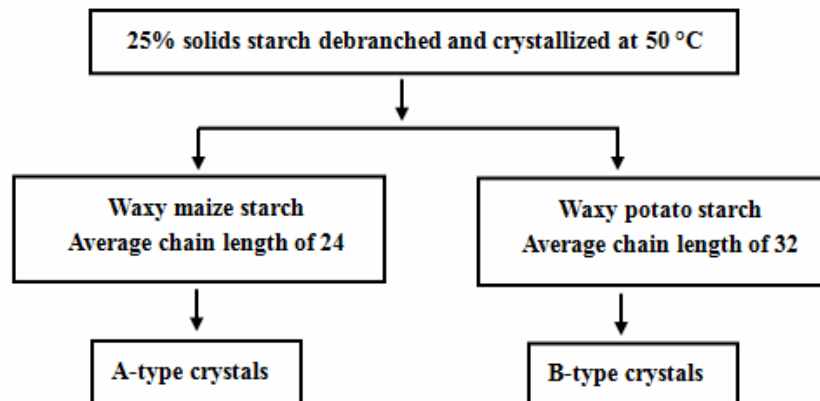


**Figure 5.2** Wide-angle X-ray diffraction of short-chain amylose prepared from debranched waxy maize starch with different (A) solids concentration, (B) crystallization temperatures, and (C) debranched waxy potato starch before and after annealing

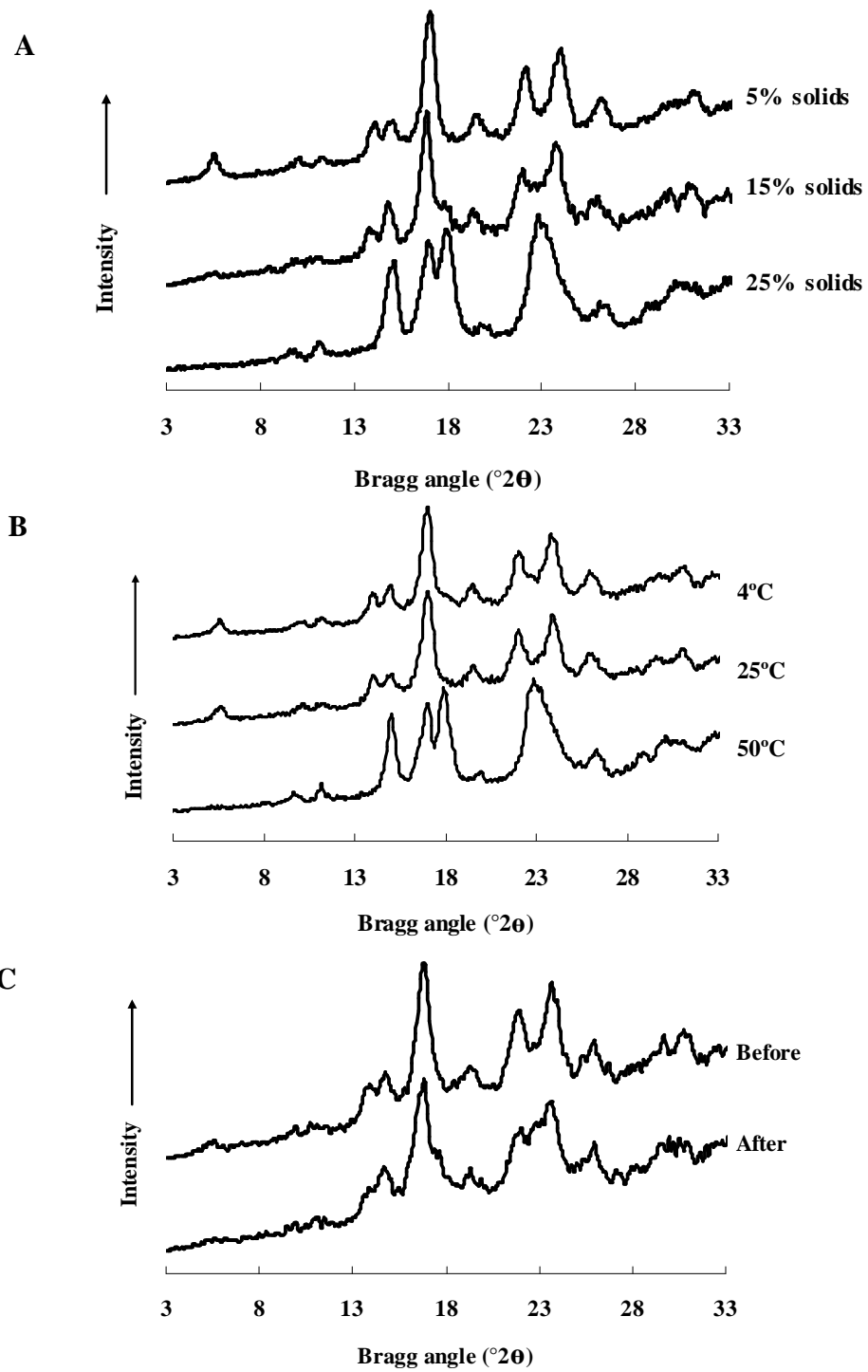


**Figure 5.3** Molecular weight distribution of short-chain amylose prepared from debranched waxy maize starch with different (A) solids concentration, and (B) crystallization temperatures, and (C) debranched waxy potato starch before and after annealing

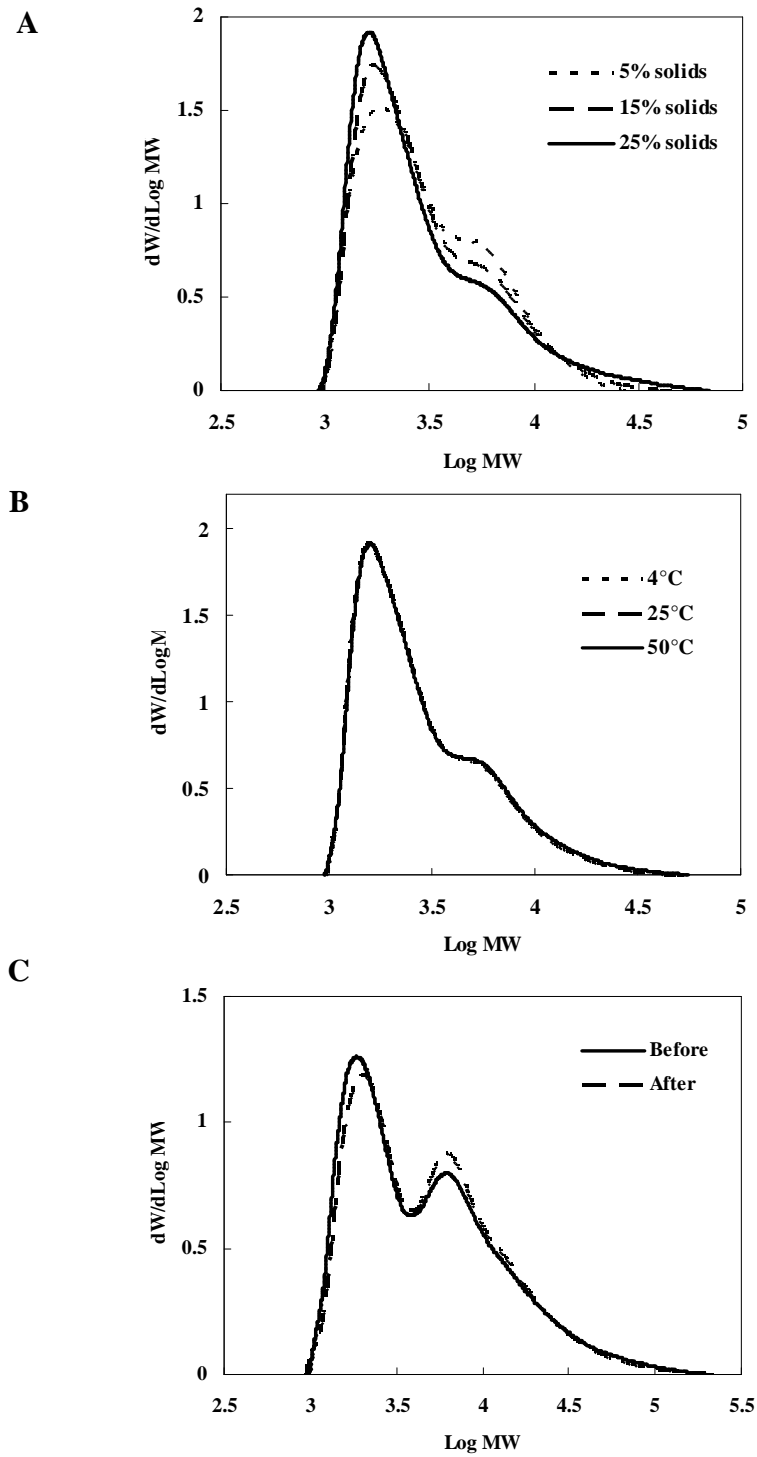


**Figure 5.4** Scanning electron microscopic images of short-chain amylose prepared from debranched waxy maize starch with different starch solids concentration: A and B, 5% solids; C and D, 15% solids; E and F, 25% solids

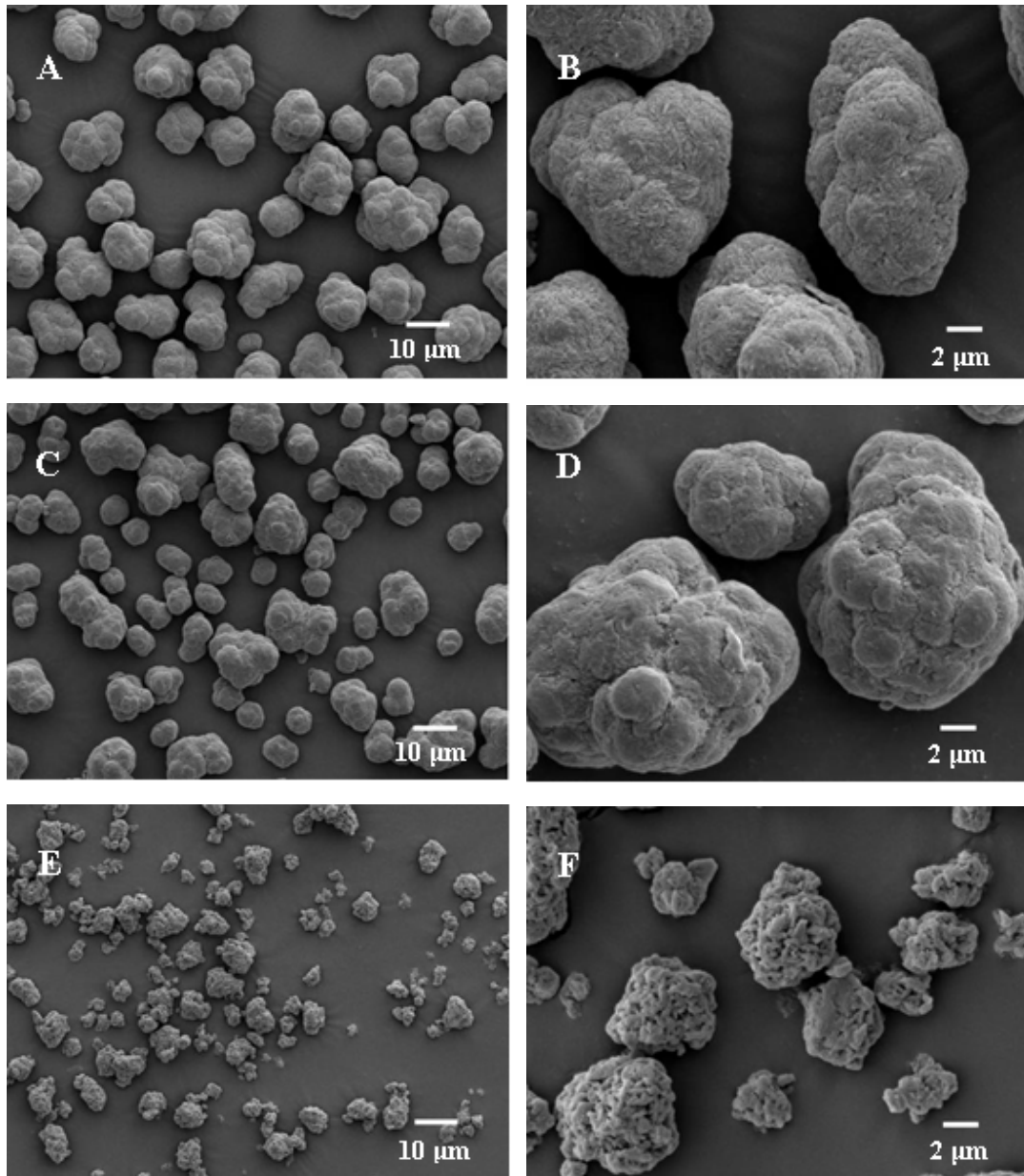


**Figure 5.5** Scanning electron microscopic images of short-chain amylose prepared from debranched waxy maize starch with different crystallization temperature: A and B, 4°C; C and D, 25°C; E and F, 50°C

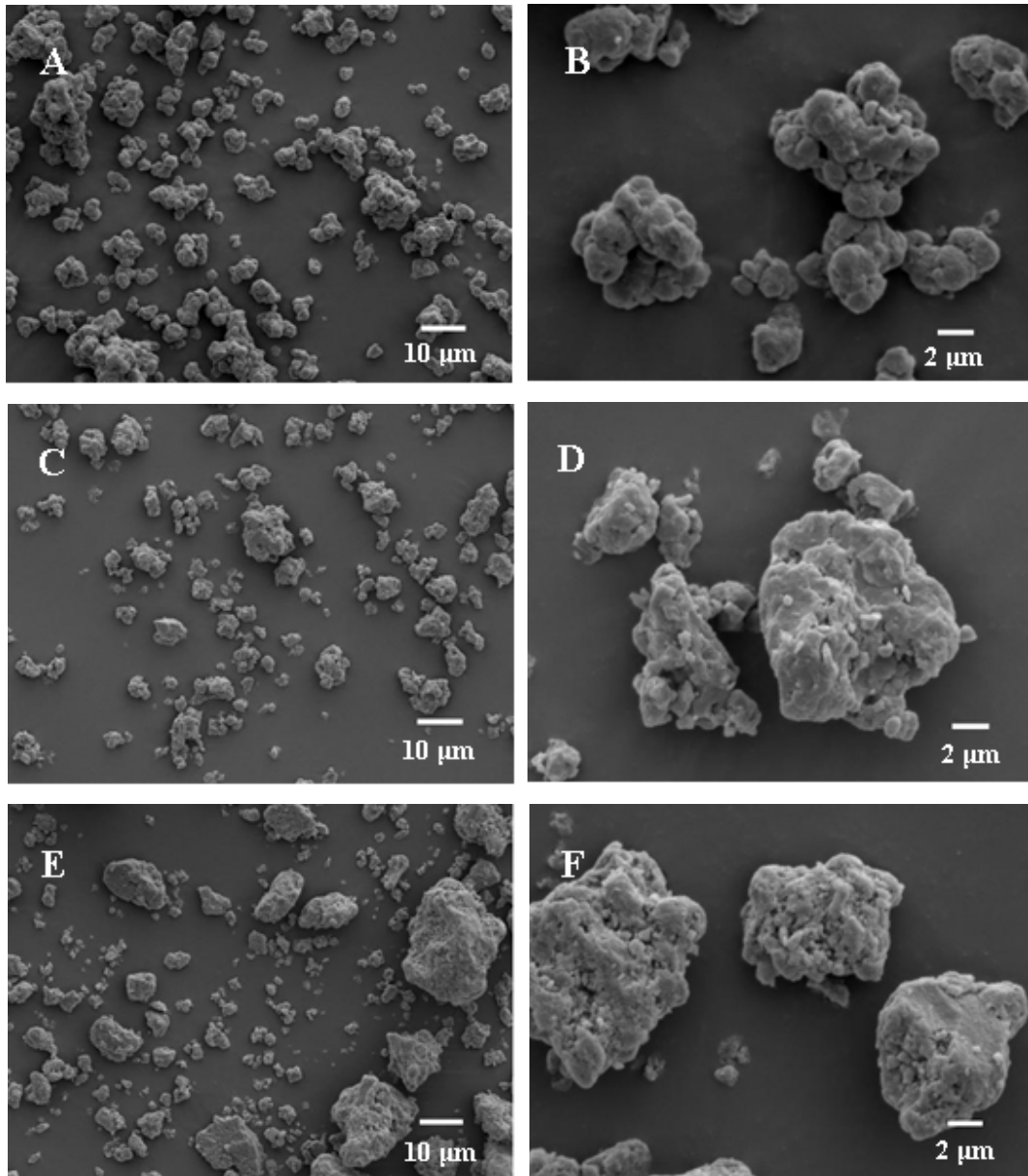


**Figure 5.6** Scanning electron microscopic images of short-chain amylose prepared from debarnched waxy potato starch: A and B, before annealing; C and D, after annealing

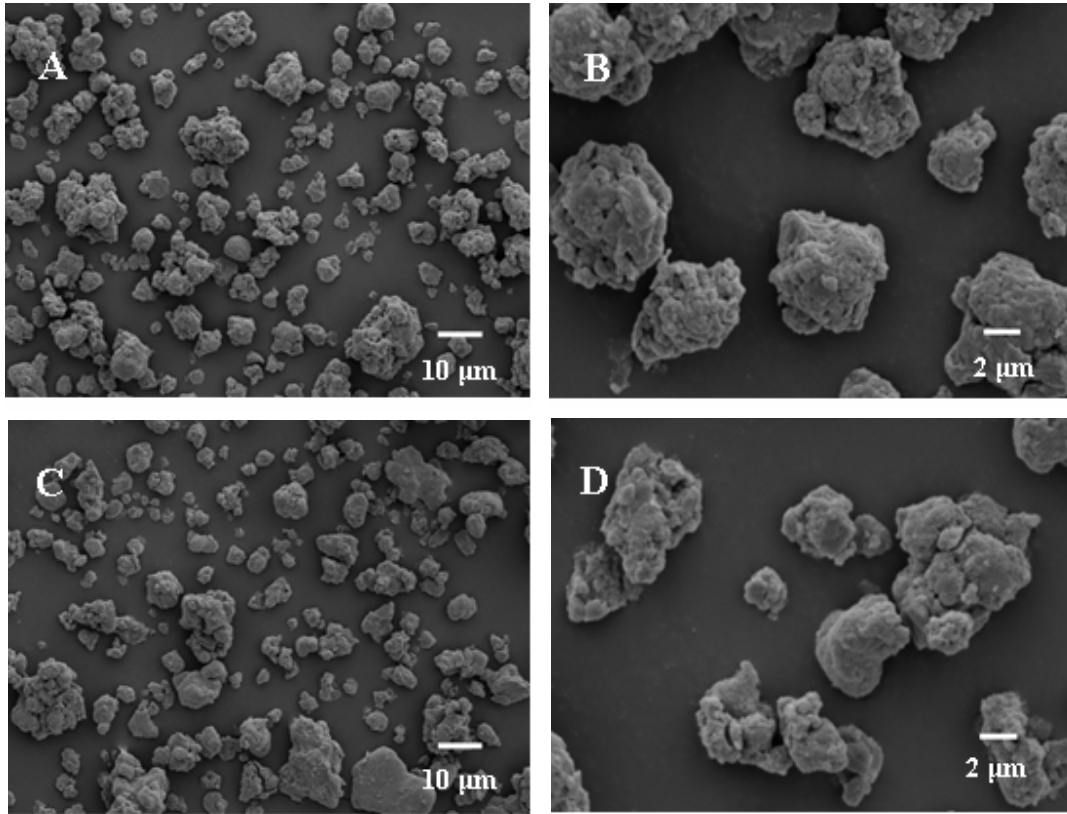


**Figure 5.7 Particle size distributions of short-chain amylose prepared from debranched waxy maize starch at different starch solids concentration: A, 5% solids; B, 15% solids; C, 25% solids**

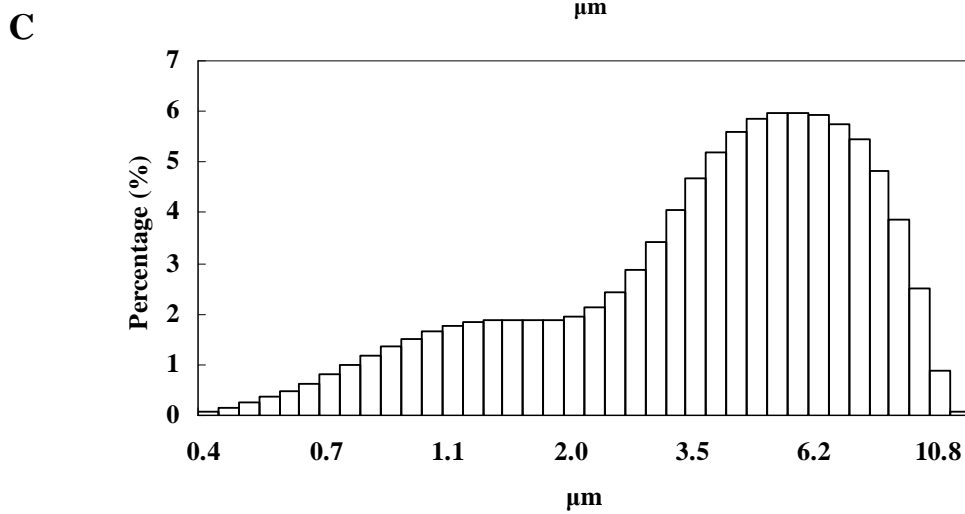
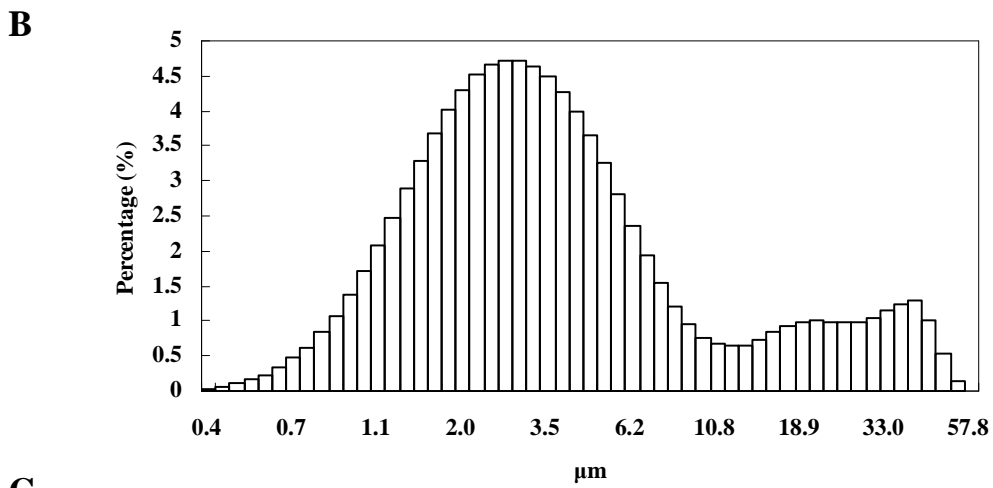
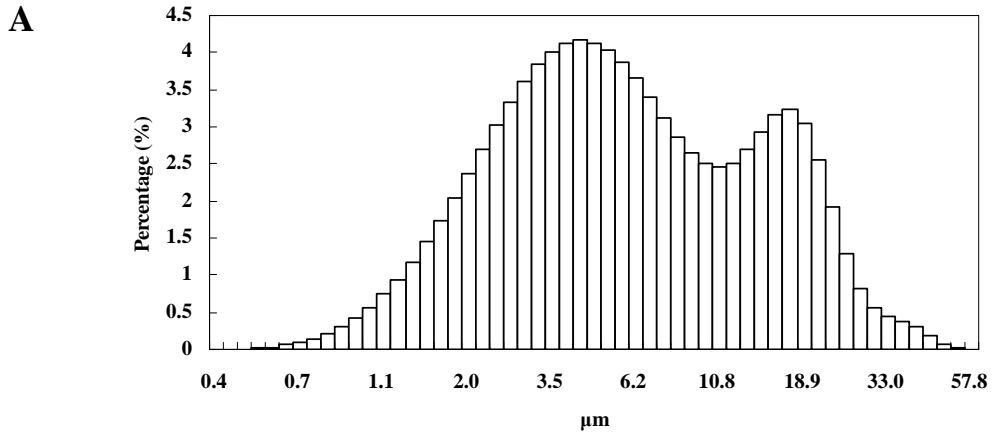


**Figure 5.8 Particle size distributions of short-chain amylose prepared from debranched waxy maize starch with different crystallization temperature: A, 4°C; B, 25°C; C, 50°C**

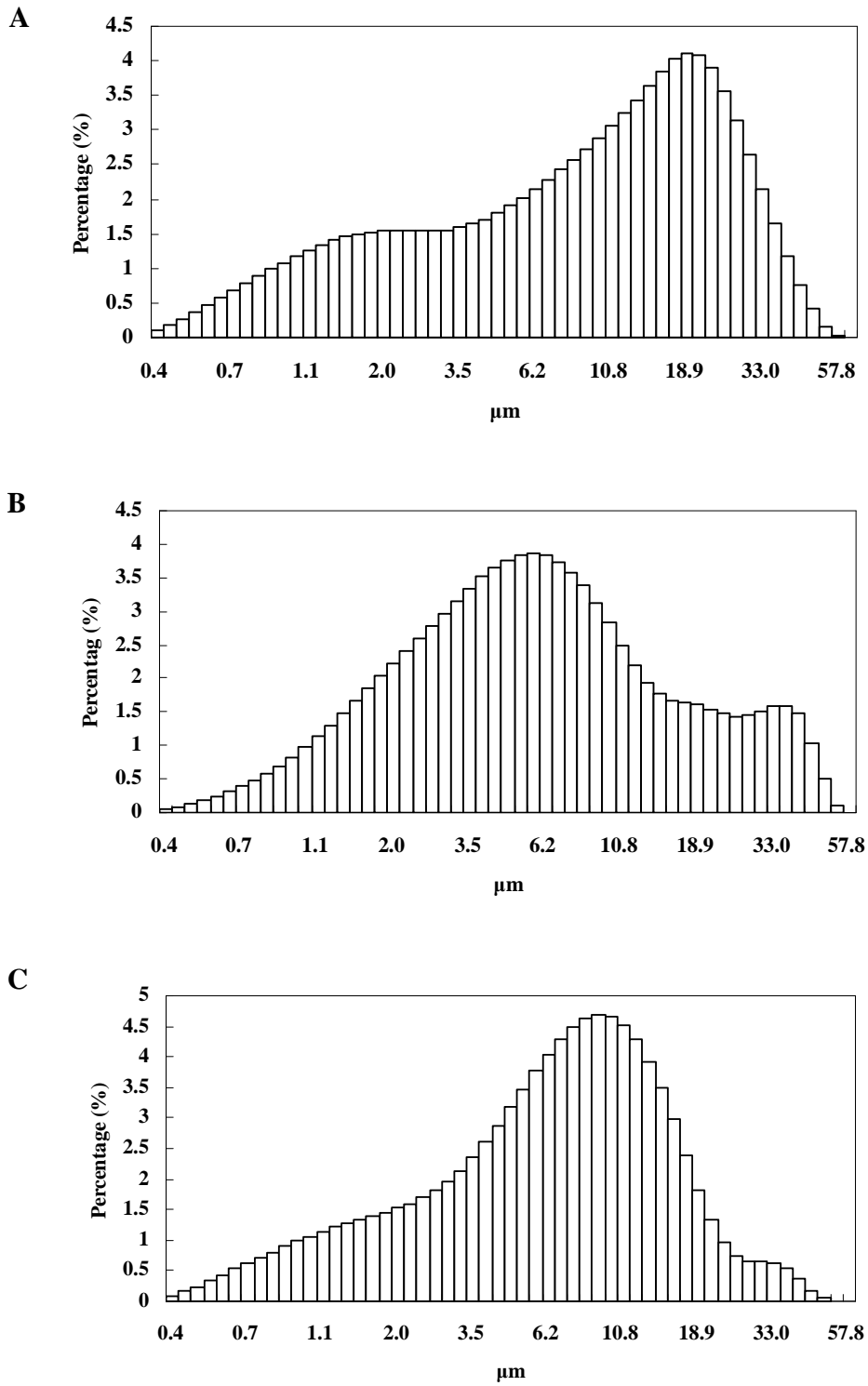
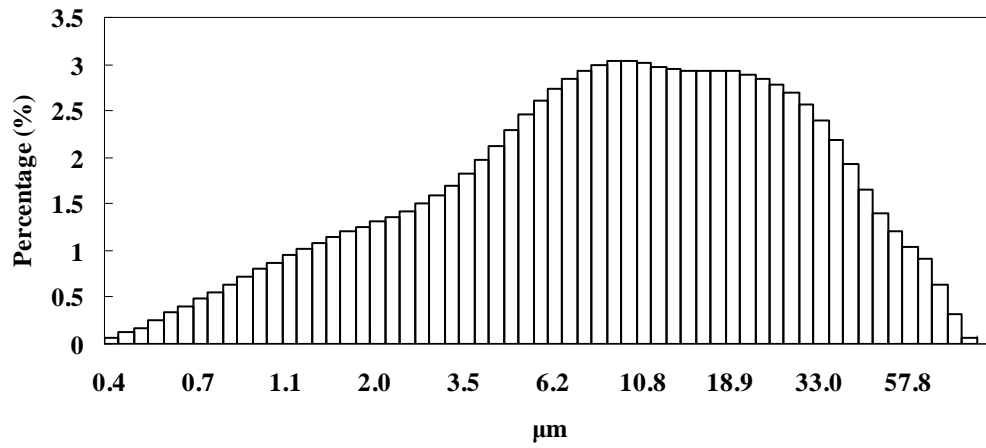




**Figure 5.9 Particle size distributions of short-chain amylose prepared from debranched waxy potato starch: A, before annealing; B, after annealing**

**A**



**B**

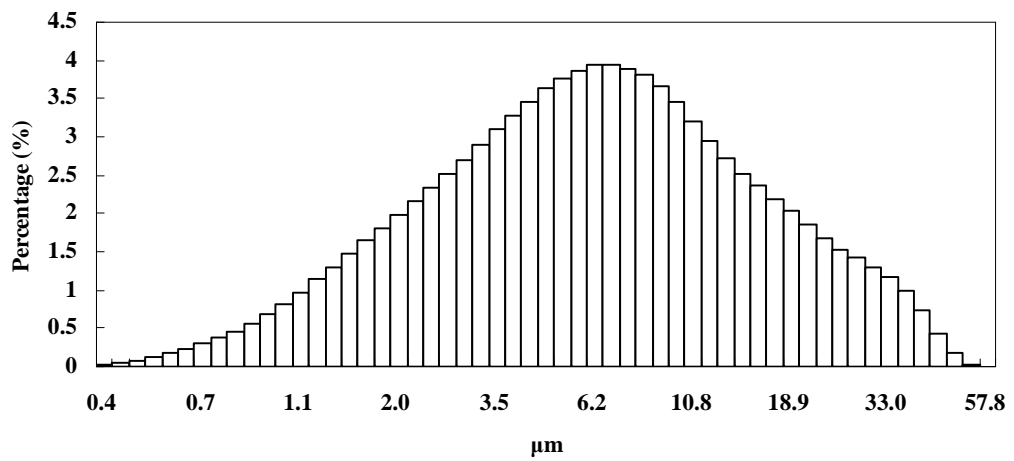


**Figure 5.10 Thermal properties of short-chain amylose prepared from debranched waxy maize starch with different (A) solids concentration, and (B) crystallization temperatures, and (C) debranched waxy potato starch before and after annealing**

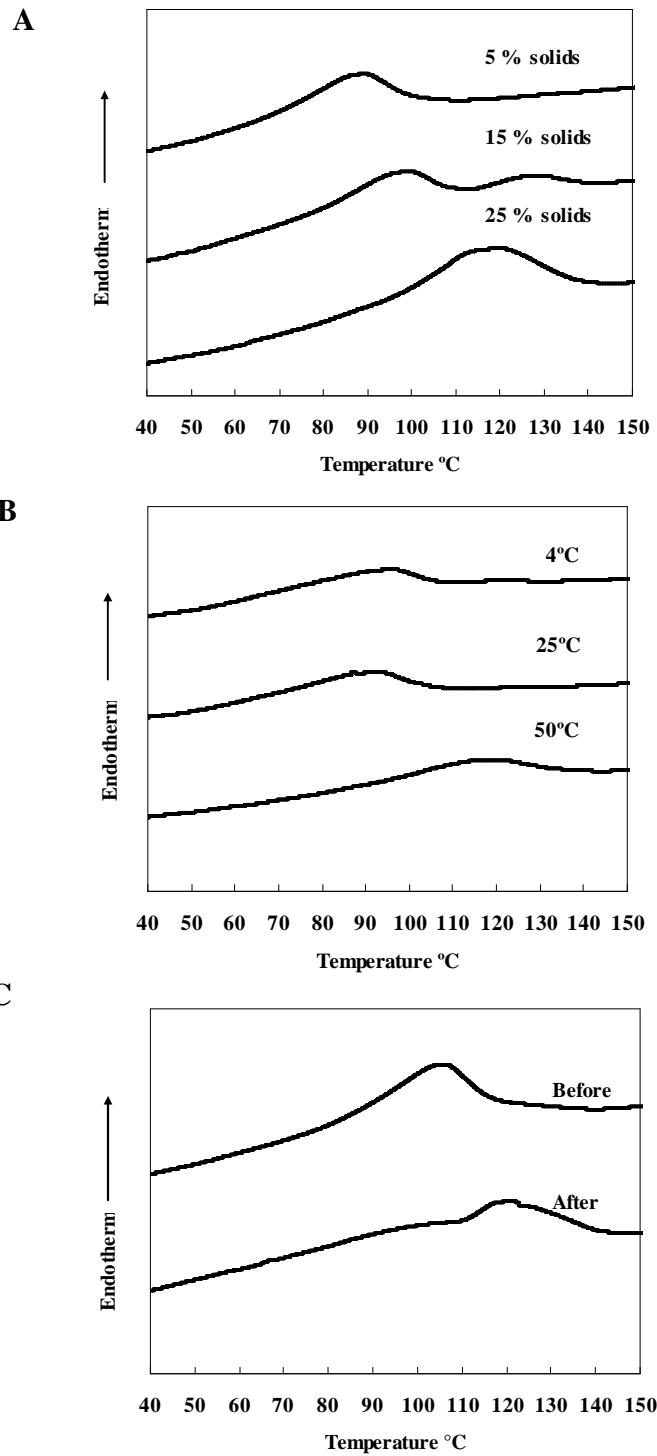


**Figure 5.11** *In vitro* digestion profile of short-chain amylose prepared from debranched waxy maize starch with different (A) solids concentration, and (B) crystallization temperatures, (C) debranched waxy potato starch before and after annealing, and (D) the method by Planchot et al (1997)

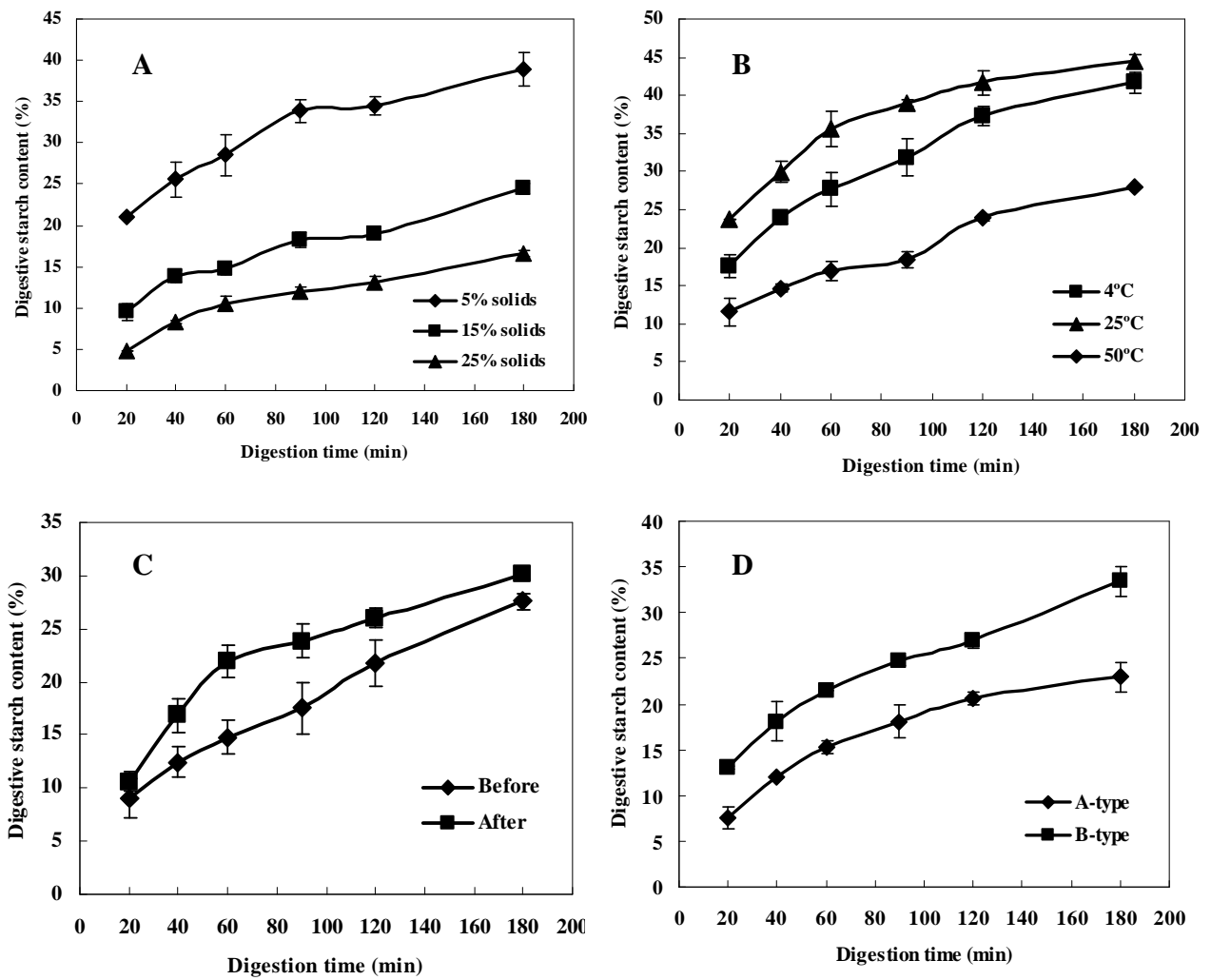
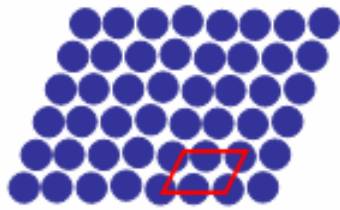
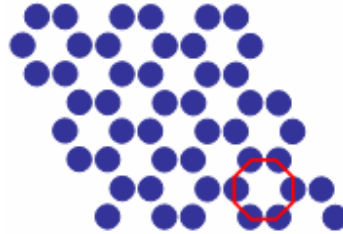


**Figure 5.12 Arrangement of double helices in A- and B-type short-chain amylose (Dot represents double helix)**



**A-type**



**B-type**

## **Chapter 6 - Formation of spherulites from short-chain amylose in relation to their digestibility**

### **Abstract**

A novel process was developed to produce spherulites from short linear  $\alpha$ -glucans (short-chain amylose, SCA) with controlled enzyme digestibility. SCA was obtained by completely debranching of waxy maize starch (25% solids) and heated to 180 °C followed by cooling and crystallization to form well-developed spherulites. Formation of spherulites involved three steps: conformational changes from coils to double helices, orderly arrangement of double helices into lamella structure, and radical orientation of aggregates of lamellar stacks into spherulites. Spherulites prepared at low temperatures (4 and 25 °C) had a large spherulite size (5-10  $\mu\text{m}$ ), a B-type X-ray diffraction pattern, a lower melting temperature (70-110 °C), and a higher digestibility, whereas spherulites crystallized at 50 °C had small dimensions (1-5  $\mu\text{m}$ ), an A-type polymorph, a higher melting temperature (100-140 °C), and a lower digestibility. The lower susceptibility of enzymatic hydrolysis was probably due to the tighter packing pattern of double helices in A-type spherulites than that in their B-type counterparts.

### **Introduction**

Spherulites are important structural features found in many polymers crystallized from the melt (Bower, 2002). Starch based spherulites can be obtained by cooling the starch suspension pre-heated into a solution state without disturbance (Nordmark and Ziegler, 2002 a,b; Steeneken and Woortman, 2009; Ziegler et al, 2003). The overall morphology of spherulites is dependent on starch sources, amylose content, and crystallization conditions such as heating temperature, concentration of starting materials, cooling rate and crystallization temperature (Singh et al, 2010; Ziegler et al, 2003). High-amylose starches could form spherical structure with birefringence more readily than normal and waxy starches (Nordmark and Ziegler, 2002 a,b; Singh et al, 2010). Spherulites may be formed over a wide range of cooling rates (1-250°C/min) provided that amylose solution (10 to 20%, w/w) was pre-heated to greater than 170°C (Creek et al, 2006). Those spherulitic crystals had dimensions and structural characteristics consistent with the hilum and core region of native granules, thus was proposed as a model for starch granule initiation *in vivo* (Ziegler et al, 2005). However, in these studies (Creek et al, 2006; Ziegler et al,

2005), amylose used was essentially linear long chains and isolated from granular starch by an aqueous leaching process, thus had a low yield. Moreover, the sample was heated in a differential scanning calorimeter (DSC) pan. A small sample size was used, and not enough for conducting digestion study.

Spherulitic crystallization from short-chain amylose (SCA) solution has been documented as well (Helbet et al, 1993; Ring et al, 1987; Planchot et al, 1997; Williamson et al, 1992; Whittam et al, 1990). Helbert et al (1993) prepared spherulites by mixing ethanol with hot aqueous solutions of low molecular weight amylose followed by slow cooling to 4°C. The precipitates had a diameter in the order of 10 µm and exhibited an A-type X-ray diffraction pattern. In contrast, spherulites with B-type polymorph and a dimension of 10-15 µm were produced by direct cooling 5-20% w/w aqueous SCA solution to 2 °C (Ring et al, 1987). Since A- and B- amylose spherulites mimic both granular morphology and the crystalline types of native starches, they were used as model systems to study the enzymatic hydrolysis of starch crystallites (Planchot et al, 1997; Williamson et al, 1992). The materials they used to prepare spherulites were obtained by extensive acid hydrolysis of native starches, as a result, causing a significant loss of starch during treatment and presumably still containing branched points (Planchot et al, 1997; Williamson et al, 1992).

Instead of using acid resistant fractions from acid hydrolyzed starches, we prepared completely short linear chains from debranched waxy maize starch by using isoamylase (Cai et al, 2010). Highly pure A- and B-type crystals with a high yield and aggregate morphology were prepared from those short chains and their digestibility was examined (**Chapter 5**). In this study, a novel process was developed to produce both highly pure A- and B-type crystalline spherulites from waxy maize starch at high solids concentration in an aqueous environment. The conditions and mechanism of self-assembly of short linear chains into spherulites in relation to their digestibility were investigated. Our specific goals were to (1) investigate the necessary heating temperature for SCA to form spherulites, (2) study the effects of crystallization temperatures on morphology and crystalline structure of resulting products, and (3) relate the structure of spherulites formed to their enzyme digestibility.

## **Materials and methods**

### ***Materials***

Waxy maize starch was obtained from National Starch LLC (Bridgewater, NJ, USA), and isoamylase (EC 3.2.1.68) was obtained from Hayashibara Biochemical Laboratories, Inc. (Okayama, Japan). The enzyme activity was  $1.41 \times 10^6$  IAU/g, and 1 IAU was defined as the amount of isoamylase that increased reducing-power absorbance of the reaction mixture by 0.008 in 30 min under the conditions of the isoamylase assay (FAO JECFA Monographs, 2007). All chemicals were reagent-grade.

### ***Starch debranching and spherulites formation***

Waxy maize starch (25g, dry basis) was mixed with acetic acid buffer (0.01M, pH4.0) in a pressure bottle (Ace Glass Incorporated, Vineland, NJ, USA) to prepare 25% solids starch suspension and cooked in a boiling water bath with continuously stirring for 30 min, then put into 120°C oven for 30 min. After the mixture was cooled to 50°C, 1% isoamylase based on the dry weight of starch was added. The mixture was kept at 50°C with stirring for 24 h. Part of the mixture (15 mL) was taken, sealed in a pressure tube (Ace Glass Incorporated, Vineland, NJ, USA) and heated in an oven at 180°C for 20 min. The tube was stored at 4, 25 and 50°C for 24 h, respectively. The precipitate was filtered, washed by water, dried at 40 °C in an oven overnight and ground by a pestle and mortar. To determine the minimum heating temperature required to form spherulites, the mixture (15 mL) was sealed and heated to 170 and 190°C for 20 min, respectively, and crystallized at 4°C for 24h.

To determine the yield of spherulites, an aliquot (1.0 mL) of starch slurry was taken and centrifuged ( $\times 13,226$  g) for 10 min. The carbohydrate concentration in the supernatant was determined with a portable refractometer (Fisher Scientific Inc., Pittsburgh, PA, USA). The blank reading was determined by the same procedure on uncooked starch slurry mixed with isoamylase. The level of precipitation of carbohydrate was calculated by reading the difference between the sample and the blank. Each measurement was done in duplicate.

### ***Light microscopy***

A drop of sample suspension was deposited on a microscopy slide, and covered with a glass. The sample was observed by an Olympus BX51TF microscope (Olympus Optical Co. Ltd.,

Shinjuku-ku, Tokyo, Japan). The images in both normal light and polarized light backgrounds were captured using SPOT 18.2 Color Mosaic camera (Diagnostic Instruments Inc., Sterling Heights, MI, USA).

### ***Gel permeation chromatography (GPC)***

The molecular weight distribution of spherulites was examined by GPC as previously described in Chapter 2.

### ***Scanning electron microscopy (SEM)***

The morphology of spherulites was investigated by SEM as previously described in Chapter 2.

### ***Wide-angle X-ray diffraction***

The crystalline structure of spherulites was studied by wide-angle X-ray diffraction as previously described in Chapter 3.

### ***DSC***

The thermal properties of spherulites were analyzed by DSC as previously described in Chapter 2.

### ***Synchrotron small-angle X-ray scattering***

Small-angle X-ray experiments were carried out as previously described in Chapter 2. Both as is and hydrated samples (ca. 50% moisture) were examined.

### ***In vitro digestion method***

The *in vitro* digestion test of spherulites was determined by a modified Englyst procedure as previously described in Chapter 2. After 3 h, the digestion was stopped by adding 200 mL ethanol. The digestive residues were recovered by filtration and dried at an oven at 40 °C overnight. The *in vitro* digestion of above digestive residues was determined by the same modified Englyst procedure as previously described in Chapter 2.



## Results

### *Molecular weight (MW) distribution and yield*

**Figure 6.1** shows the MW distribution of SCA spherulites as determined by GPC. A bimodal distribution with low and high MW peaks, was observed for all spherulites crystallized at different temperatures. Spherulites obtained at 4°C had a slightly larger proportion of the low MW fractions compared to those produced at 25 and 50°C. The observation suggested that shorter linear chains ( $DP < 10$ ) could continue to associate together and precipitate out when temperature was decreased.

The MW distribution results were also consistent with the yield data listed in **Table 6.1**. The recovery of SCA spherulites increased from 50% to 87.6%, as crystallization temperature decreased from 50°C to 4°C. Similar phenomenon was observed during debranching and crystallization of high solids concentration waxy maize starch (Cai et al, 2010). The yield of precipitate increased to about 90%, after debranching and crystallization of waxy maize starch at 50°C for 24 h followed by precipitation at 25° for 6 h (Cai et al, 2010). The high yield of SCA spherulites and their possible recovery by filtration make them great application potentials.

### *Morphology*

Microscopic images of SCA spherulites under both normal and polarized light backgrounds are shown in **Figure 6.2**. For materials crystallized at 4°C and 25°C, birefringence and Maltese cross were observed under polarized light (**Figure 6.2B** and **D**). The size of the spherulites ranged from 5 to 10  $\mu\text{m}$  (**Figure 6.2A-D**). Increasing the crystallization temperature to 50°C resulted in less well-developed spherulites with a reduced particle size (ca. 1 to 5 $\mu\text{m}$ ), a weak birefringence and Maltese cross pattern (**Figure 6.2 E** and **F**).

The spherulites were not well developed when cooling from 170°C. Instead, small size particles (ca. 1 to 5 $\mu\text{m}$ ) with week birefringence were observed (**Figure 6.3A** and **B**). Spherulites were observed when cooling from 190°C (**Figure 6.3C**), but the Maltese cross pattern was weak (**Figure 6.3D**). Thus, the necessary heating temperature for high solids SCA aqueous solution to form spherulites upon cooling was above 170°C. Similar conclusions were reported for long chain amylose (Ziegler, 2003). They suggested that conformational change from a helix to a coil

structure of linear chains above 170°C increased the chain flexibility and induced the spherulite formation.

**Figure 6.4** shows the SEM images of SCA spherulites produced from different crystallization temperatures. Similar morphology and size were shown for spherulites formed at 4°C (**Figure 6.4A** and **B**) and 25°C (**Figure 6.4C** and **D**). Spherulites crystallized at 50°C had a smaller size (ca. 1-5  $\mu\text{m}$ ) (**Figure 6.4 E** and **F**).

#### *Characterization of crystalline structure*

The wide-angle X-ray diffraction patterns of spherulites are shown in **Figure 6.5**. Spherulites formed at 4 and 25°C exhibited the B-type crystallinity, whereas the A-type polymorph was formed at 50°C. According to Gidley (1987), A-type structure of starch is a thermodynamic product whereas B-type polymorph is a kinetic event. The dissolution temperature of SCA spherulites is largely dependent on their polymorphs and water content (Whittam et al, 1990). The thermal properties of spherulites prepared at different crystallization temperatures were shown in **Figure 6.6**. An endothermic peak that centered around 90°C was observed for spherulites obtained at 4 and 25 °C. The endotherm of spherulites formed at 50 °C shifted to a higher peak melting temperature of 120°C, indicating that differences in crystallization temperature could lead to different melting temperatures. Our results showed that A-type structure prepared from 50°C was more thermal stable (about 30°C higher) than B-type structure obtained from 4 and 25°C (**Figure 6.6** and **Table 6.2**). These phenomena were in agreement with the work conducted by Whittam et al (1990). They found that A-type SCA spherulites melted at temperatures about 20°C higher than B-type spherulites at a water content more than 40% (w/w).

Peak melting temperature of the B-type SCA spherulites prepared from lintnerized potato starch was 70-80°C in the excess water conditions (Ring et al, 1987; Williamson et al, 1992; Whittam et al, 1990), while a peak melting temperature of about 90°C was observed for A-type spherulites (Williamson et al, 1992; Whittam et al, 1990). It is interesting to note that for the same crystalline type, spherulites made in this study had 20-30 °C higher melting temperature than those documented in the literature. We hypothesized that completely linear short chains generated from debranched waxy starch could form more stable double helices than SCA obtained from acid hydrolysis, which contained branch points. However, except the molecular

chain distribution pattern, other factors such as starch solids concentration, crystallization temperature and medium, might also contribute to these results.

Unlike SCA, spherulites from long chain amylose (isolated from native starch) were only reported to reveal the B-type X-ray diffraction pattern, and showed a higher dissolution temperature than B-type SCA spherulites (Nordmak and Ziegler, 2002a; Creek et al ,2006). According to Nordmak and Ziegler (2002a), amylose purified from high amylose maize starch could form spherulites with an endotherm ranged from ca. 90 to 140°C and a peak melting temperature of 125-130°C. Creek et al (2006) reported that spherulitical materials obtained from pre-heated maize amylose with a wide range of cooling rates showed a dissolution temperature ranged from 100 to 140 °C. The endotherm does not change significantly in response to a change in cooling rate. It is possible that double helices in long chain amylose spherulites associated more tightly and were more resistant to disassociation upon heating. According to Moastes et al (1997), the dissolution temperature of amylose crystals at a volume fraction of water of 0.8 increased from 57°C to 119°C with a chain length increased from 12 to 55 residues, while extrapolated dissolution temperature for the high molecular weight polymer was 147°C.

The small-angle X-ray scattering curves of spherulites samples were presented in **Figure 6.7**. This peak was not observed when the moisture content was low (ca.5%) but was evident when the samples were hydrated (ca.50%). The water functions as plasticizer to hydrate the starch molecules via hydrogen bonds and align the short linear chains into order (Donald et al, 2001). However, unlike narrow 9 nm lamella peak in native starch granules (Donald et al, 2001), the peak of spherulites was broad (ranged ca. 0.3 to 1.2 nm<sup>-1</sup>), which might be attributed from the large variation of their lamella size. Nevertheless, all the lamella peaks of shperulites were centered around 0.7 nm<sup>-1</sup> (**Figure 6.7**), thus the average length of the repeating stacking containing alternative crystalline and amorphous region is about 9 nm, similar as that in the granular starches (Donald et al, 2001). The lamella peak of spherulites formed at 4°C was more evident than those formed at 25 and 50 °C, suggesting that spherulites as well as lamella structure were less well developed at higher crystallization temperatures.

### ***In vitro digestion profile***

Given the well-defined morphology and remarkable highly pure crystallinity, SCA spherulites were ideal models that could be used to study the enzymatic digestibility of native

starches with A- and B-type structures. As shown in **Figure 6.8A**, spherulites prepared at 50 °C showed the lowest digestibility. Only 15.4% of the spherulites were digested after 3 hours. For spherulites formed at 4 and 25°C, the digestive starch content at 3 hour was 20.4% and 21.9%, respectively. Interestingly, the digestion curve of spherulites formed at 4 °C was essentially linear as a function of digestion time. Digestion profiles of residues showed similar kinetic curves as the parent spherulites (**Figure 6.8B**), demonstrating that the spherulites had an essentially constant digestion rate. The residues from spherulites formed at 50°C were more enzyme resistant than those formed at 4 and 25 °C. A slight increase of digestion was observed for all the spherulite residues in comparison with their parent counterparts, which may be attributed from the altered morphology and structure of residues after the enzyme digestion test.

To further understand the digestion mechanism, we examined the digestive residues of spherulites by the light microscope again (**Figure 6.9**). Individual spherulites with clear Maltese cross along with small pieces of fragments were observed, suggesting that some spherulites were weak and more susceptible to enzyme attack, whereas some stronger spherulites were more resistant to the enzyme digestion. SEM showed rough surface structure for all the spherulite digestive residues (**Figure 6.10**), indicating that surface erosion rather than the endo-corrosion was occurred during starch digestion. It is known that the enzymatic degradation of native starch is not homogeneous. The enzymes generate holes through penetrating the weak points on the granule surface and hydrolyze the less resistant regions. In contrast, no holes or pores were observed for the spherulites.

Our results indicated that spherulites with A-type structure were more resistant to enzymatic hydrolysis than B-type spherulites. This observation was opposite to the works conducted by Williamson et al (1992) and Planchot et al (1997). They prepared A- and B-type spherulite crystals from lintnerized potato starch and found that B-type spherulites were more resistant to  $\alpha$ -amylase digestion than A-type spherulites. However, it is worth noting that the A- and B-spherulites prepared by Williamson et al (1992) and Planchot et al (1997) contained branched points. As pointed out by those authors, the presence of  $\alpha$ -1,6- linkages and the ratio of linear and branched chains may affect the amylolysis susceptibility. In the present work, the A- and B- crystals were confirmed to be linear and had similar molecular weight distribution (**Figure 6.1**).

Regardless of spherulite size and thermal stability, B-type spherulites was more susceptible to enzymatic hydrolysis than A-type polymorph (**Figure 6.8**), suggesting that the enzyme resistance of B-type native starch was probably due to its starch granular structure rather than the crystalline types. It is known that the packing pattern of double helices in A-type structure is more condensed than in its B-type counterpart (Imberty et al, 1988; Imberty and Perez, 1988; Takahashi et al, 2004; Popov et al, 2009). This tighter packing might inhibit the access of enzymes to double helices and lead to a lower digestibility of A-type spherulites in this study.

## Discussion

Amylose is known to be the effective starch component inducing the formation of spherulites (Nordmak and Ziegler, 2002a, b; Sigh et al, 2010; Ziegler et al, 2005). In this study, short linear chains obtained from debranched waxy maize starch were used to prepare spherulites for the first time. Schematic drawing of transition from starch granules to SCA spherulites is presented at **Figure 6.11**. By modeling the small angle X-ray scattering data, native starch internal granules are proposed to contain three different types of regions: amorphous growth rings, amorphous and crystalline lamella in a repeating stack (Donald et al, 2001). After being cooked at a high temperature, the starch granules were disrupted and the crystalline structure was destroyed, allowing branched points to be cleaved by isoamylase, and producing completely linear chains.

Cloudy SCA slurry (25% solids concentration) was observed after debranched starch molecules were crystallized at 50°C, but the mixture was converted into a clear solution after it was heated to 140°C. When the solution was cooled from this temperature (or the temperature range of 140-170°C), aggregates of particles with irregular shapes were observed. Those materials showed weak birefringence and a sharp wide-angle X-ray diffraction pattern, confirming the formation of double helices and crystalline structure; however, Maltese cross was not observed under polarized light and no peak was detected using small-angle X-ray scattering, indicating that the double helices were not arranged into order to form the lamella structure. Interestingly, when the solution was cooled from 180°C, lamella structure was formed as a broad peak was observed at small-angle X-ray scattering curves of hydrated spherulites samples (**Figure 6.7**).

According to Zieger et al (2005), the overall morphology of spherulitic crystals depended on the relative rates of phase separation and polymer association. It is possible that molecular interaction/crystallization occurred predominantly in this range of temperature and acted as a barrier to inhibit the formation of spherulite structure. Only when the phase separation was induced well before the nuclei initiate crystallization could the spherulites be formed (Creek et al, 2006). At the temperature of 180°C, amylose shifted from helix to coil state and separated into polymer-poor and polymer-rich phases. Upon cooling, double helices were formed in polymer-rich phase, aligned into order and precipitated out as spherulites. Thus, the spherulites formation involved (1) conformational transition from coils to double helices, (2) orderly arrangement of double helices into lamella structure, and (3) radical orientation of aggregates of lamellar stacks into spherulites.

### **Conclusions**

A novel process was developed to convert waxy maize starch to spherulites with controlled enzyme digestibility. Regardless of spherulite size and thermal stability, the A-type spherulites were more resistant to enzymatic hydrolysis than the B-type spherulites. Our findings are opposite to the fact that native starches with a B-type structure are more enzyme resistant than those with an A-type structure, suggesting that the crystalline type is not the key factor determining the digestibility of native starches.

## References

- Bower, D. I. (2002). An introduction to polymer physics. pp 133-136. UK: Cambridge University Press.
- Cai, L., Shi, Y-C., Rong, L., & Hsiao, B.S. (2010). Debranching and crystallization of waxy maize starch in relation to enzyme digestibility. *Carbohydrate Polymers*, 81, 385-393.
- Creek, J. A., Ziegler, G. R., & Runt, J. (2006). Amylose crystallization from concentrated aqueous solution. *Biomacromolecules*, 7, 761-770.
- Donald, A. M., Perry, P. A., & Waigh, T. A. (2001). The impact of internal granule structure on processing and properties. In T.L. Barsby, A. M. Donald, & P. J. Frazier. *Starch: Advances in structure and functionality* (pp. 45-52). Cambridge, UK: The Royal Society of Chemistry.
- FAO JECFA Monographs (2007). Joint FAO/WHO expert committee on food additives. 4, 21-23.
- Gidley, M. J. (1987). Factors affecting the crystalline type (AC) of native starches and model compounds- A rationalization of observed effects in terms of polymorphic structures. *Carbohydrate Research*, 161, 301-304.
- Helbert, W., Chanzy, H., Planchot, V., Buleon, A., & Colonna, P. (1993). Morphological and structural features of amylose spherocrystals of A-type. *International Journal of Biological Macromolecules*, 15 (3), 183-187.
- Imberty, A., Chanzy, H., Perez, S., Buleon, A., & Tran, V. (1988). The double-helical nature of the crystalline part of A-starch. *Journal of Molecular Biology*, 201, 365-378.
- Imberty, A., & Perez, S. (1988). A revisit to the 3-dimensional structure of B-type starch. *Biopolymers*, 27, 1205-1221.
- Moates, K. G., Noel, R. T., Parker, R., & Ring, G. S. (1997). The effect of chain length and solvent interactions on the dissolution of B-type crystalline polymorph of amylose in water. *Carbohydrate Research*, 298, 327-333.
- Nordmark, T. S., & Ziegler, G. R. (2002a). Spherulitic crystallization of gelatinized maize starch and its fractions. *Carbohydrate Polymers*, 49, 439-448.
- Nordmark, T. S., & Ziegler, G. R. (2002b). Structural features of no-granular spherulitic maize starch. *Carbohydrate Research*, 337, 1467-1475.
- Planchot, V., Cononna, P., & Buleon, A. (1997). Enzymatic hydrolysis of  $\alpha$ -glucan crystallites. *Carbohydrate Research*, 298, 319-326.
- Popov, D., Buleon, A., Burghammer, M., Chanzy, H., Montesanti, N., Putaux, J.-L., Potocki-Veronese, G., & Riekkel, C. (2009). Crystal structure of A-amylose: A revisit from synchrotron microdiffraction analysis of single crystals. *Macromolecules*, 42, 1167-1174.
- Ring, S. G.; Miles, M. J., Morris, V. J., Turner, R., & Colonna, P. (1987). Spherulitic crystallization of short chain amylose. *International Journal of Biological Macromolecules*, 9(3), 158-160.
- Singh, J.; Lelane, C.; Stewart, R. B.; Singh, H. (2010). Formation of starch spherulites: Role of amylose content and thermal events. *Food Chemistry*, 121, 980-989.
- Steeneken, P.A.M; & Woortman, A.J.J. (2009). Superheated starch: A novel approach towards spreadable particle gels. *Food Hydrocolloids*, 23, 394-405.
- Takahashi, Y., Kumano, T., & Nishikawa, S. (2004). Crystal structure of B-amylose. *Macromolecules*, 37, 6827-6832.

- Whittam, M. A., Noel, T. R., & Ring, S. G. (1990). Melting behavior of A-type and B-type crystalline starch. *International Journal of Biological Macromolecules*, 12, 359-362.
- Williamson, G., Belshaw, N. J., Self, D. J., Noel, T. R., Ring, S. G., Cairns, P., Morris, V. J., Clark, S. A., & Parker, M. L. (1992). Hydrolysis of A-type and B-type crystalline polymorphs of starch by Alpha-amylase, Beta-amylase and Glucoamylase-1. *Carbohydrate Polymers*, 18, 179-187.
- Ziegler, G. R., Creek, J. A., & Runt, J. (2005). Spherulitic crystallization in starch as a model for starch granule initiation. *Biomacromolecules*, 6, 1547-1554.
- Ziegler, G.R.; Nordmark, T.S.; Woodling, S.E. (2003). Spherulitic crystallization of starch: influence of botanical origin and extent of thermal treatment. *Food Hydrocolloids*, 17, 487-494.



**Table 6.1 Yield of short-chain amylose spherulites produced by heating debranched waxy maize starch (25% w/w) to 180°C and crystallized at different temperatures<sup>A</sup>**

Crystallization Temperature (°C)	4	25	50
Yield (%)	87.6 ±2.1	72±1.4	50±1.6

<sup>A</sup> Mean ± standard deviation values are reported.

**Table 6.2 Thermal properties of short-chain amylose spherulites produced by heating debranched waxy maize starch (25% w/w) to 180°C and crystallized at different temperatures as determined by differential scanning calorimetry <sup>A</sup>**

Crystallization Temperature (°C)	T <sub>o</sub> (°C)	T <sub>p</sub> (°C)	T <sub>c</sub> (°C)	ΔH(J/g)
4	64.8±1.2	91.4±2.3	108.5±0.7	20.9±0.1
25	73.5±0.32	91.8±1.9	109.1±0.9	21.0±0.4
50	99.9±1.1	117.5±1.9	139.1±0.5	20.5±0.5

<sup>A</sup> Waxy maize starch (25% solids) was debranched and heated to 180 °C and cooled to different crystallization temperatures.

**Figure 6.1** Molecular weight distribution of short-chain amylose spherulites produced by heating debranched waxy maize starch (25% w/w) to 180°C and crystallized at different temperatures

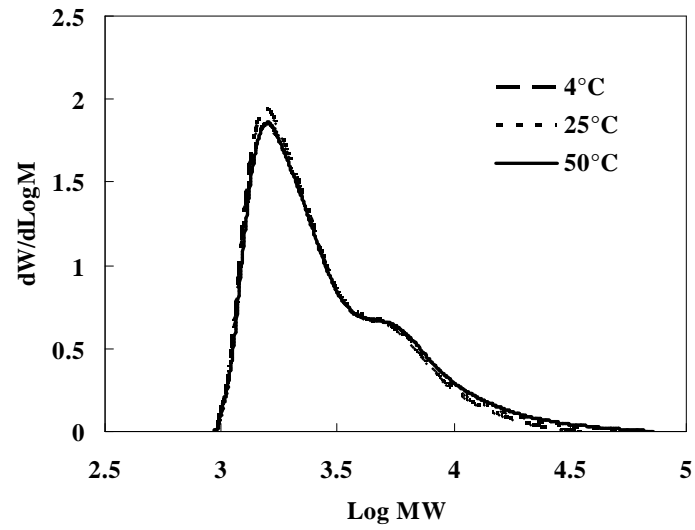


**Figure 6.2** Microscopic images of short-chain amylose spherulites produced by heating debranched waxy maize starch (25% w/w) to 180°C and crystallized at different temperatures: A and B, 4°C; C and D, 25°C; E and F, 50°C. All scale bars represent 10 μm

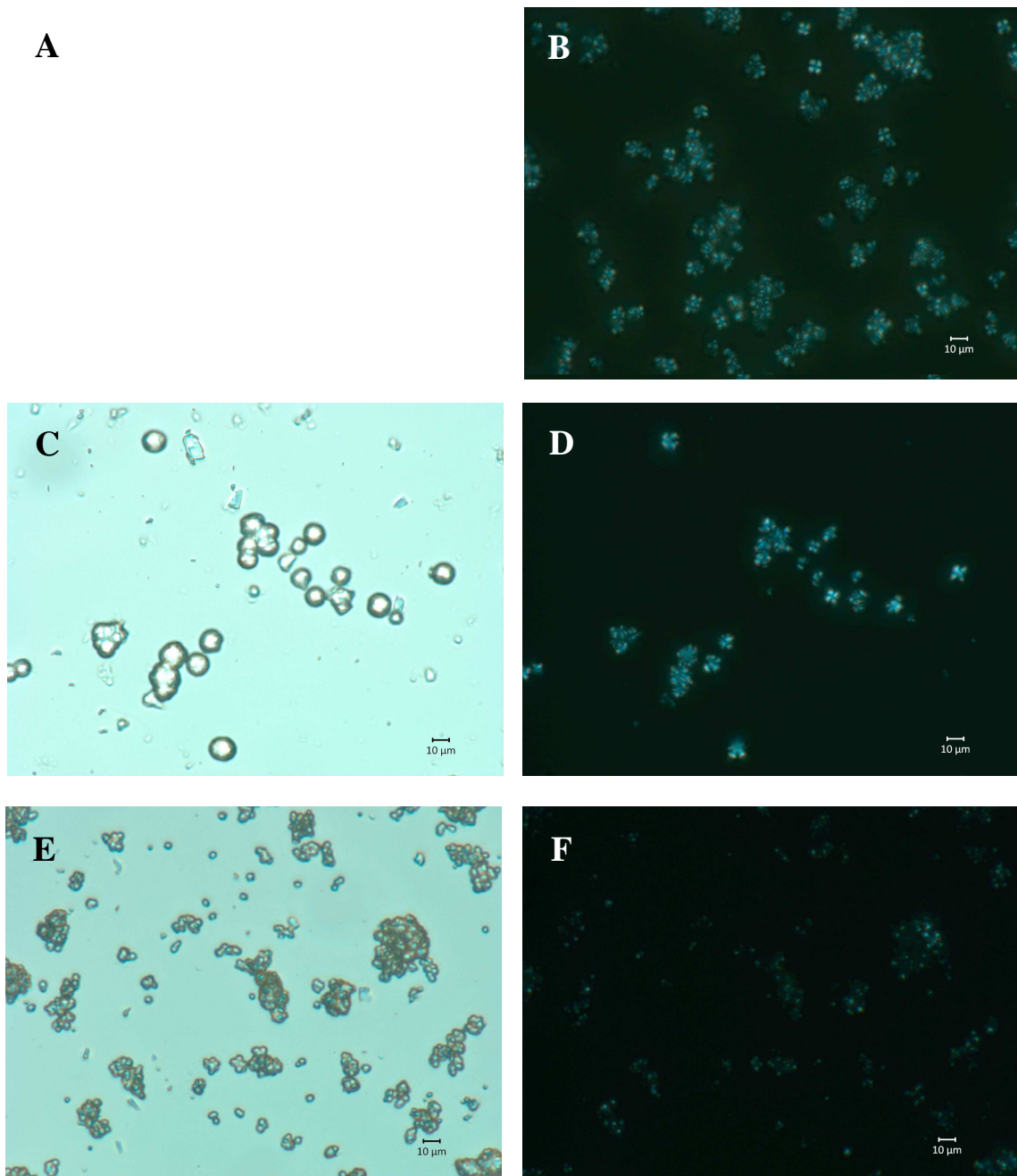


**Figure 6.3** Microscopic images of short-chain amylose produced by cooling debranched waxy maize starch (25% w/w) from A and B, 170°C; C and D, 190°C, and crystallized at 4°C. All scale bars represent 10 μm

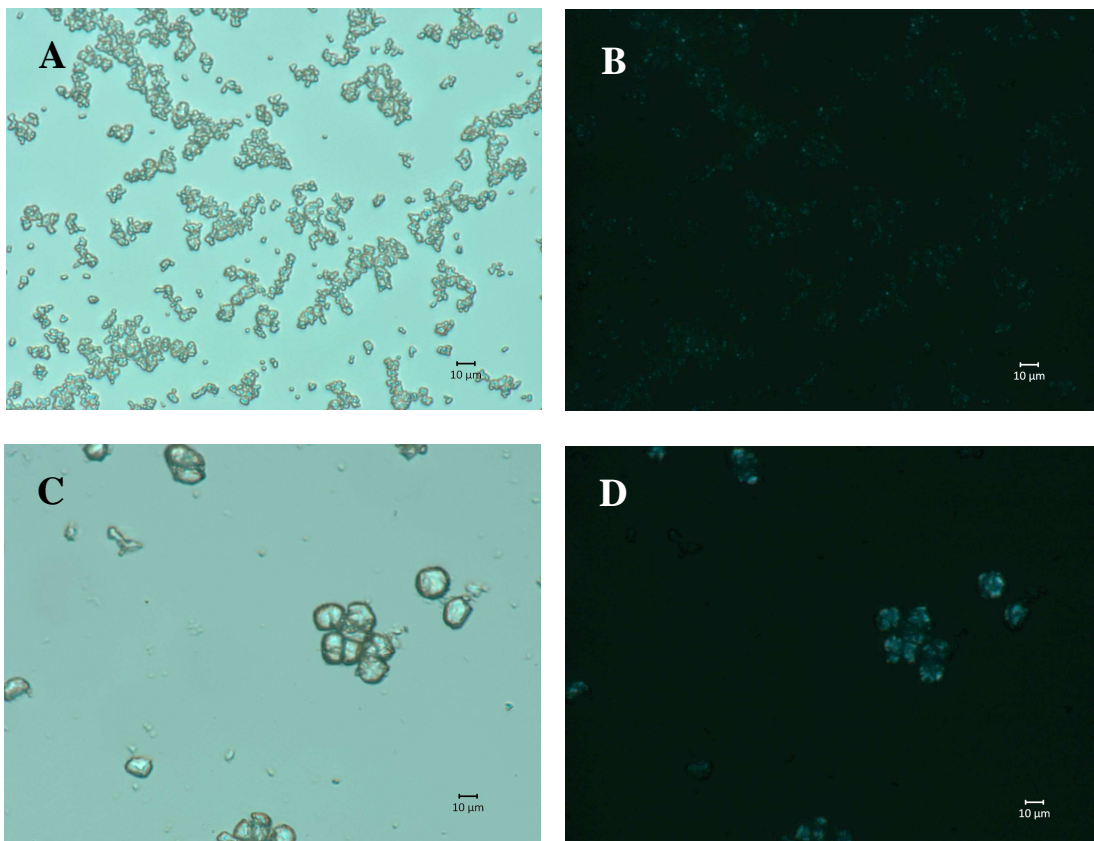


**Figure 6.4** Scanning electron microscopic images of short-chain amylose spherulites produced by heating debranched waxy maize starch (25% w/w) to 180°C and crystallized at different temperatures: A and B, 4°C; C and D, 25°C; E and F, 50°C

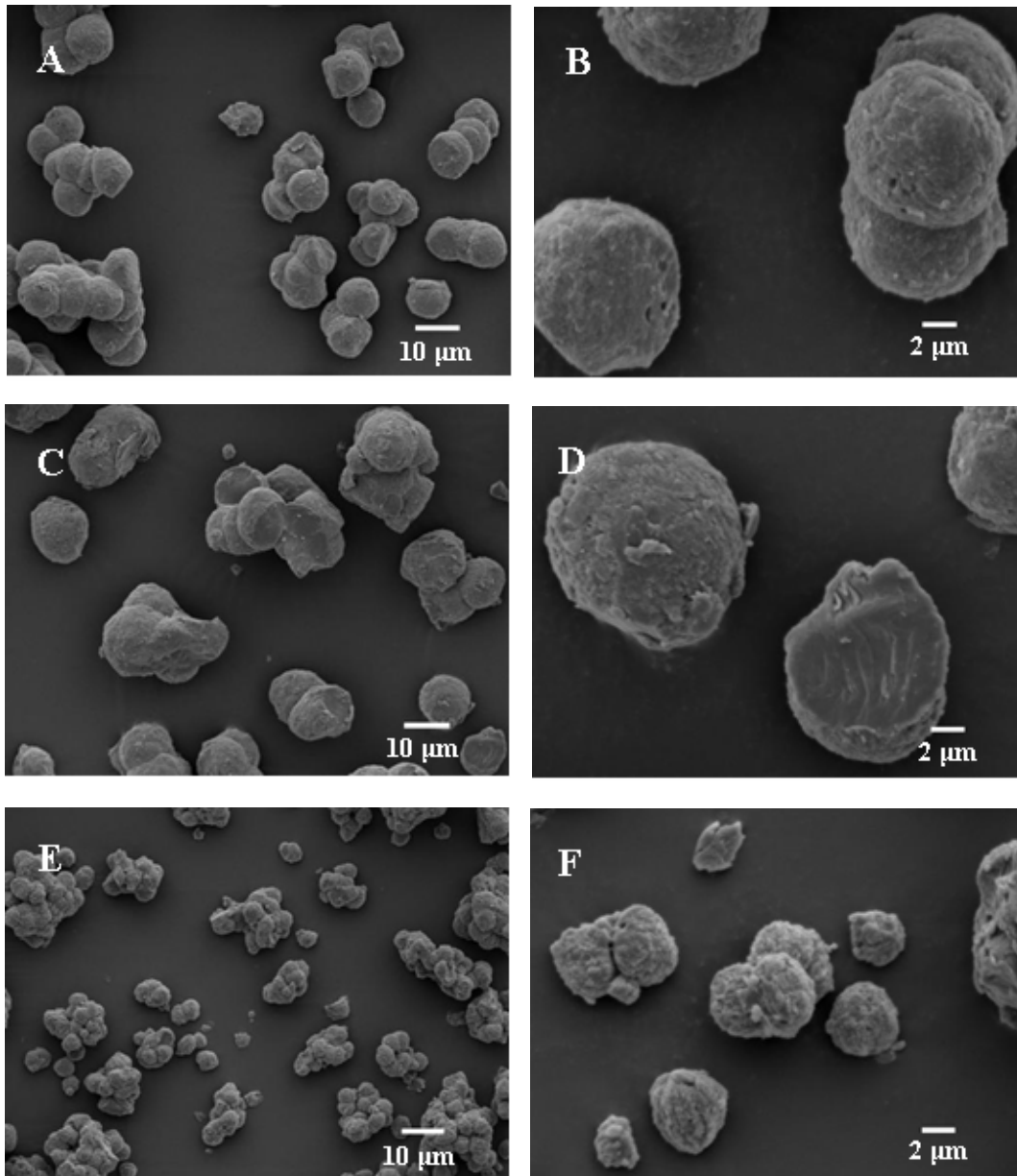


**Figure 6.5** Wide-angle X-ray diffraction of short-chain amylose spherulites produced by heating debranched waxy maize starch (25% w/w) to 180°C and crystallized at different temperatures

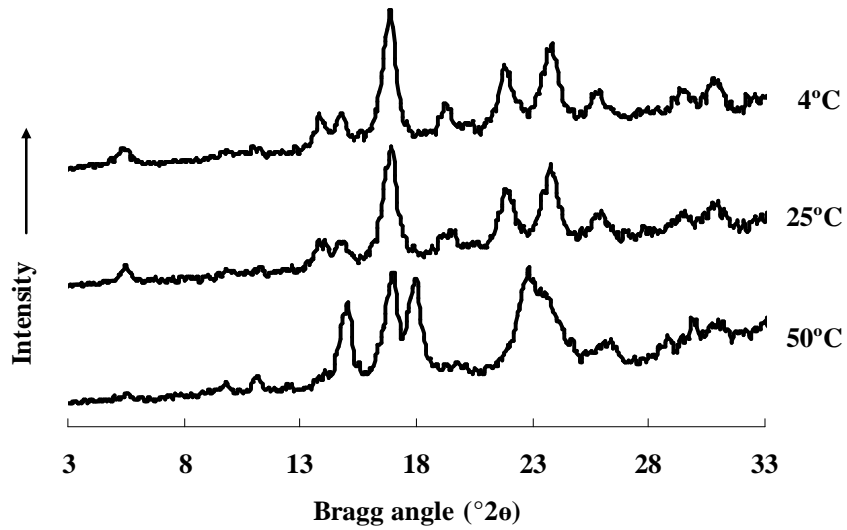


**Figure 6.6** Thermal properties of short-chain amylose spherulites produced by heating debranched waxy maize starch (25% w/w) to 180°C and crystallized at different temperatures as determined by differential scanning calorimetry

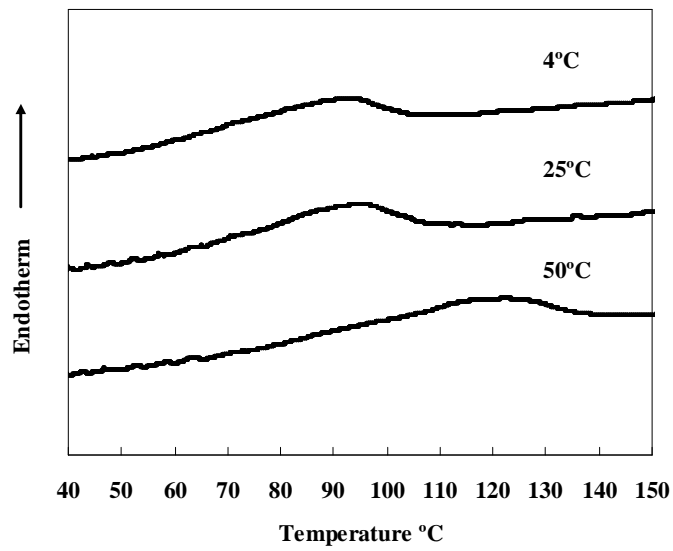




**Figure 6.7** Synchrotron small-angle X-ray scattering of short-chain amylose spherulites produced by heating debranched waxy maize starch (25% w/w) to 180 °C and crystallized at different temperatures: (A) 4 °C, as it; (B) 4 °C, hydrated; (C) 25 °C, as it; (D) 25 °C, hydrated; (E) 50 °C, as it; and (F) 50 °C, hydrated

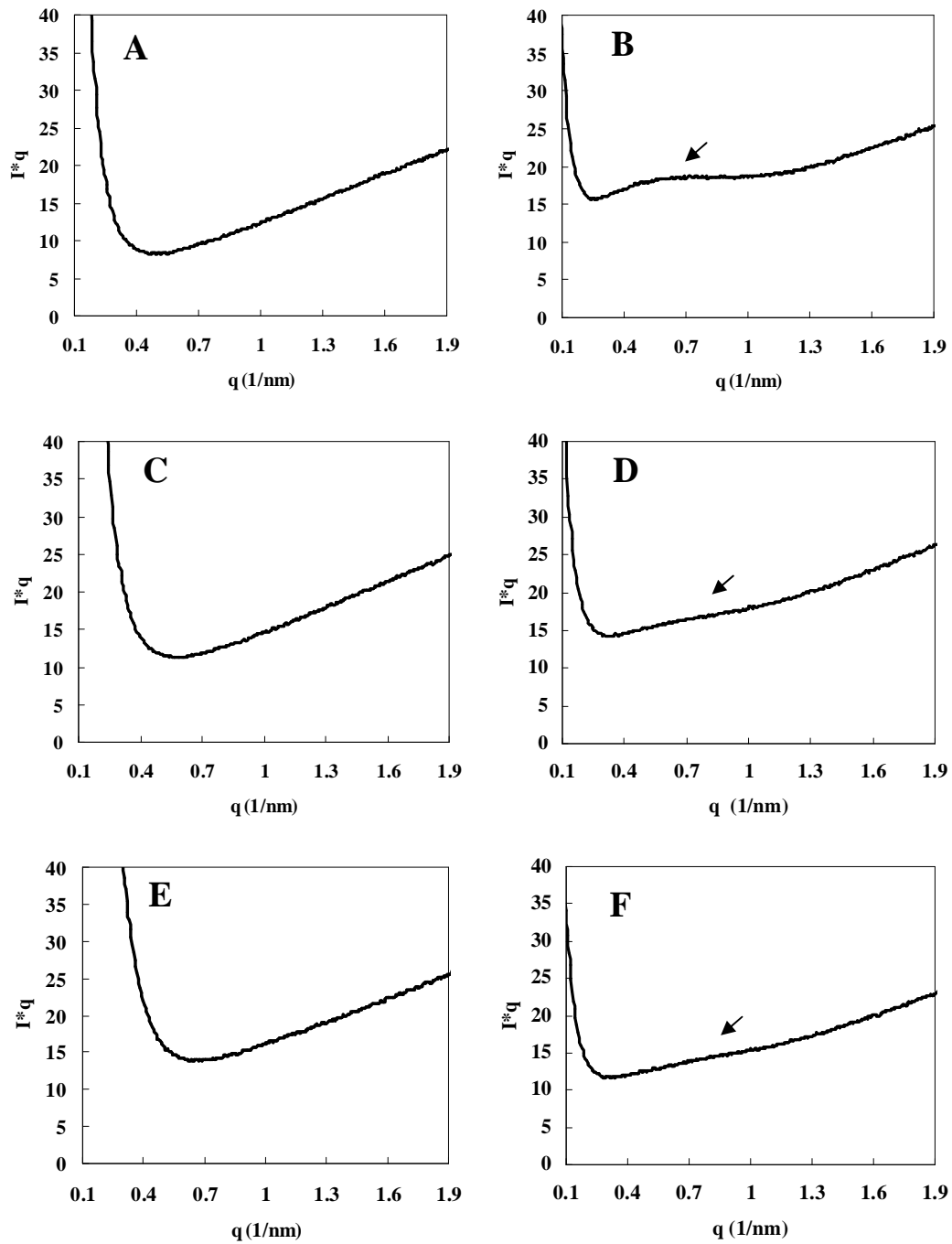


**Figure 6.8** *In vitro* digestion profile of (A) short-chain amylose spherulites produced by heating debranched waxy maize starch (25% w/w) to 180 °C and crystallized at different temperatures; and (B) their digestive residues

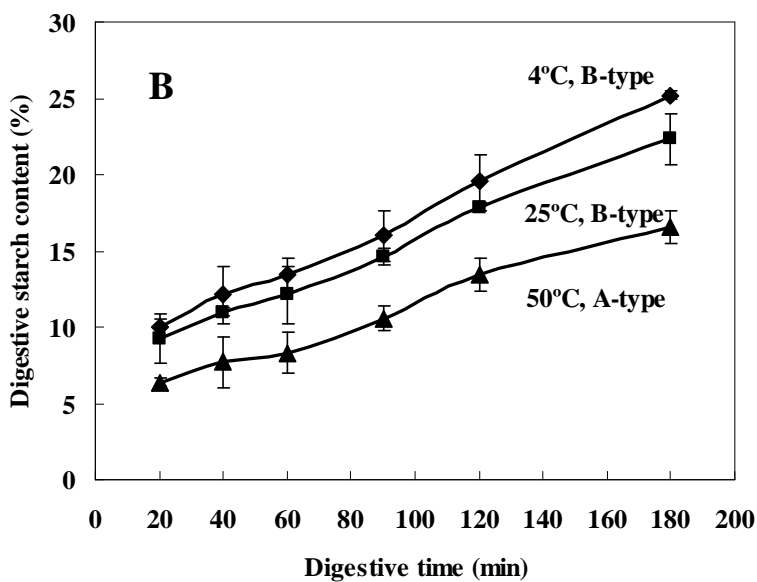
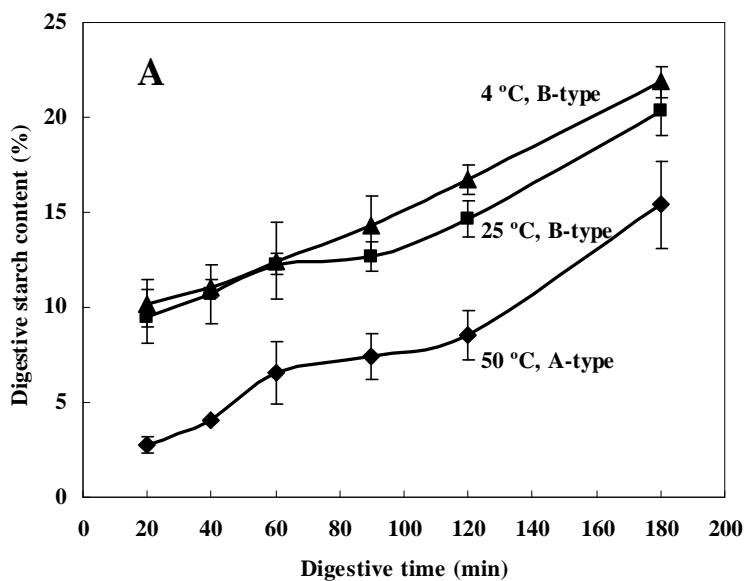


**Figure 6.9** Microscopic images of digestive residues from short-chain amylose spherulites produced by heating debranched waxy maize starch (25% w/w) to 180 °C and crystallized at different temperatures: A and B, 4 °C; C and D, 25 °C; E and F, 50 °C. All scale bars represent 10 μm.

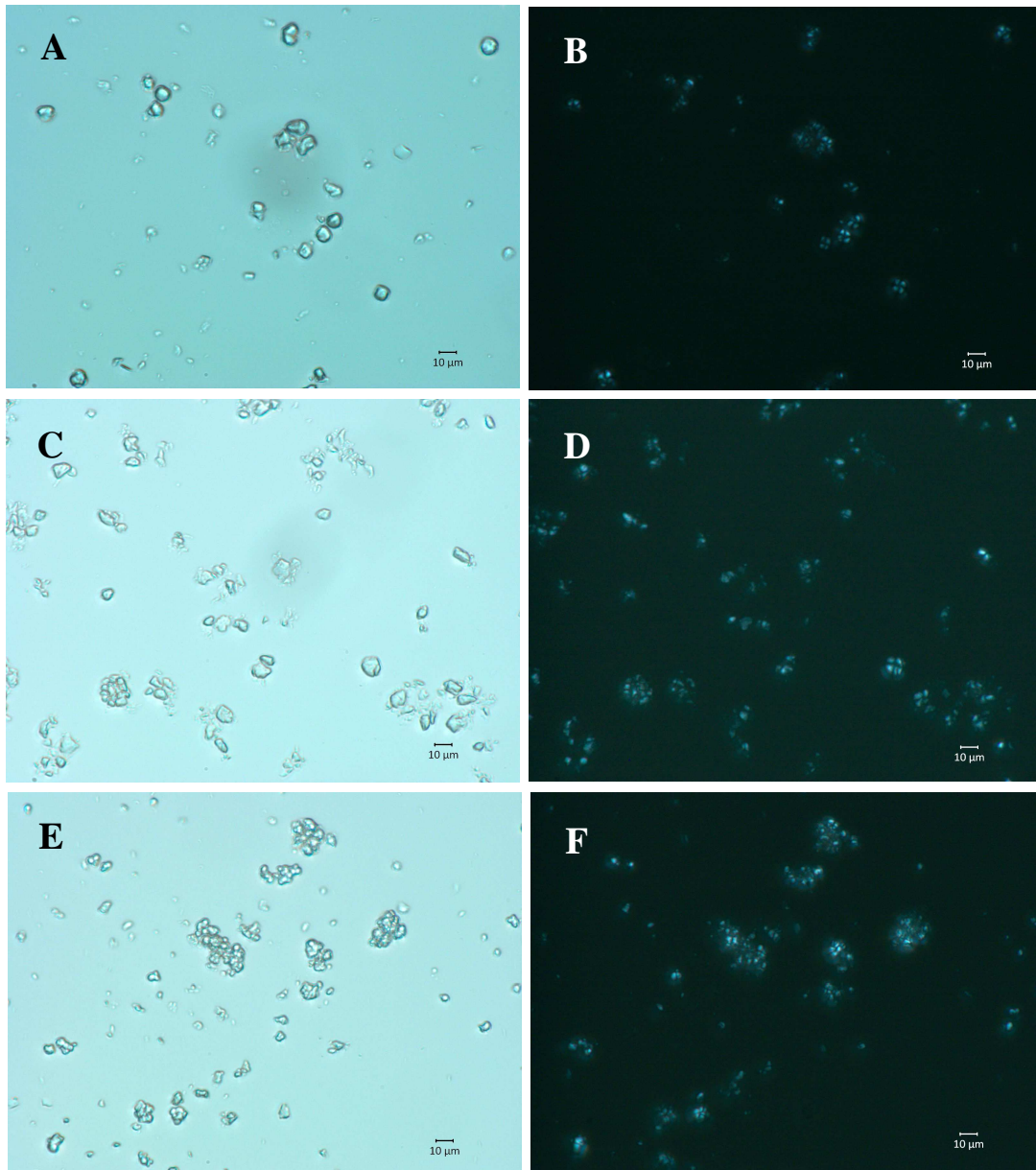


**Figure 6.10** Scanning electron microscopic images of digestive residues from short-chain amylose spherulites produced by heating debranched waxy maize starch (25% w/w) to 180 °C and crystallized at different temperatures: A and B, 4 °C; C and D, 25 °C; E and F, 50 °C.

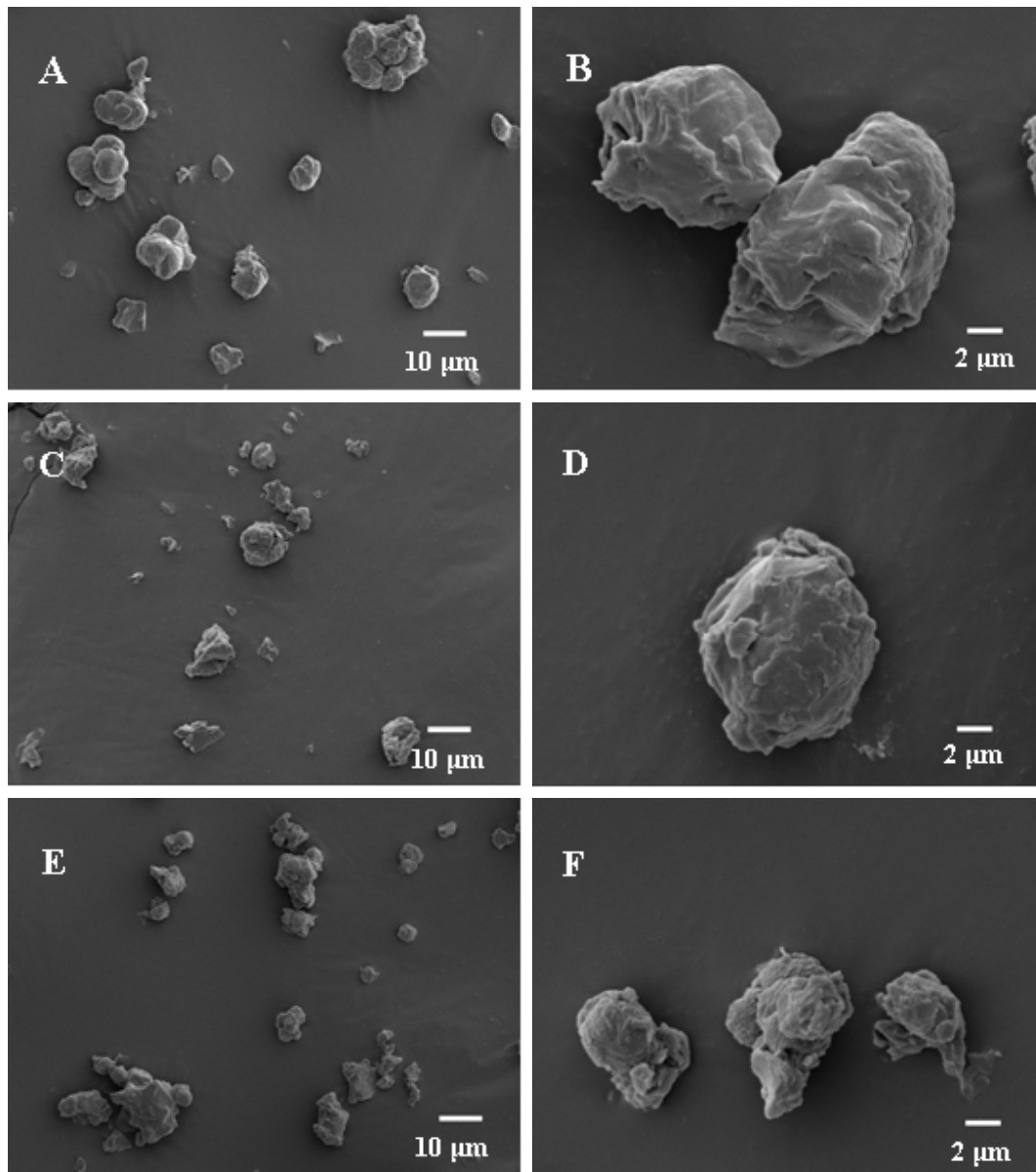
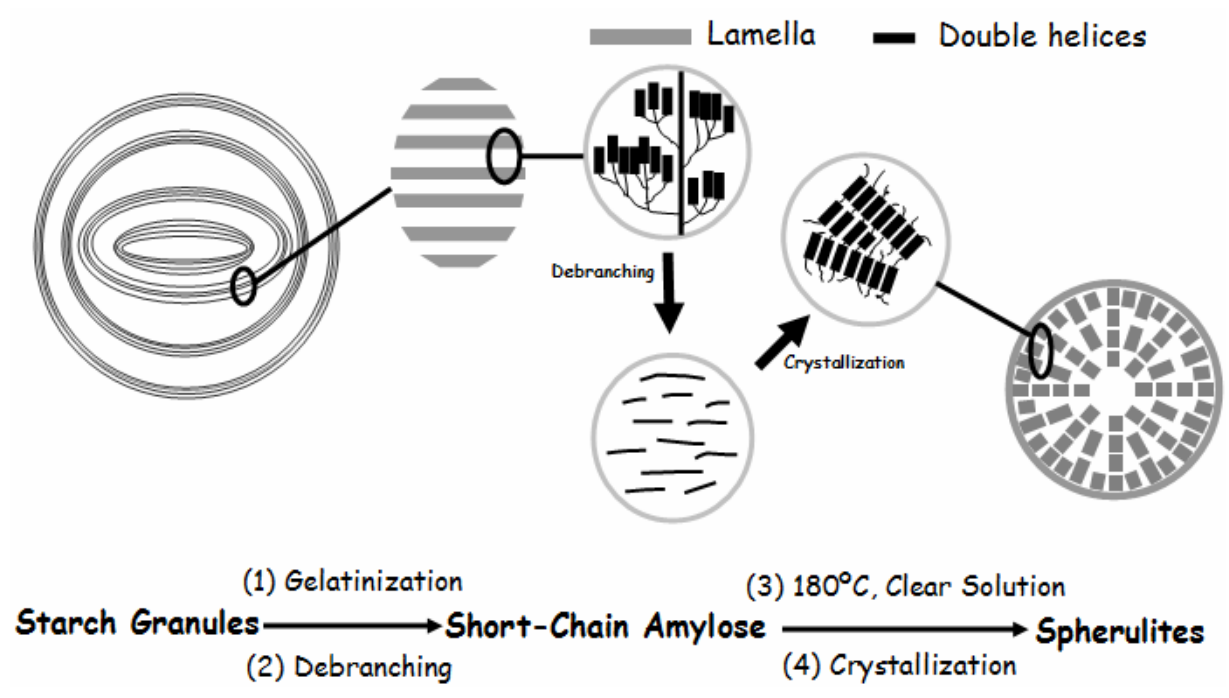


**Figure 6.11 Schematic drawing of transition from starch granule to short-chain amylose spherulites.**



## Chapter 7 - Conclusions and Perspectives

Starch is the most important source of food energy. However, the information about the metabolic quality of starchy foods is scarce. There is growing interest in understanding the relationships between digestion of starch and its impact on human health. The essential tasks of this project are to understand starch molecular architecture during crystallization, structural formation of different types of crystals (A- and B-types), and to provide new insights into how these crystalline starches are digested by enzyme. The successful completion of this project leads to a thorough understanding of how starch molecules assemble to form a specific structure and why starches with different crystalline structure have different digestibility. The enhanced understanding will have broad implications, and further help to control digestion in starchy foods, and to develop new ingredients and foods to improve human health.

The integrated project included study of debranching and crystallization of high solids waxy maize starch, structure and digestibility of crystalline short-chain amylose (SCA) generated from three different waxy starches, investigation of melting and crystallization of SCA in real time, comparison on digestibility of A- and B-type starch crystals, and formation of spherulites from SCA in relation to enzyme digestibility.

At high solids (25%) condition, crystalline precipitates rather than gel materials could be obtained from debranched waxy maize starch slurry by continuous stirring. SCA crystallized upon release from amylopectin during debranching. The yield of the crystallized product was ca. 90% after the starch was completely debranched at 50°C and further precipitated at 25°C. The filtered materials were characterized with an A-type crystalline structure, high melting temperature (90°C to 140°C), and high resistant starch content (71.4%).

Compared to debranched waxy wheat and waxy maize starches, debranched waxy potato starch had a higher average chain length of 32.1, resulting in a higher yield (72.6%) of crystallized product with stronger crystalline structure, higher peak melting temperature (116.2°C), and higher resistant starch content (77.8%). It is suggested that the double helices formed from the longer chains in waxy potato starch are stronger, more resistant to enzyme hydrolysis, and have better thermal stability. Therefore, waxy potato starch is the preferred starch to make a product with high resistant starch content by debranching and crystallization.

Amorphous SCA from debranched waxy starches could immediately crystallize into B-type polymorph when hydrated with ca.50% moisture content at 25°C. SCA from debranched waxy potato starch with higher average chain length showed relatively low crystallinity and higher melting temperature. It could not be completely melted at 100°C and remained a B-type polymorph during rapid cooling. In contrast, SCA from debranched waxy wheat and waxy maize starches contained large portion of low molecular weight fractions, resulted in higher crystallinity and lower melting temperature. When melted, it could predominantly reform into an A-type polymorph under rapid cooling.

Spherulites were prepared by heating high solids concentration (25%) debranched waxy maize starch to 180 °C and cooling at different temperature levels ( 4, 25 and 50°C, respectively). The spherulites prepared at low temperature (4 and 25°C) had large spherulite size (10-15 µm), B-type X-ray diffraction pattern, and lower dissolution temperature (ca. 70-110°C), whereas the spherulites crystallized at 50°C showed small particle dimension (5-10 µm), A-type polymorph, and higher dissolution temperature (100-140°C). Regardless of spherulite size and thermal stability, the A-type spherulites were more resistant to enzymatic hydrolysis than B-type spherulites.

In conclusion, A-type crystals could be formed at high concentration, high temperature and short chain length, whereas B-type polymorph was produced at low concentration, low temperature and long chain length. Digestion results (combined  $\alpha$ -amylase and glucoamylase) showed that A-type structure was more resistant to enzyme digestion than its B-type counterpart. A-type structure had higher thermal stability than B-type polymorph. Annealing increased the melting peak of the B-type crystals, making it similar to that of the A-type crystals, but did not improve the enzyme resistance. The possible reason for these results was due to a more condensed double helices packing pattern of A-type crystallites. Our observations were opposite to the fact that B-type native starches are more enzyme resistant. It is suggested that crystalline types are not the key factor that impact the digestibility of native starch granules. The susceptibility of native starches to enzymes mainly depends on the organization of starch granules.

Our work on relating starch structure and digestibility was based on *in vitro* enzyme methods. Further research is needed to determine the digestibility by using *in vivo* methods and estimate health impacts of starches with different structure on human. We are also looking for

the opportunities to conduct further work with industry partners to seek to commercialize the products developed from this work. The products could be recovered by filtration with a high yield, and may have potentials to be used as dietary fiber to increase the nutrient claims in the food products, and as bulking agents and control release agents in pharmaceutical applications.